Gelatin Nanoparticles as Potential Nanocarriers for Macromolecular Drugs

Dissertation

zur

Erlangung des Doktorgrades

der Naturwissenschaften

(Dr. rer. nat.)

dem

Fachbereich Pharmazie der

Philipps-Universität Marburg

vorgelegt von

Saeed Ahmad Khan

aus **Pakistan**

Marburg/Lahn **Jahr 2014**

Erstgutachter: **Prof Dr. Marc Schneider**

Zweitgutachter: **Prof. Dr. Udo Bakowsky**

Eingereicht am **11.06.2014**

Tag der mündlichen Prüfung am **23.07.2014**

Hochschulkennziffer: 1180

Table of Contents

Short Summary

With an objective of designing gelatin based nanoparticulate delivery system for macromolecules, some of the important challenges associated with gelatin nanoparticles are addressed in this thesis. The first goal is to avoid aggregation, one of the most often encountered problems during nanoparticle formation from gelatin. In this context, different parameters involved in nanoprecipitation technique are investigated, in order to obtain optimum preparative conditions. Effective loading of FITC-dextran as a model hydrophilic macromolecule shows good potential of the system for macromolecular drugs. Attempts are also made to modify the surface of gelatin nanoparticles with PEI, in order to facilitate surface adsorption of negatively charged macromolecules. However, the size of nanoparticles is substantially increased after PEI coating. Moreover, the particles strongly positively charged particles showed an increased toxic behavior after surface modification with PEI.

The second main challenge in gelatin nanoparticles is the use of crosslinkers for stabilization of particles. Since crosslinkers not only crosslink gelatin but also the active sites of therapeutic proteins, this may lead to biological inactivity of proteinaceous compounds. Therefore, we introduce an alternative approach of stabilization. Gelatin nanoparticles are entrapped in nanospheres made of synthetic polymers, using a unique technique of nanoprecipitation-emulsion solvent evaporation. PLGA seems to be ineffective, while Eudragit® E100 efficiently entraps gelatin nanoparticles in nanosphere matrix depending on concentration.

Kurzzusammenfassung

Die Herstellung gelatinebasierter nanopartikulärer Drug Delivery Systeme für Makromoleküle birgt viele Herausforderungen. Diese Arbeit beschäftigt sich mit einigen der wichtigsten Schwierigkeiten bei der Herstellung von Gelatine-Nanopartikeln.

Das erste Ziel stellt die Vermeidung der Partikelaggregation dar, eines der häufigsten Probleme mit dem die Herstellung von Gelatine-Nanopartikeln assoziiert ist. Zur Identifikation der diesbezüglich optimalen Herstellungsbedingungen wurden verschiedene Parameter der Nanopräzitations-Technik untersucht. Durch die effektive Beladung mit dem hydrophilen Modellmakromolekül FITC-Dextran konnte das hohe Potential dieses Trägersystems für makromolekulare Wirkstoffe gezeigt werden. Darüber hinaus wurde versucht die Oberfläche der Gelatine-Nanopartikel mit PEI zu modifizieren, um die Oberflächenadsorption von negativ geladenen Makromolekülen zu erleichtern. Neben der erfolgreichen PEI-Adsorption und der damit verbundenen positiven Oberflächenladung, nahm die Partikelgröße deutlich zu und die positiven Ladungen führten zu einer verstärkten Beeinträchtigung der Zellviabilität. Ein weiteres Problem bei der Herstellung von Gelatine-Nanopartikeln stellt die Verwendung von Quervernetzer zur Stabilisierung der Partikel dar. Derartige Quervernetzer können nicht nur Gelatine, sondern auch aktive Zentren von therapeutischen Proteinen vernetzen, wodurch diese ihre biologische Aktivität verlieren können. Um dem entgegenzuwirken, wurde im Rahmen dieser Arbeit ein alternativer Ansatz zur Partikelstabilisierung entwickelt. Hierbei wurden die Gelatine-Nanopartikel unter Nutzung der einzigartigen Nanopräzipitation-Emulsions-Evaporations-Technik in Nanosphären verkapselt, die aus einem synthetischen Polymer bestehen. PLGA hat sich diesbezüglich als ungeeignet erwiesen, wohingegen Eudragit® E100 die konzentrationsabhängige Verkapselung von Gelatine-Nanopartikel in Nanosphären auf effiziente Weise ermöglicht.

1. Background and Literature Survey

1.1. Introduction

Conventionally most of the pharmacologically active compounds have been of low-molecular weight. However advances in biotechnology have paved new ways for macromolecular drugs to become new therapeutics for several major disorders [1, 2]. These so-called biologicals are expected to occupy about 50 % sale of the top hundred drugs by 2018 [3]. Due to high molecular weight, macromolecules have limited ability to cross biological barriers. Hence, the factors required for delivery of appropriate amount of macromolecular drugs to the desired site of the body are significantly different from those required for conventional small therapeutic moieties.

1.2. Delivery of Macromolecules

Macromolecules are conventionally administered in aqueous solution using needles and syringes [4]. For the improvement in therapeutic efficacy of macromolecules, several approaches have been utilized e.g., photochemical internalization [5, 6], pH gradient exploitation [7], hydrogels [8-11], microneedles [12, 13], microparticles [14, 15], and nanoparticles [16, 17]. Nanoparticles have been proved to be one of the most promising delivery systems. The submicron size of nanoparticles favors intracellular uptake compared to larger carriers [18, 19]. Consequently, nanoparticles have gained increasing attention for the delivery of macromolecules [20, 21]. However, these systems are mostly based on hydrophobic polymers, which may induce unfolding and hence inactivation of hydrophilic macromolecules [22-24]. For this reasons, interests are diverting towards biopolymers as nanomaterial for the delivery of labile macromolecular drugs [25, 26], since biopolymers exhibit congruent properties in terms of their suitability for macromolecular drugs [27].

1.3. Biopolymers

Biopolymers are polymers produced and isolated from living organisms. They are typically safe materials having immense applications in devices intended for application in pharmaceutical and medical fields [28].

Pharmaceutically used biopolymers are classified into two major classes: (1) polysacharides (e.g., chitosan, hyaluronan, dextran, cellulose, pullulan, chondroitin sulfate, alginate, etc.), and (2) proteins (e.g., collagen, gelatin, gliadin, albumin, etc.). Both groups are hydrophilic, biocompatible and biodegradable. However, comparison of both groups based on their merits is difficult because each group possesses its characteristic advantages. Some of the typical examples for naturally occurring biopolymers and their chemical structures are given in table 1.1.

1.4. Gelatin

Gelatin, as a prominent biopolymer, is a generic name for the mixture of purified protein fractions obtained from collagen [29]. It is isolated mainly from bovine hide, pork skin, and cattle bones. However, non-mammalian sources e.g. fish are also gaining interest [30-32]. Commercially two different types of gelatin (type A & type B) are available depending on the method of collagen hydrolysis. Type A gelatin is obtained by acid hydrolysis of gelatin. Acid processing barely affect the amide groups of glutamine and asparagine, resulting in an higher isoelectric point (IEP), i.e., 7-9 [33]. Contrarily, alkaline treatment hydrolyses asparagine and glutamine to aspartate and glutamate, respectively. Thus type B gelatin possesses a greater proportion of carboxyl groups, rendering it negatively charged and lowering its IEP (i.e. 4.5-6.0) [34].

Table. 1.1. Common biopolymers used in preparation of nanoparticulate drug delivery

Biopolymers	Bio-Source	Chemical Structure	Ref.
Polysaccharides			
Cellulose	Wood and agricultural residues		[35]
Chitosan	Shells of marine crustaceans		[36]
Dextran	Brown algae *Leuconostoc mesenteroides*		[28]
Alginate	Bacteria e.g., Azotobacter and Pseudomonas species.		[37]
Hyaluronan	Cartilage, skin, rooster combs, etc., Bacteria e.g., *Streptococcus zooepidemicus*.		[38]
Pullulan	Bacterium *Aureobasidium pullulans*		[39]
Chondroitin sulfate	Animal cartilage		[40]
Proteins			
Animal Proteins			
Gelatin	Animal bones or skin		[41]
Albumin	Human or animal albumin	-	[42]
Plant Proteins			
Gliadin	Wheat gluten		[43]
Zein	Maize (corn)	-	[44]
Soy Proteins	Soybeans	-	[45]
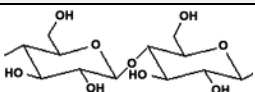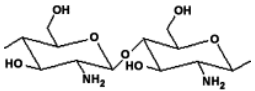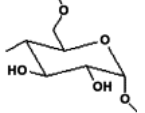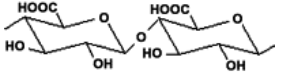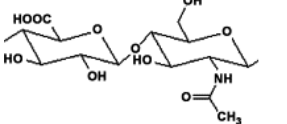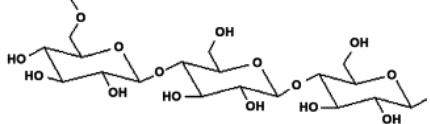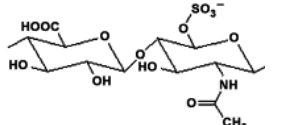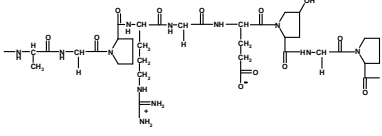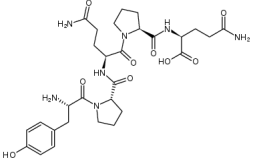
Gelatin dissolves in warm water forming a solution of uniformly distributed gelatin molecules. At temperature >35-40 °C gelatin-water mixture exists as sol [46]. At further lower temperature the intra-molecular hydrogen bonding induces a transition from sol to a structured three dimensional gel, at concentration higher than approximately 1% [47]. Lower concentration does not have sufficient molecules to support infinite three-dimensional gel network [48]. Various grades of gelatin are commercially available with different granule size, molecular weight etc. and grading is usually done by jelly strength (Bloom strength) [32].

Being a versatile natural polymer, gelatin has a broad range of applications i.e. food, photographic, medical and pharmaceutical products. In the food products, it is utilized as film former, gelling agent providing texture and shape to food [49, 50]. In the medical field it is used in artificial organs and tissue engineering [51, 52]. In pharmaceutical field it is conventionally used as emulsifier [53, 54], binder [55], gelling agent [56], vaccine stabilizer [57], and plasma expander [58]. Due to its innate properties it has gained new interests in drug delivery systems [59] such as hydrogels [60], films [61], microcapsules [62], nanoparticles, etc. [63-65].

1.5. Gelatin Nanoparticles (GNPs)

The potentials of gelatin as nanomaterial was explored in 1980s for the first time [66, 67]. Biodegradability and biocompatibility are some of the important merits of gelatin nanoparticles development for *in vivo* application [68, 69]. Drugs can be effectively incorporated or attached to the surface of the nanoparticle matrix. Its proteinaceous origin has raised specific interest, due to the presence of different accessible functional groups. This provides multiple opportunities for modification e.g. attachment of targeting-moieties, crosslinkers and shielding substances [70-72]. All these virtuous properties of gelatin make it

an attractive biomaterial for nanoparticulate drug delivery systems [73].

1.5.1. Preparation Techniques

Different preparation techniques have been adopted by various investigators for gelatin nanoparticles, summarized in table 1.2. For instance, emulsion/solvent evaporation [74, 75], reverse phase preparation [76], inverse miniemulsion [77], coacervation [66, 67, 78-80], desolvation [63, 81-85], and more recently nanoprecipitation [86]. Some of the frequently used techniques are discussed as follows.

Simple w/o Emulsion Method

Cascone and Lazzeriet [75] introduced solvent evaporation technique based on single water-in-oil (w/o) emulsion. Typically, the gelatin aqueous solution is homogenized in nonpolar phase comprised of poly(methylmethacrylate) (PMMA) dissolved in chloroform/toluene. Size of droplets is reduced by homogenization to obtain nanoemulsion, which is subsequently crosslinked to produce homogeneous solid gelatin nanoparticles in the size range 100-200 nm. Despite of difficult washing steps to remove PMMA, emulsion solvent evaporation was used by some researchers [74, 87].

Reverse Phase Preparation Technique

In this method the particles are formed inside the inner aqueous core of reverse micellar droplets formed by surfactant bis(2-ethylhexyl sulphosuccinate) (AOT) in n-hexane [76]. Gelatin aqueous solution is accommodated in the internal aqueous core which is subsequently crosslinked. This method yields gelatin nanoparticles in the size range 40 nm. Nevertheless, the use of apolar solvent, and complexity in washing step are the main disadvantages of this technique [88].

Inverse Miniemulsion Technique

In this method two inverse miniemulsions are formed (i.e. emulsions A and B). Gelatin aqueous solution in *p*-Xylene, containing emulsifier comprises emulsion A. Similarly emulsion B is formulated by emulsifying glutaraldehyde (crosslinker) aqueous solution in p-Xylene. Both crude emulsions are separately sonicated to form miniemulsions which are subsequently mixed and sonicated in an ice bath to fuse the droplets and produce crosslinked gelatin nanoparticles. Fusion and fission is considered to be the governing phenomenon for nanoparticles formation by inverse miniemulsion [77, 89]. Higher polydispersity, difficulty in removal of p-Xylene and repeated sonication are the main demerits of this technique.

Coacervation Technique

In coacervation/desolvation process, nanoparticles are formed by addition of sodium sulfate as coacervating agent to the gelatin solution [66]. This leads the system to liquid-liquid phase separation. Consequently a polymer rich dense phase (coacervate phase), is induced due to rolling up of gelatin molecules. Hence nanoparticles are formed due to the dehydration of gelatin molecules [67, 78], which are subsequently crosslinked by glutaraldehyde. Despite the addition of tween 20, the GNPs produced by sodium sulfate coacervation have bigger sizes and a broader size distribution [79, 80] than other techniques.

Desolvation Technique

In desolvation technique gelatin aqueous solution is desolvated at controlled pH by the addition of a desolvating agent (e.g., alcohol) under continuous stirring. Typically nanoparticles are formed as controlled precipitates when the solvent composition is changed from 100% water to 65% hydro-alcoholic solution [81, 90-92]. After crosslinking gelatin nanoparticles in the size range 200-500 nm are produced [82-84, 93-98]. Nanoparticles

produced by this technique are heterogeneous in size and have stability issues [85]. Besides, the reproducibility for different batches of nanoparticles and phase separation after a slight excess of ethanol, are some of the problems associated with desolvation [99]. Desolvation of gelatin aqueous solution is a very complex phenomenon. It can be affected by many factors such as pH, temperature, ethanol concentration and molecular weight [100]. The process of aggregation by ethanol induced desolvation is explained in detail by Mohanty et al [81, 91, 92].

Two-Step Desolvation Technique

In an attempt to solve the stability problems associated with conventional desolvation, an important progress was made by Coester et al. in 2000 [85]. They introduced a two-step desolvation technique for gelatin nanoparticles. Typically, the low molecular weight portion of gelatin is discarded after the first desolvation. The high molecular weight precipitate is dissolved in water and re-desolvated at controlled pH. This technique produces particles in the size range of 100-300 nm. Two step desolvation has been one of the most widely employed techniques for preparation of GNPs [63, 99, 101-104]. Nevertheless, this technique works at a narrow pH range i.e., 2.3 to 4.0 before the second desolvation. Moreover, the temperature of gelatin solution, the amount of precipitate after the first desolvation step, and the speed of acetone addition during the second desolvation are some of the important factors affecting the size and homogeneity of produced nanoparticles [99]. The Asymmetrical Flow Field Flow Fractionation (AF4) and Multi Angle Light Scattering (MALS) showed that lowering the amount of low molecular weight fraction in gelatin bulk material omits the need of first desolvation step [102]. More specifically, gelatin batches containing less than 20 % (w/w) of <65 kDa molecular weight peptides resulted in successful nanoparticles formation by one-step desolvation. On the other hand gelatin with increased amount of high molecular weight

component >104 kDa failed to yield nanoparticles by one step desolvation. Thus, contrary to the earlier study of Farrugia & Groves [100], it is not essential to have increased amount of the high molecular weight fraction for the production of stable and homogeneous gelatin nanoparticles. Rather reduction of very low molecular weight components (<65 kDa) is critical for the stability and homogeneity of produced nanoparticles [99, 102]. Two-step desolvation enables the production of homogeneous gelatin nanoparticles. However, critical requirement for molecular weight and a narrow pH range are some of the drawbacks limiting the flexibility and reproducibility of the technique for broader application range.

Nanoprecipitation Technique

In order to produce gelatin nanoparticles without changing the native pH of gelatin solution and to avoid pretreatment of gelatin bulk material, i.e., removal of low molecular weight portion, nanoprecipitation technique was introduced [86]. Nanoprecipitation requires two miscible solvents; the polymer can be dissolved in one (the solvent) but not in the other (the nonsolvent). Typically, gelatin aqueous solution is dropped into the nonsolvent containing poloxamer as stabilizer. An interfacial turbulence is created due to solvent diffusion. Subsequently, a violent spreading occurs because of the solvent/nonsolvent mutual miscibility. Thus droplets of nanometer range are torn from the interface [105-107]. Nanoparticles are formed immediately when water diffuses to the nonsolvent, leaving behind the poloxamer stabilized gelatin nanoparticles. Those are then crosslinked with glutaraldehyde in order to obtain stable nanoparticles [108]. The size of nanoparticles can be tuned by changing gelatin concentration in the solvent phase and altering the composition of nonsolvent as described in chapter two.

Table 1.2. Advantages and disadvantages of different preparation techniques for gelatin nanoparticles.

Preparation Method	Size (nm)	Positive aspects	Negative aspects	Reference
Desolvation	200-500	Simple procedure	Agglomeration, Polydispersity and stability issues.	[83]
Two step desolvation	100-300	Homogeneous size	Narrow pH range, Specific molecular weight requirement.	[85, 109]
Emul./solvent evaporation	100-200	Homogeneous size	Hectic procedure of washing for nanoparticles isolation	[75]
Reverse phase preparation	40	Small size	Nanoparticles isolation	[76]
Inverse miniemulsion	150-200	No special gelatin needed	High polydispersity and difficult procedure	[77]
Nanoprecipitation	250-350	Simple and straight forward procedure	High amount of surfactant needed.	Described in Chapter 2

1.5.2. Drug Loaded Gelatin Nanoparticles

Nanoparticles for drug delivery systems should ideally have high loading capacity so that a lower amount of carrier is required for delivery of a certain dose of the drug. Drug loading of the nanoparticles is achieved by two ways: The drug is either incorporated in the polymer solution before nanoparticle preparation, or by soaking the particles in drug solution, i.e., the drug is sorbed into the particles after preparation. A good incorporation method is thought to exhibit efficient loading compared to soaking method [110-113].

Different outcomes have been reported for various drugs in terms of loading and release (summarized in table 1.3). Overall, no concrete conclusion can be drawn for encapsulation efficiency. However, some of the factors can be assumed as important parameters, such as

solubility, ionization, and bloom strength of gelatin etc. For instance, Vandervoort and Ludwig [82] observed the important role of solubility in encapsulation. Such as, about 50% encapsulation was observed for hydrophilic compound pilocarpine HCl. The protonated pilocarpine molecule was considered to be attracted by negatively charged gelatin B. Comparatively lesser entrapment (i.e. 35%) was observed for hydrocortisone, a well know hydrophobic compound, however conjugation with cyclodextrins increased the encapsulation of hydrocortisone to 45%. On the other hand loading as high as 70% and 90% was observed for hydrophobic compounds like didanosine and cyclosporine respectively [114-116]. Thus encapsulation efficiency of the drug cannot be solely attributed to the solubility. Decrease in entrapment was observed for methotrexate upon increase in drug-polymer ratio [75]. Moreover, drug loading was also affected by the crystallinity of drug. For example entrapment efficiency of 33% was observed for an extremely hydrophobic compound paclitaxel because it existed in amorphous state. However, the entrapment of paclitaxel increased to 78% with higher bloom gelatin [117]. This means bloom strength also has an effect on entrapment. For instance 26% cycloheximide was loaded into gelatin nanoparticles prepared with 75 bloom, while the entrapment efficiency increased to 41% when gelatin of 300 bloom was used [118].

The release of drug from nanoparticles may be controlled by diffusion or dissolution. The mechanism of drug release from gelatin nanoparticles is considered to be controlled by diffusion, since the crosslinked nanoparticles matrix does not degrade in normal release medium [74]. Therefore, swelling of gelatin matrix, solubility of drug, molecular size of drug and involvement of drug in crosslinking can be considered critical in defining the release pattern of gelatin nanoparticles [119]. For instance, didanosine a sparingly water soluble compound showed a release of 50% in 24 hours, while a biphasic release with an initial burst release was observed for the water insoluble drug amphotericin B [120, 121]. A very rapid release of i.e.,~90% release after 2 h was observed for paclitaxel from gelatin nanoparticles.

The reason for such a fast release was explained to be the amorphous nature of encapsulated paclitaxel [117]. Moreover, the extent of crosslinking obviously affects the drug release, i.e., gelatin nanoparticles with higher crosslinking degree exhibited slower release [74, 87, 119]. Moreover, the release rate and extent of release was dependent on the amount of drug loaded. Faster release was observed when higher amount of drug was used in formulation [74, 75]. Another important property of gelatin is the bloom strength. Gelatin with lower bloom showed faster release compared to higher blooms [118]. This may be due to better mechanical properties of gel network prepared with higher bloom [122].

Table. 1.3. Examples of studies conducted on drug loaded gelatin nanoparticles

Encapsulant	Loading method	Nanoparticle preparation method	E.E (%)	Ref.
Methotrexate	incorporation prior nanoparticle formation	Emulsion	5-15	[75]
Chloroquine phosphate	Swelling post nanoparticles formation	Emulsion	15-20%	[74]
BSA	incorporation prior nanoparticle formation	Emulsion	-	[123]
Cytarabine	Swelling post nanoparticles formation	Emulsion	-	[74]
Paclitaxel	Mixed with desolvating agent	Desolvation with sodium sulfate	33-78%	[117]
Pilocarpine	incorporation Prior nanoparticle formation	Desolvation with ethanol	50 %	[82]
Hydrocortisone	incorporation Prior nanoparticle formation	Desolvation with ethanol	35 %	[82]
Doxorubicin	incorporation Prior nanoparticle formation	Desolvation with sodium sulfate	42 %	[78-80]
Didanosine	incorporation Prior nanoparticle formation	Two-step desolvation	70 %	[116]
Sulphamethaxazole	Swelling post nanoparticles formation	Emulsion method	18-39 %	[87]
Cycloheximide	incorporation prior nanoparticle formation	Two-step desolvation	25-40 %	[118]
Cyclosporine	incorporation Prior nanoparticle formation	Emulsion method	90 %	[114]
Rosiglitazone	incorporation Prior nanoparticle formation	Two-step desolvation	90 %	[115]
Amphotericin B	incorporation prior nanoparticle formation	Two-step desolvation	45%	[120]
Iron oxide	incorporation prior nanoparticle formation	Two-step desolvation	-	[124]
FITC-dextran	incorporation Prior nanoparticle formation	One step desolvation	10-80%	[98]

1.5.3. Modified Gelatin Nanoparticles

The presence of various functional groups (Figure 1.1) in the structure of gelatin makes it an interesting nanomaterial. Depending upon the purpose and intended application, gelatin provides different modification opportunities [83, 125].
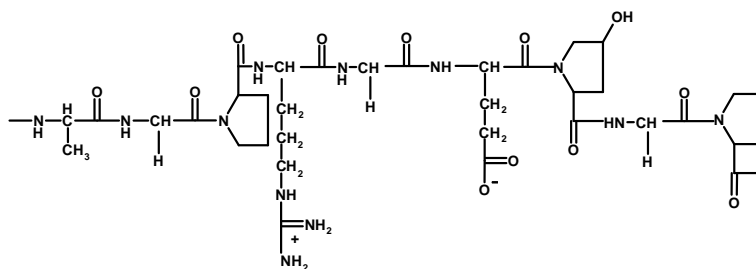
Figure 1.1. Chemical structure of gelatin

Modification can be done before or after nanoparticle formation. Different modification strategies are summarized in table 1.4. For instance, the α-amino groups of gelatin can be modified to free thiol groups by 2-iminothiolane (Traut's reagent), succinimidyl 3-(2-pyridyldithio) propionate (SPDP), and succinimidyl 4-(p-maleimidophenyl) butyrate (SMPB). Alternatively, by quenching the aldehyde groups of the crosslinker glutaraldehyde (GTA) with cysteine, free sulfhydryl groups are generated on the surface of gelatin nanoparticles [126]. Similarly, carboxylic groups can be attached to other ligands by 1-Ethyl-3-(3-dimethylaminopropyl) carbodiimide hydrochloride (EDC), and dicyclohexyl carbodiimide (DCC).

Modification for Extended Circulation Time

Poly(ethylene-glycol) modification (PEGylation) is one of the most widely used approach to improve the circulation time of bioavailable drugs, hence decreasing dosing frequency [42–47]. For this purpose Kaul and Amiji [83] modified gelatin nanoparticles by reacting them

with PEG-epoxide. In a different approach, Kim and Byun [127] adopted the approach of coupling carboxylated mPEG to amine groups of gelatin nanoparticles. PEGylated nanoparticles showed extended circulation time in breast tumor (MDA-MB-435)-bearing nude mice [97]. (PEG)–modified thiolated gelatin nanoparticles were developed as a long-circulating passively targeted delivery system, which released the load in response to intracellular glutathione to enhance DNA delivery and transfection [96]. Furthermore, The mean residence time, and the area-under-the-curve (AUC) of PEGylated gelatin nanoparticles were significantly higher than those of the unmodified gelatin nanoparticles [94, 95].

Modification for Cell Specific Trafficking

In an attempt to link avidin, the surface functional groups of the gelatin nanoparticles were thiolated and linked through a bifunctional spacer at high levels. Biotinylated peptide nucleic acid (PNA) was effectively complexed by the avidin-conjugated nanoparticles in order to explore the potential of the carrier system for biotinylated drug derivatives in antisense therapy. Likewise biotinylated epithelial growth factor (EGF) molecules were conjugated with gelatin nanoparticles to target lung adenocarcinoma (which contains EGF receptors) [40]. This increased uptake into adenocarcinoma cells (A549) compared to the uptake in normal lung cells (HFL1) [128, 129]. Balthasar et al [70] attached biotinylated anti-CD3 antibodies to gelatin nanoparticles by avidin-biotin-complex formation. The resulting nanoparticles could specifically target T-lymphocytes. A similar strategy was used for targeting CD3-positive human T-cell leukemia cells. An anti-CD3-antibody was conjugated with gelatin nanoparticles [130]. Furthermore, Kaur et al reported three times increase in uptake of gelatin nanoparticles into macrophage rich organs (lung, liver, and lymph nodes), by modification with mannose.

Modification for DNA and RNA delivery

Surface modified gelatin nanoparticles as a potential carrier system for double stranded DNA and RNA oligonucleotides is reported. Zwiorek et al [131] modified the free carboxylic groups of gelatin nanoparticles with a quaternary amine (cholamine). This rendered the particles positively charged. These particles were then incubated with DNA solution in order to bind the negatively charged DNA electrostatically to the positively charged cholamine. The DNA transfection efficiency and cell viability studies were performed on the cultured human cells. The amount of nucleic acid loading was found to be dependent on the particle's zeta potential and the type of incubation medium [132, 133].

Table. 1.4. Approaches for modification of gelatin nanoparticles

Modification Purpose	Modifying moiety	Therapeutic improvement	References
Modification for hydrophilization	PEG	Long circulation	[83, 93]
	PEG	Targeting subcutaneous lewis lung carcinoma cells	[95]
	PEG	Targeting murine fibroblast cells (NIH3T3).	[84, 96, 97]
Modification for site specific trafficking	Biotinylated epithelial growth factor (EGF)	Targeting adenocarcinoma cells (A549)	[40, 128, 129]
	Anti-CD3 antibodies	Targeting CD3-positive human T-cell leukemia cells	[70]
	Anti-CD3-antibody	Targeting CD3-positive human T-cell leukemia cells	[130]
	Mannose	Targeting macrophages containing tissues (lung, liver, and lymph nodes)	[116]
Modification for DNA or RNA delivery	Cholamine	Positively charged for gene delivery	[132, 133]

2. Aim and Scope of the Thesis

Most of the preparation techniques for gelatin nanoparticles are either tedious, require specific proportion of certain molecular weight fraction or need a narrow range of relevant pH. The requirement of extreme acidic or basic pH for successful nanoparticle preparation may affect the macromolecules to be loaded. Therefore the first objective was to offer an optimized technique without altering the intrinsic properties of gelatin. In this context a straight forward technique of nanoprecipitation will be presented. The effects of various parameters involved in the particle preparation process were investigated, in order to obtain optimum preparative conditions. FITC-dextran will be employed to assess the possible potential of macromolecular loading. The surface of gelatin nanoparticles will also be modified with PEI, in order to facilitate surface adsorption of negatively charged macromolecules.

Secondly, an alternative approach for stabilization of gelatin nanoparticles without crosslinking will be presented. Since loading of proteinaceous drugs in gelatin nanoparticles due to the generalized reaction of crosslinkers with proteins seems to be impossible with no involvement in crosslinking. Therefore, a method of gelatin nanoparticles stabilization without crosslinking is needed. To date, no study has been performed to address this issue of gelatin nanoparticles. Therefore, we will present a novel technique for maintaining the structural integrity of gelatin nanoparticles in polymeric nanospheres, using nanoparticles in nanospheres (NiNOS) concept. The effect of different parameters and the physicochemical properties of nanosphere preparation will be investigated to get optimum formulation.

3. Improvement of Nanoprecipitation for Gelatin Nanoparticles Preparation

3.1. Abstract

This chapter deals with the improvement of a previously developed nanoprecipitation technique for the preparation of gelatin nanoparticles. A sub-micrometer size range relevant for nanomedicines with a narrow size distribution was aimed for. An optimum preparation technique was established, which was based on the addition of an aqueous gelatin solution to a nonsolvent containing a stabilizer. Subsequent crosslinking with glutaraldehyde resulted in stable gelatin nanoparticles. Several factors of the preparation process, such as the surfactant concentration, type of surfactant, type of nonsolvent and gelatin concentration in the solvent phase were evaluated. Gelatin nanoparticles in the size range of 200-300 nm can be produced with 20-30 mg/ml of gelatin concentration in the solvent phase. Minimum stabilizer (Poloxamer 407 or Poloxamer 188) concentration of 7% w/v in the nonsolvent phase was needed. Furthermore, acetone and acetonitrile as nonsolvents yielded nanoparticles of size around 250 nm and 340 nm respectively at the same gelatin concentration. However, the size can be changed by varying the acetone/acetonitrile ratio. Moreover, the entrapment and release of FITC-dextran as a model macromolecular drug was dependent on molecular weight. About 70% and 90% entrapment efficiency was observed for 42kDa and 167kDa FITC-dextran. Faster and consistent release was exhibited by small molecular weight FITC-dextran. Complete release was only possible after enzymatic digestion with trypsin. Furthermore, as a proof of biocompatibility cytotoxicity against L929 and SKOV-3 cell lines was investigated not indicating an acute toxicity.

3.2. Introduction

In the past nanoparticles from gelatin were prepared by desolvation with sodium sulfate [134]. However, due to the polyampholytic nature and broad molecular weight distribution of gelatin, it has always been a challenging task to prepare stable and monodisperse nanoparticles from gelatin, without aggregation during crosslinking [99]. Therefore, various investigators have utilized different techniques for preparation of gelatin nanoparticles [74-77, 81-84, 119, 135]. In this context Coester et al. introduced a two-step desolvation technique [136], which differed from the previous approaches in the sense that low molecular weight gelatin was discarded before formation of nanoparticles. This procedure allowed to form homogeneous sized nanoparticles. As a consequence, two-step desolvation has become the most widely used method so far [137-139]. However, removal of a major portion of gelatin and a narrow pH range (i.e. highly acidic or basic) as mandatory requirement for successful preparation are some of the drawbacks in two-step desolvation. Therefore, we explored the potential of nanoprecipitation for gelatin nanoparticle preparation, as a straightforward technique without altering the intrinsic properties of gelatin [86].

Nanoprecipitation requires two miscible solvents. The polymer is soluble in one solvent (the solvent), but not in the second (the nonsolvent). The polymer in the solvent phase is added to the nonsolvent containing stabilizer [86, 140]. Interfacial turbulence due to solvent diffusion reduces the size to the nano range [23]. Nanoparticles are formed due to polymer aggregation in the stabilized droplets [141, 142]. The major drawback in nanoprecipitation was that it could only be used for nanoparticles formation from hydrophobic polymers. Thus encapsulating hydrophilic drugs especially macromolecules had always been difficult due to incompatible with the hydrophobic polymers [22, 23, 143]. Keeping in view this challenge, our focus was to explore the potential of nanoprecipitation for the encapsulation of a model

hydrophilic macromolecule (FITC-dextran) within gelatin nanoparticles. In this context, we also aimed to improve the nanoprecipitation technique for gelatin nanoparticles, and to define parameters for a stable gelatin nanoparticle formulation. Hence, the effect of various preparation parameters was investigated allowing to determine a reproducible formulation with uniform size. Furthermore, we also compared our technique with the most commonly used two-step desolvation technique for gelatin nanoparticles preparation.

3.3. Experimental

3.3.1. Materials

Gelatin B bloom75 from bovine skin, Pluronic F-68 (Poloxamer 188), FITC-dextran (42 kDa, 167 kDa and 580 kDa) and polysorbate 80 were obtained from Sigma-Aldrich. Lutrol® F127 (Poloxamer 407) was obtained from BASF, Germany. Trypsin was from Sigma life science, USA. Ethanol, Methanol and n-Propanol were supplied by Sigma-Aldrich Germany (adjusted to 95% to favor dissolution of stabilizer). Acetone and Acetonitrile were obtained from Fisher Chemicals Germany. PBS ready mix was used to prepare phosphate buffered solution. TritonX-100 and glutaraldehyde were provided by BDH-Prolabo Chemicals. Polysorbate 20 was obtained from Atlas Chemicals (Houston, USA). Millipore water with a resistivity of 18.2 MΩ·cm was used throughout the experiments.

3.3.2. Nanoparticles Fabrication by Nanoprecipitation

20 mg gelatin was dissolved in 1ml of de-ionized water at 50 °C, it was then added drop-wise to 10 ml of ethanol containing Lutrol® F127 (7% w/v), and subsequently crosslinked with 0.5 ml glutaraldehyde solution (2%, w/v). The system was stirred overnight to allow crosslink formation in the particles.

3.3.3. Formulation Optimization

Gelatin nanoparticles tend to aggregate during the preparation process, which is augmented by the crosslinking reaction. Thus the formulation was optimized to obtain stable nanoparticle dispersions. In this regard, various parameters were investigated for their effects on particle size before and after crosslinking reaction.

Stabilizer Type and Concentration

To see the suitability of various stabilizers, poloxamer 407, poloxamer 188, polysorbate 80, polysorbate 20 and tritonX-100 were investigated at various concentrations (2-10%). The gelatin concentration in the solvent phase (20 mg/ml), solvent/nonsolvent ratio (1:10), and the glutaraldehyde amount (0.5 ml of 2% w/v) was kept constant.

Nonsolvent Type and Volume

In order to investigate the effect of the nonsolvent type, different nonsolvents (i.e. ethanol, methanol, isopropanol, acetonitrile, and acetone) were studied. Besides that, the effect of the solvent (aqueous phase) to nonsolvent (ethanol phase) ratio on the size was assessed.

Gelatin concentration in the solvent phase was kept constant at 20 mg/ml. Furthermore, the mass ratio of gelatin to stabilizer (i.e. 1/32) and glutaraldehyde amount (0.5 ml of 2% w/v) was maintained unchanged.

Gelatin Concentration in the Solvent Phase

The ratio of solvent/nonsolvent(1/15), mass ratio of gelatin to stabilizer (1/32), glutaraldehyde amount (0.5ml of 2%w/v), and the volume of nonsolvent(15 ml ethanol) were kept constant. However, gelatin concentration in the solvent phase was varied from 20 mg/ml to 35 mg/ml. Similarly using acetone as nonsolvent, gelatin nanoparticles with different

gelatin concentrations were also prepared.

Comparison with Two-step Desolvation Technique

Nanoprecipitation was compared with two-step desolvation for the effect of gelatin concentration on particle size and PDI.

Particles preparation by two-step desolvation adopted the following protocol:

200-400 mg of gelatin was dissolved in 10.0 ml water at 50 °C and then 10.0 ml acetone was added drop-wise. The solution was kept stagnant for two minutes to allow the high Mw fraction to sediment. After discarding the supernatant, the precipitate was redissolved in 10.0 ml water at 50 °C, the pH was adjusted to 8.35. Then 25 ml of acetone was added drop-wise under vigorous stirring. The nanoparticles were crosslinked with 2.5 ml glutaraldehyde (2%) overnight. The nanoparticles were purified by three times centrifugation (10,000g/15 minutes) and redispersion in water and subsequently freeze dried.

3.3.4. Loading of Gelatin Nanoparticles with Model Drug

FITC-Dextran was chosen as a model macromolecular drug, because it lacks primary amino groups in its structure, thereby does not participate in the crosslinking process [144].

Loaded gelatin nanoparticles were produced with typical procedure; briefly 22 mg of gelatin was dissolved in water containing 0.22 mg of FITC-dextran, it was subsequently added to ethanol. The produced nanoparticles after overnight crosslinking, were isolated and washed with water by three centrifugation/redispersion cycles and then freeze dried.

Three different molecular weight FITC-dextrans (42 kDa, 167 kDa and 580 kDa) were used to see the effect of molecular weight.

26

Blank particles were prepared in the same way except that no FITC-dextran was added to the gelatin solution.

3.3.5. Size and Zeta Potential of Nanoparticles

Samples from crude nanosuspension were withdrawn just after production, as well as after overnight crosslinking, and 100 times diluted with the respective nonsolvent (ethanol, methanol, n-propanol or acetone). Then the mean size and polydispersity were measured three times for each batch by dynamic light scattering (DLS), using a Zetasizer nano-ZS (Malvern Instruments Ltd., UK).

Size determination of the washed particles was done with 100 times diluted samples in water. Zeta potential of the dispersed particles was measured at different pH values using Zetasizer nano-ZS (Malvern Instruments Ltd., UK).

3.3.6. Morphological Analysis

Scanning Probe Microscopy (SPM)

The crosslinked nanoparticles were centrifuged for 20-min cycles at $10,000 \times g$. Afterwards the samples were redispersed and the procedure was repeated three times in order to gradually remove the dispersing medium and excess stabilizer. These samples were then evaluated by SPM.

SPM analysis was performed at room temperature; the washed nanoparticles were diluted with ethanol. A drop of ethanol dispersed particles (to avoid agglomeration of particles during drying) was placed on a freshly cleaved mica sheet (Plano Planet GmbH, Wetzlar, Germany), and subsequently dried overnight. SPM imaging was performed under atmospheric conditions using a Bioscope® with a NanoscopeIV controller (DI Digital Instruments, Bruker

Corporation) in tapping mode. A cantilever with a spring constant of 40 N/m and a scan rate of 0.5 Hz (256 lines per image) was used for image acquisition. Raw data was processed by a flattening algorithm to remove background slopes, and hence analyzed by *Nanoscope SPM* software regarding size.

Scanning Electron Microscopy (SEM)

The morphology of nanospheres was also confirmed by SEM. For sample preparation, a silicon wafer was mounted on a metal hub using carbon adhesive tape. A drop of the washed nanosuspension was dropped onto the silicon wafer. Samples were dried by overnight evaporation under ambient conditions. Samples were coated with platinum. SEM images were obtained by JSM-7500F SEM (JEOL (Germany), München, Germany).

3.3.7. Determination of Crosslinking Extent

The extent of crosslinking in the gelatin nanoparticles was determined by an established trinitro benzenesulfonic acid (TNBS) assay [145]. 10-12 mg freeze dried gelatin nanoparticles (crosslinked and un-crosslinked) were dispersed in 1 ml 4% $NaHCO_3$ and 1 ml 0.5% TNBS and heated at 40 °C for 4 hours. 3 ml of 6 M HCl was added and the mixture was autoclaved for 1 hour at 120 °C. The hydrolysate was diluted to 10 ml with water, and extracted with ethyl acetate to remove un-reacted TNBS. 5 ml aliquot of the aqueous phase was diluted to 25 ml with water and the absorbance was measured at 349 nm (using PerkinElmer Lambda35 UV/VIS spectrophotometer) against a blank.

Blanks were prepared by the same procedure as above except that no gelatin was added. The number of primary amino groups as a parameter for crosslinking extent was obtained by the following formula:

$$\frac{\text{Moles of primary amino groups}}{\text{Mass of gelatin in gram}} = \frac{2(\text{absorbance})(0.025\text{L})}{(1.46\times10^4\text{L/mole.cm})(b)(x)}$$

where 1.46×10^4L/mole.cm is the molar absorbtivity of TNB-lys, b is the path length in cm, and x is the sample weight in grams.

3.3.8. Measurement of Drug Content and In Vitro Release

FITC-dextran content in nanoparticles was evaluated in terms of entrapment efficiency (E.E%), which was determined by fluorescence intensity after enzymatic degradation. Briefly, 5 mg of freeze dried particles were dispersed in 5 ml PBS (pH 7.4) at room temperature (23 $\pm2°$C), containing 2.5 mg trypsin. After six hours of digestion the samples were diluted to 25 ml and filtered using 0.22 µm filter. Fluorescence intensity was measured by Infinite$^®$M200 plate reader (Tecan group, Switzerland). Calibration curve was prepared with different FITC-dextran concentration in PBS (the presence of gelatin and trypsin had no effect on the fluorescence intensity). Unloaded particles (no FITC-dextran) were used as blank. The entrapment efficiency was calculated by the following equation:

$$\text{Entrapment Efficiency (\%)} = \frac{\text{Weight of drug in nanoparticles / Weight of nanoparticles}}{\text{Weight of drug used / Weight of gelatin used}} \times 100$$

For estimation of the *in vitro* release process, 5 mg of gelatin nanoparticles were dispersed in 25 ml PBS (pH 7.4). 2 ml samples were withdrawn at defined time intervals, and were centrifuged for 20 min at $10{,}000\times g$. Then 1 ml aliquots were withdrawn from the supernatant, 1 ml PBS was added to the pellets. The pellets were redispersed and added to the original dissolution medium keeping the particle concentration constant. In the aliquots withdrawn, the amount of FITC-dextran was quantified. After five days gelatin nanoparticles were digested with trypsin (0.5 mg trypsin per mg of gelatin nanoparticles), in order to estimate total amount of FITC-dextran.

The turbidity of nanoparticles in PBS (pH 7.4) was measured in terms of absorbance at 600 nm (using PerkinElmer Lambda 35 UV/VIS spectrophotometer), to correlate the release of FITC-dextran with dissolution of particles.

In order to study the effect of molecular weight on the release, around 5 mg of freeze dried FITC-dextran (42 kDa, 167 kDa and 580 kDa) loaded particles were dispersed in 10 ml of phosphate buffer solution (pH 7.4). Aliquots of 1 ml were taken out in different Eppendorf tubes and incubated at 37°C. At different time intervals the tubes were centrifuged at 20000×g for 15 minutes. Supernatant was collected and analyzed for fluorescence intensity.

3.3.9. MTT Assay

Cell viability was performed using the 3-(4,5-dimethythiazol-2-yl)-2,5-diphenyl tetrazolium bromide (MTT) assay, to determine *in vitro* toxicity of particle. This is a colorimetric assay based on reduction of MTT by mitochondrial succinate dehydrogenase in metabolically active cells. The MTT is converted to a dark purple colored formazan product, which is solubilised with DMSO and quantified spectrophotometrically as a measure for viability of the cells, since reduction of MTT can only occur in metabolically active cells.

L929 murine fibroblast, one of the most intensively used cell line for cytotoxicity studies was used. Additionally, SKOV-3 human ovarian carcinoma cell line was used as a representative for human cancer. Cell were cultured at a density of 1×10^4 cells per well in a 96-well plate for 24 h. 100µl of nanoparticles diluted with cell culture media were put in each well and incubated at 37ºC for 24 hours. After the exposure time 100µl of cell culture medium containing MTT was added to each well and incubated for further four hours. After removal of the culture medium 100µl DMSO was added in each well to dissolve formazan product, which was measured by spectrophotometer at 495nm. Cells without any treatment were used

as negative control and cells treated with TritonX-100 were used as positive control. The cell viability was calculated using the following equation.

$$\text{Cell Viability}\,(\%) \;=\; \frac{(\text{Sample} - \text{Positive control})}{(\text{Neagative control} - \text{Positive control})} \times 100$$

3.4. Results and Discussion

The original nanoprecipitation technique was based on poly-(D,L-lactide) (PLA) nanocapsules, being prepared by deposition of the polymer at the o/w interface following acetone displacement from oily nanodroplets [106]. The organic solvent phase was a serious constraint in the procedure, since it rendered the technique only suitable for water insoluble polymers [22]. However, the procedure was modified to produce nanoparticles from gelatin as a hydrophilic polymer [86]. This simple technique is shown schematically in Figure 3.1. Nanoparticles are formed instantaneously after addition of gelatin solution to nonsolvent. The mechanism of particle formation is explained by the interfacial turbulence created due to the solvent diffusion. Subsequently, a violent spreading occurs because of the solvent/nonsolvent mutual miscibility. Thus droplets of nanometers range are torn from the interface, which are eventually needed to be stabilized by a surfactant. Consequently aggregation of polymer chains leads to the formation of nanoparticles [107].
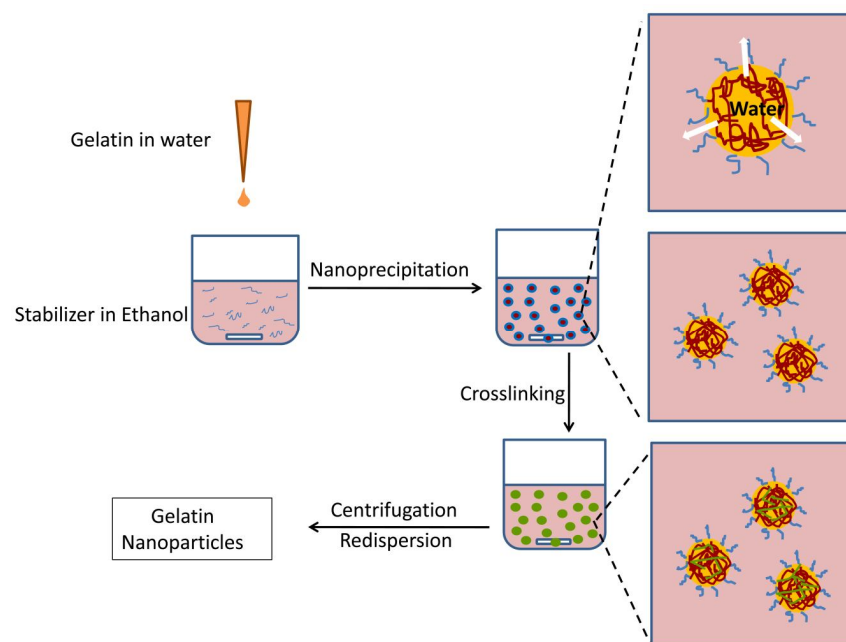
Figure 3.1. Schematic representation of gelatin nanoparticle formation by nanoprecipitation technique.

3.4.1. Effect of Stabilizer Type and Concentration

Gelatin is a polyampholyte, containing both positively and negatively charged segments in the polymer backbone. In the presence of nonsolvent, sequential intermolecular charge neutralization of gelatin molecules takes place; this intermolecular interaction typically leads to agglomeration [146]. Besides this, gelatin based devices readily lose shape in water, hence abruptly releasing the load [147]. Therefore crosslinking is an inevitable step in the preparation of gelatin nanoparticles. For crosslinking bifunctional crosslinkers are usually used e.g. glutaraldehyde, formaldehyde, carbodiimide [148]. The crosslinking step may also form inter-particular crosslinks simultaneous to intra-particular crosslinks, which may lead to aggregation as illustrated in Figure 3.2.
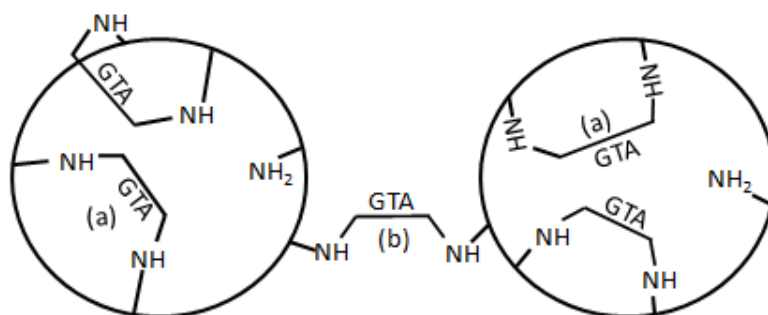
Figure 3.2. Schematic representation of glutaraldehyde crosslinked gelatin nanoparticles, (a) intraparticular crosslinks, (b) interparticular crosslinks.

In order to circumvent possible instabilities due to agglomeration, stabilizers were used in the nonsolvent. Polysorbate 20 and Polysorbate 80 did not stabilize the suspension, while the effect of Poloxamers was concentration dependent. Poloxamer concentration affected the mean size of particles (Figure 3.3). Particles increased by 2-3 fold in the presence of 2% stabilizer. A similar trend was seen with stabilizer concentration as high as 5%. The increase in size is probably due to the formation of interparticular aggregates resulting in an inhomogeneous size distribution, which is apparent from the high value of the polydispersity index (PDI of 0.4-0.5) (Figure 3.3). Further increase of the stabilizer concentration to 6%, reduced the PDI to around 0.25 but it is still higher than that before crosslinking i.e. 0.1. At a stabilizer concentration of 7% or more (up to 10%), the mean size and PDI remained stable during crosslinking. Thus it can be said that a minimum of 7% poloxamer is necessary to produce stable nanoparticles in the size range of 150-250 nm.
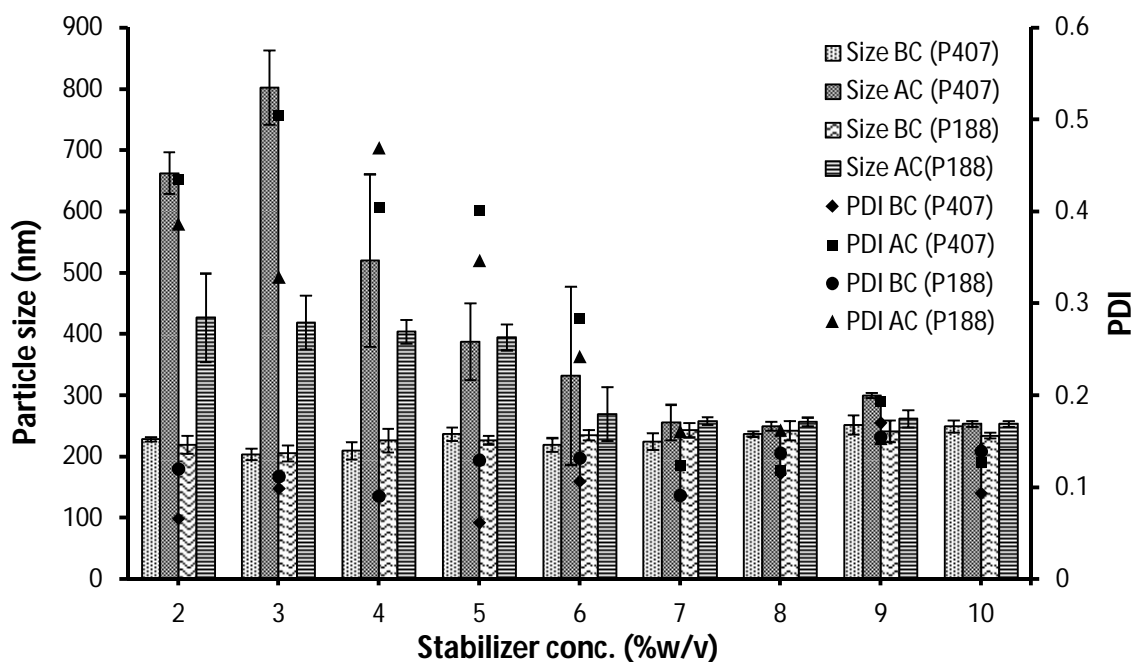
Figure 3.3. Effect of stabilizer concentration on the particle size and polydispersity. In the figure, BC=Before crosslinking, AC=After crosslinking, P407=Poloxamer407, P188=Poloxamer188, PDI=Polydispersity index.

SPM investigation showed spherical particles with smooth surfaces (Figure 3.4). Image analysis for particles size by SPM revealed smaller sizes than that measured by the Zetasizer (as shown in Table 3.1). The smaller size of nanoparticles shown by SPM is most likely due to the drying effects of the sample, whereas particles in dispersion are swollen and yield hydrodynamic radii. In addition, the presence of some larger particles in SPM micrographs (Figure 3.4) underlines the broader size distribution (obvious from PDI values in Table 3.1).
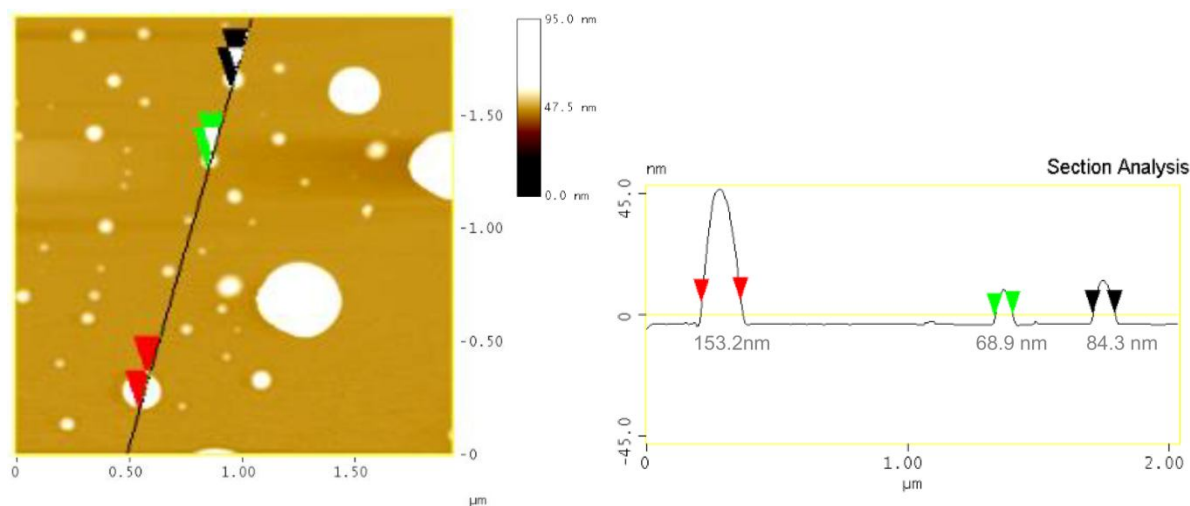
Figure 3.4. SPM analysis of gelatin nanoparticles highlighting some of the particles used in section analysis, (Formulation: 25 mg/ml gelatin in solvent phase).

Table 3.1. Size characterization of gelatin nanoparticles by two methods

Stabilizer	Mol.Wt	a	b	Size in nm ± S.D	
				Zeta sizer	AFM
Poloxamer 407	12000	75	30	249.9 ±7.1 (0.12)*	100.8 ±52.3
Poloxamer 188	8350	98	67	258.6 ±6.5 (0.16) *	138.2 ±56.4

a, number of poly oxypropylene chains; b, number of polyoxyethylene chains.
Formulation: Gelatin concentration: 25 mg/ml, nonsolvent: Ethanol (10 ml).
*Values in parenthesis represent polydispersity index.

3.4.2. Effect of Nonsolvent

In preliminary experiments we had found that acetone and acetonitrile could not produce nanoparticles. Indeed, as soon as the polymer solution was dropped into these nonsolvents, the polymer underwent intense agglomeration and formed a visible precipitate. We thought the possible reason for nanoprecipitation failure might be the big difference in the solubility parameter values. However, we have found that the reason was actually the inefficient stabilizer chosen. Actually, we had used TritonX-100 instead of Poloxamer, due to the

35

insolubility of Poloxamer. In fact poloxamer can be dissolved if a portion of acetone is replaced with water. Hence, nanoparticles can be produced with these acetone and acetonitrile if poloxamer is used as a stabilizer. Figure 3.5 shows that the mean size of nanoparticles obtained with ethanol as nonsolvent was 244 nm, while acetone produced nanoparticles of around 250 nm. Nanoparticles produced with acetonitrile as nonsolvent were around 350 nm in size. However, the size can be changed by altering acetone/acetonitrile ratio.
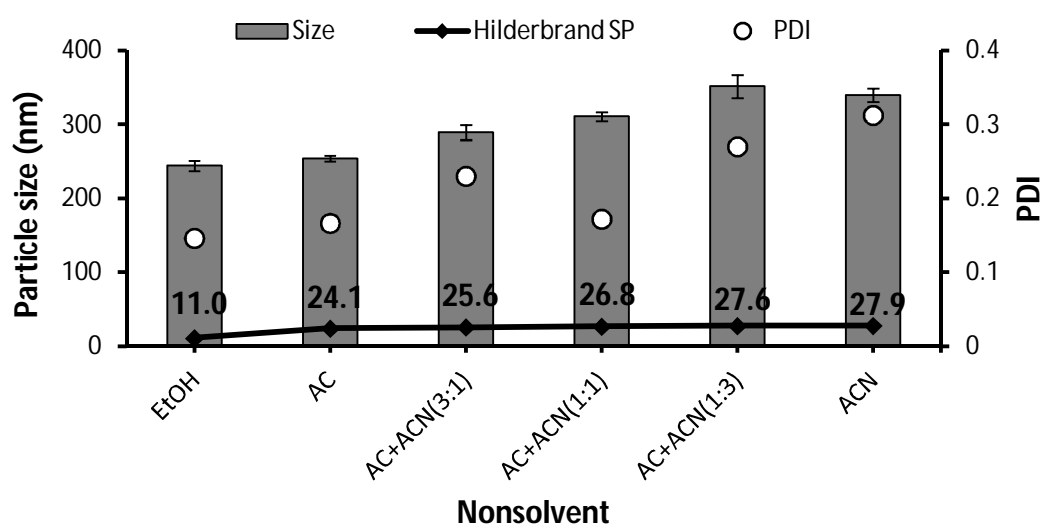

Figure 3.5. Effect of nonsolvent on particle size and polydispersity of gelatin nanoparticles

Nanoprecipitation is governed by a complex phenomenon of polymer–nonsolvent–solvent system. Hence, solvent-nonsolvent interaction parameter, X, is an important parameter to explain solvent-nonsolvent affinity [149]. Equation (1) was used to calculate X [150], in order to correlate with nanoparticles size.

$$X = \frac{V_{NS}}{RT} (\delta_S - \delta_{NS})^2 \qquad (1)$$

Where V_{NS} is the molar volume of nonsolvent, R is the gas constant, T is the absolute temperature, and δ_S and δ_{NS} are the Hildebrand solubility parameters of solvent and nonsolvent, respectively.

Solvent-nonsolvent interaction plays a vital role in the solvent diffusion phenomenon during

36

nanoparticles formation. Lower $X_{S\text{-}NS}$ values represent high affinity of the solvent for the nonsolvent, thus leading to formation of smaller nanoparticles due to faster diffusion [149]. Therefore the increase of particle size in Figure 3.5 can be attributed to an increase in $X_{S\text{-}NS}$ values, shown in Figure 3.5. However, the interaction parameter solely cannot be attributed to the solvent/nonsolvent affinity. Just as seen in case of acetone compared to ethanol as nonsolvent, where interaction parameter for acetone is 24 compared to 11 of ethanol. But the increase in size is not substantial.

3.4.3. Effect of Solvent/Nonsolvent Ratio

The solvent/nonsolvent ratio is an important parameter for preparing stable nanosuspensions; a ratio of as low as 1:7.5 lead to visible particles in the system with both the poloxamer types, though high PDI value is depicted only for poloxamer 188 as shown in Figure 3.6. Solvent/nonsolvent ratio of 1:10 could produce stable nanoparticles in the range of 250 nm. However, further increase in nonsolvent volume did not affect the size and PDI of particles.
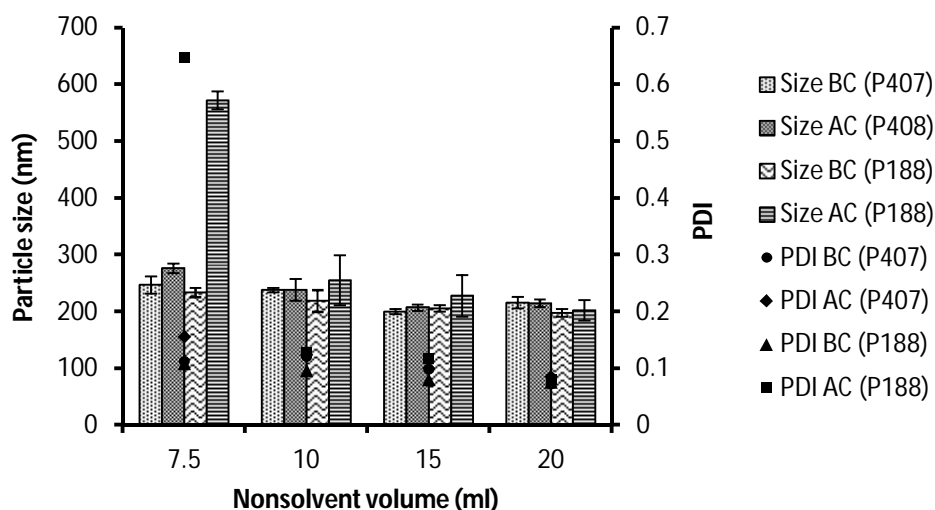

Figure 3.6. Effect of ethanol volume on particle size and polydispersity. BC=Before crosslinking, AC=After crosslinking, P407=Poloxamer407, P188=Poloxamer188, PDI=Polydispersity index.

3.4.4. Effect of Gelatin Concentration

The mean size of gelatin nanoparticles increased with increasing concentration of gelatin in the solvent phase; for instance 20 mg/ml gelatin could produce particles in the size range of around 200 nm. The mean size increased to around 250 nm with a gelatin concentration of 30 mg/ml. Additionally, SPM images reveal that the nanoparticles have spherical shape and are distinctly separated from each other. However, a concentration higher than 30 mg/ml produced big visible particles besides nanoparticles, which can be seen in figure 3.8(e) and which is also obvious from the higher mean size and polydispersity index (Figure 3.7). This might be due to the increase in viscosity of the gelatin solution, since increased viscosity of the solvent phase due to higher polymer concentration retards diffusion of the solvent toward the nonsolvent [23]. These results are in accordance with our expectations regarding similar data for other materials described in literature [151].
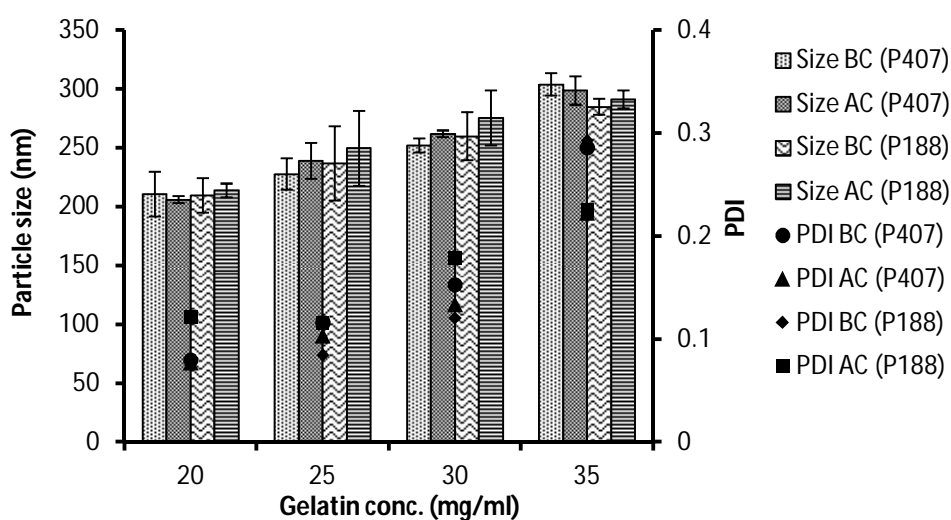

Figure 3.7. Effect of gelatin concentration on the particle size and polydispersity. BC=Before crosslinking, AC=After crosslinking, P407=Poloxamer407, P188=Poloxamer188, PDI=Polydispersity index, (ethanol as nonsolvent).
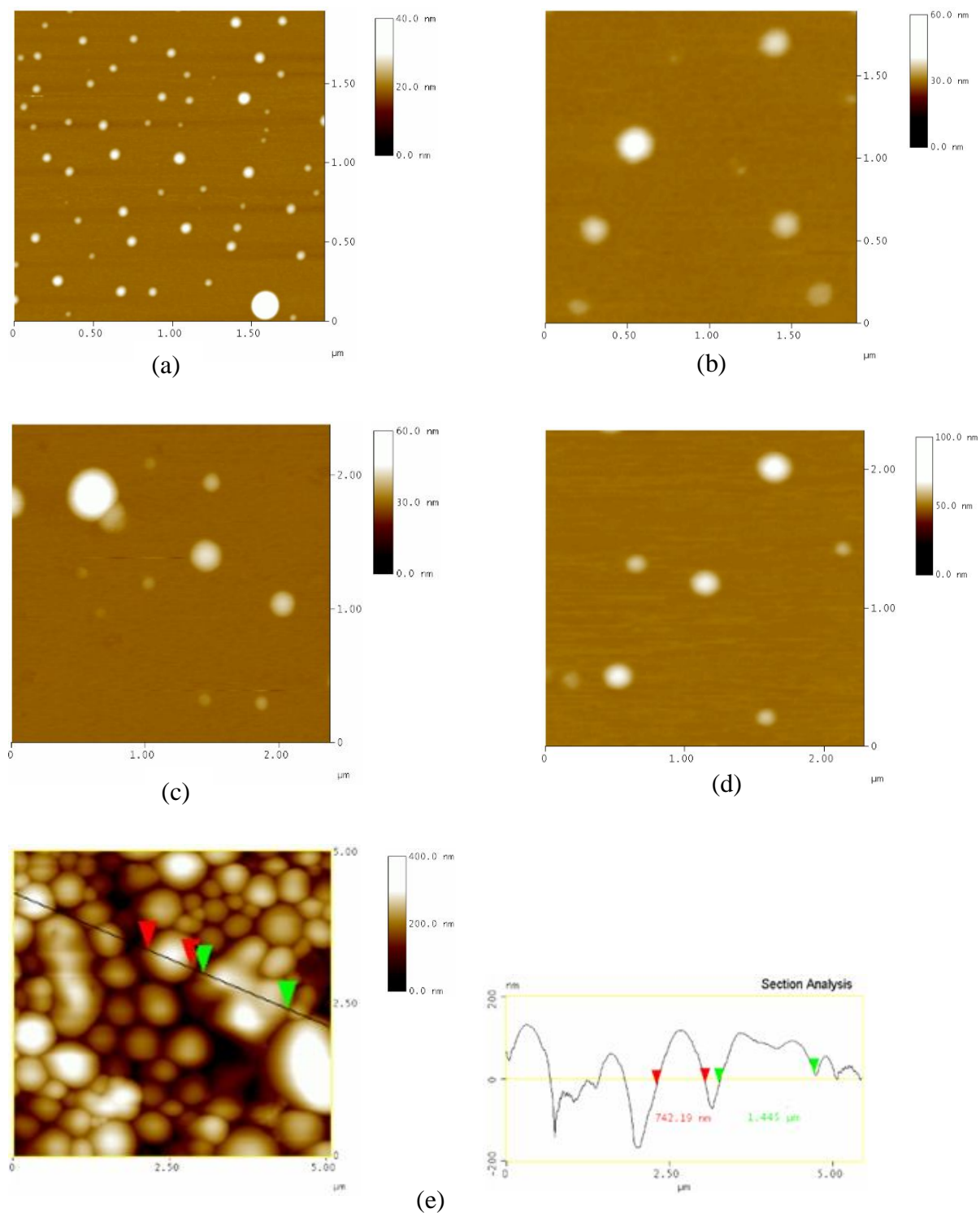
Figure 3.8. Scanning probe micrographs of nanoparticles produced by nanoprecipitation under different conditions: (a) 25 mg/ml gelatin, poloxamer407 as stabilizer; (b) 25 mg/ml gelatin, Poloxamer188 as stabilizer; (c) 30 mg/ml gelatin, poloxamer407 as stabilizer; (d) 30 mg/ml gelatin, poloxamer188 as stabilizer; (e) 35 mg/ml gelatin, poloxamer407 as stabilizer.

The effect of gelatin concentration using acetone as nonsolvent is shown in Figure 3.9. Gelatin nanoparticles of around 250 nm size can be produced with gelatin concentration 20 mg/ml. The size increased to around 300 nm when gelatin concentration was increased to 35 mg/ml gelatin. Visible aggregates appeared with gelatin concentration 45 mg/ml. This was depicted in the PDI value of 0.37. Particles produced with gelatin concentrations lower than 30 mg/ml were monodisperse showing a PDI less than 0.2. However the PDI steadily increased with higher gelatin concentrations.
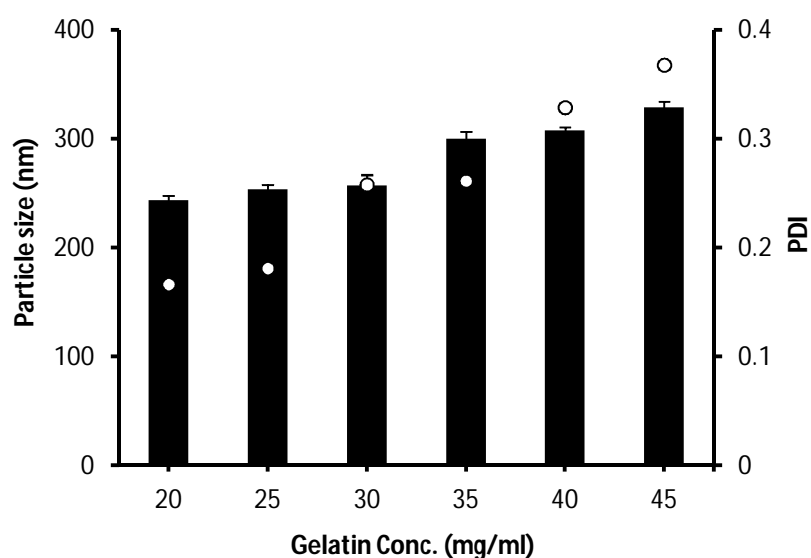

Figure 3.9. Effect of gelatin concentration on the particle size and polydispersity (Acetone as nonsolvent).

SEM images (Figure 3.10) show that nanoparticles have spherical shape. The black square shaped spot in the middle of Figure 3.10(f) is a common artifact observed in SEM analysis, due to longer exposure of sample in electron beam. The particle size calculated from SEM using imageJ® is summarized in table 3.2, which also shows the change in size due to nonsolvent and gelatin concentration. Though, the size of nanoparticles calculated from SEM image is lower than that of DLS results. This is probably due to drying effect, since the size by DLS is actually the hydrodynamic radii of particles.
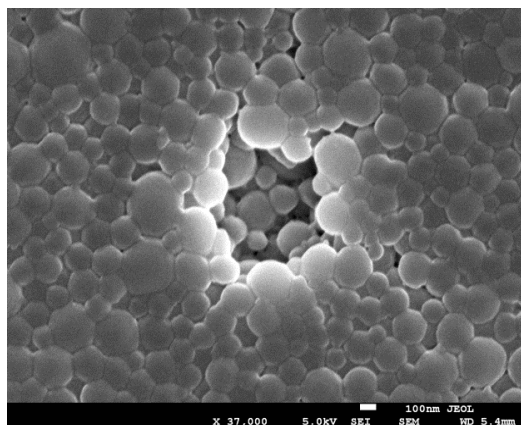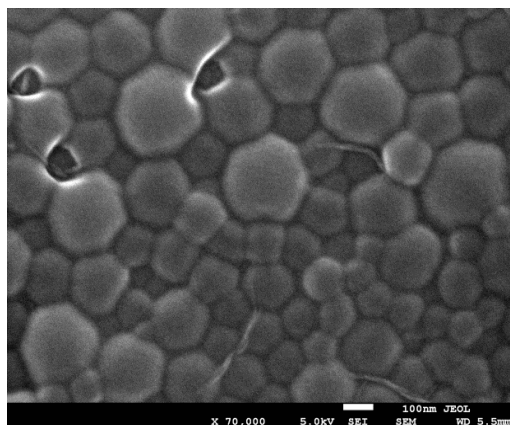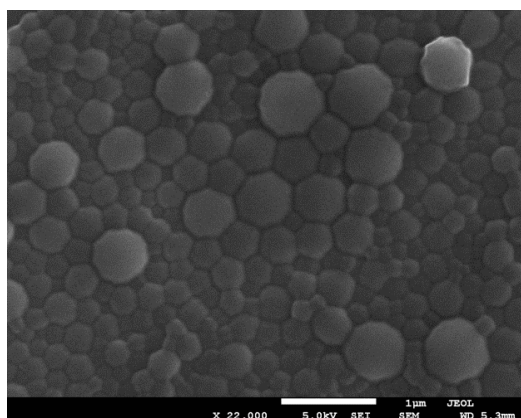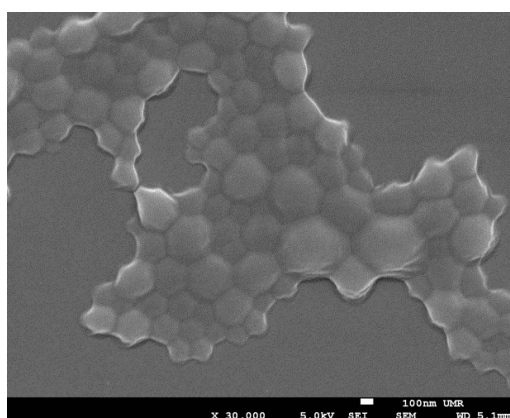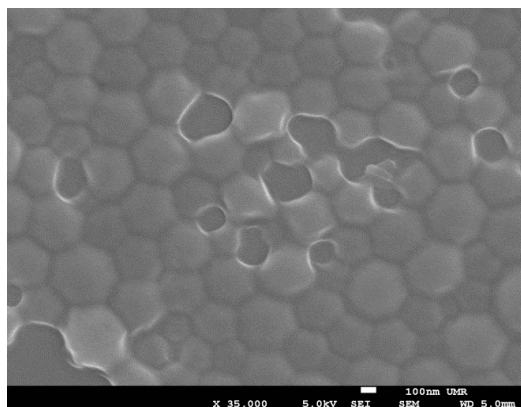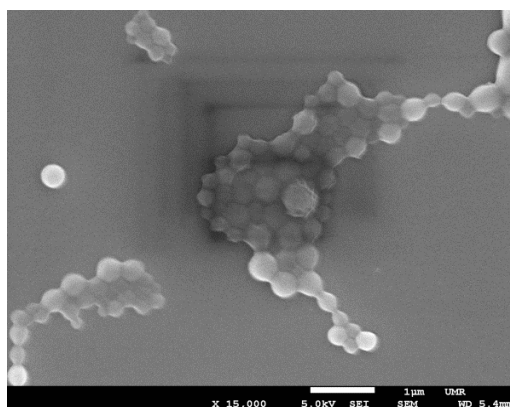
Figure 3.10. SEM images of gelatin nanoparticles produced under different conditions: (a) 20 mg/ml gelatin, ethanol as nonsolvent; (b) 20 mg/ml gelatin, acetone as nonsolvent; (c) 20 mg/ml gelatin, acetonitrile as nonsolvent; (d) 25 mg/ml gelatin, acetone as nonsolvent; (e) 35 mg/ml gelatin, acetone as nonsolvent; (f) 45 mg/ml gelatin, acetone as nonsolvent.

Table 3.2. Size characterization of gelatin nanoparticles produced at different conditions.

Nonsolvent	Conc. (mg/ml)*	[1]Size by DLS (PDI)	[2]Size from SEM
Ethanol	20	244.0 ± 3.2 (0.15)	186.7 ± 65.0
Acetone	20	253.9 ± 4.0 (0.16)	182.6 ± 49.2
Acetonitrile	20	347.4 ± 20.4 (0.31)	326.2 ± 150.8
Acetone	25	253.7 ± 4.2 (0.18)	221.8 ± 65.6
Acetone	35	300 ± 6.5 (0.26)	287.0 ± 71.8
Acetone	45	328.9 ± 5.6 (0.37)	308.1 ± 115.6

*Gelatin concentration in the solvent phase, [1] Dispersed in water after washing, [2] 50 particles analyzed using ImageJ®

3.4.5. Comparison of Nanoprecipitation with Two-Step Desolvation Technique

Nanoprecipitation and two-step desolvation were compared for the effect of gelatin concentration on the mean size of gelatin nanoparticles. In case of nanoprecipitation when the gelatin concentration was increased from 20 mg/ml to 35 mg/ml, the mean size of particles increased from 206 nm to 299 nm and 214 nm to 291 nm (using poloxamer N407 and poloxamer 188 as stabilizer, respectively, as shown in Figure 3.11a), and the PDI values almost doubled in case of both the stabilizers (Figure 3.11b). The increase in PDI can be attributed to the big visible particles produced, as shown in Figure 3.12c.

Two-step desolvation yield comparatively smaller particles than nanoprecipitation. However, a similar trend of increase in size was observed, where the particle size increased from 60 nm to 155 nm when the concentration was increased from 20 mg/ml to 35 mg/ml (Figure 3.11a). However the PDI values show that particles produced with higher concentration of gelatin were more uniform in size than those produced with smaller gelatin concentration, as shown in Figure 3.11b.
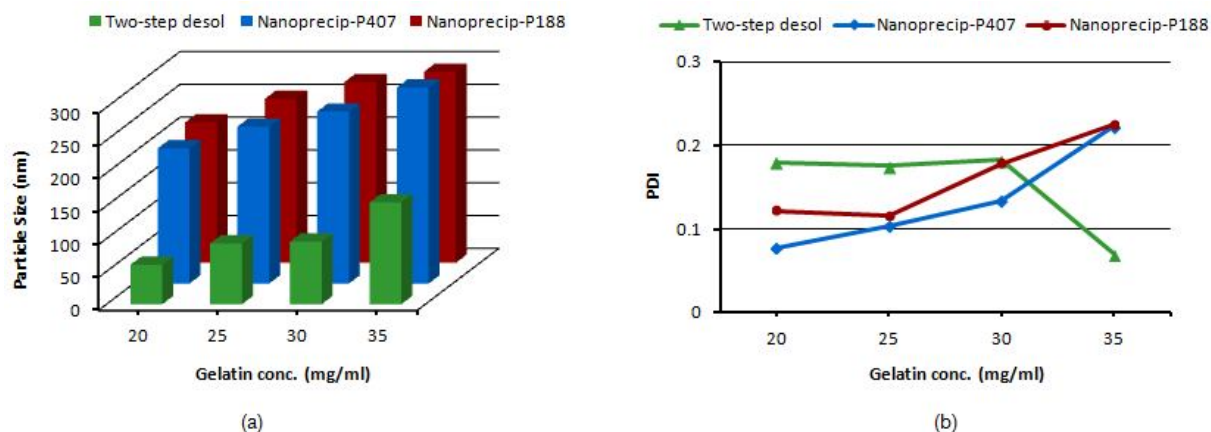
Figure 3.11. Effect of gelatin concentration on the size (a) and polydispersity index (PDI) (b) of nanoparticles produced by two stefp desolvation and nanoprecipitation.

Thus, for both techniques a general trend of increasing particle size was observed with increase in gelatin concentration. However, the increase in PDI was contrary in both cases; at higher gelatin concentration, PDI increased in case of nanoprecipitation, while a decrease in PDI was observed for two-step desolvation.

SPM images revealed that nanoparticles prepared by nanoprecipitation at low concentration (i.e. 25 mg/ml) are uniformly spherical (Figure 3.12a), while those prepared by two-step desolvation with a similar gelatin concentration are comparatively irregular in shape (Figure 3.12b) Contrarily, at higher concentration (35 mg/ml) two-step desolvation produced comparatively more spherical and uniform particles (Figure 3.12d) than nanoprecipitation (Figure 3.12c).
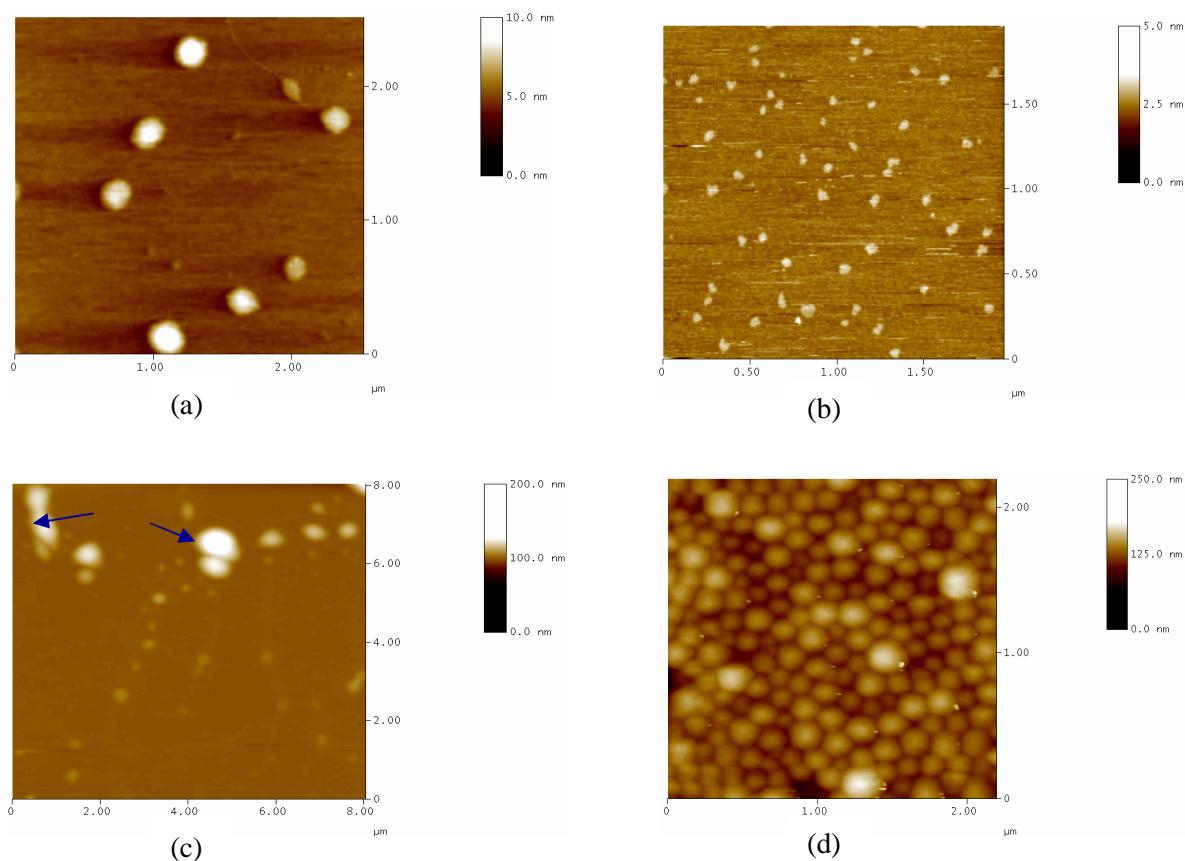
Figure 3.12. SPM analysis of gelatin nanoparticles produced by (a) Nanoprecipitation (20 mg/ml gelatin) (b) Two-step desolvation (20 mg/ml gelatin) (c) Nanoprecipitation (35 mg/ml gelatin) (d) Two-step desolvation (35 mg/ml gelatin).

3.4.6. Zeta Potential of Nanoparticles

Gelatin is a polyelectrolyte containing both anionic and cationic groups. The net charge depends on the type of gelatin and the solution pH. During nanoparticles formation, gelatin chains are crosslinked to form stable nanoparticles. However, not all the primary amino groups are crosslinked (evident from the 72% crosslinking degree in table 3.3), though the number of positively charged groups is decreased. Hence, the zeta potential profile of gelatin nanoaparticles at different pH values shows that ionized cationic groups predominate at lower pH, thus rendering the overall surface positively charged. The net charge on particles' surface is almost zero at around pH 5. While at higher pH the particles tend to be negatively charged, as shown in Figure 3.13.

44
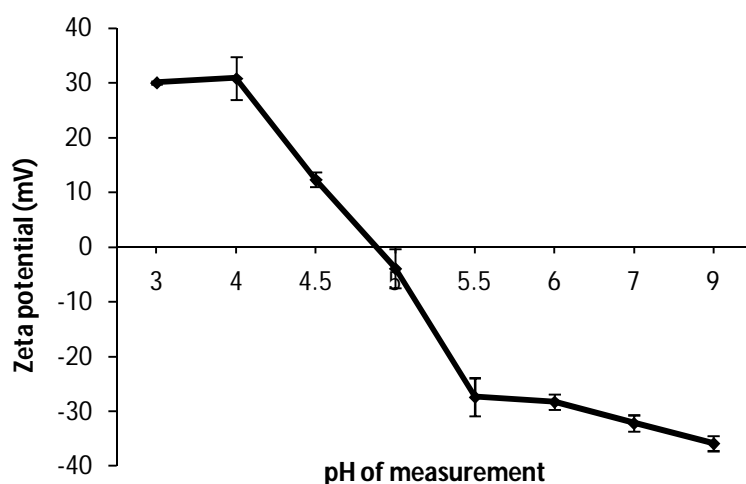
Figure 3.13. Zeta potential of gelatin nanoparticles determined at different pH values.

3.4.7. Extent of Crosslinking of Gelatin Nanoparticles

The extent of crosslinking in glutaraldehyde crosslinked gelatin nanoparticles was determined by trinitro-benzenesulphonic acid (TNBS) assay. It is based on the estimation of primary amino groups in crosslinked and uncrosslinked particles. TNBS reacts with the primary amino groups under mild alkaline conditions to produce an unstable Meisenheimer complex. Subsequent acidification rapidly converts the orange unstable product to a yellow stable trinitrophenol derivative, which has maximum absorbance at approximately 349 nm.

The absorbance of uncrosslinked and crosslinked gelatin nanoparticles is correlated with the number of free amino groups present. The result shows that gelatin nanoparticles crosslinked with 0.5 mg GTA/1 mg gelatin exhibited around 72.5 ±0.12% crosslinking extent (as shown in table 3.3).

Table. 3.3. The extent of crosslinking in gelatin nanoparticles prepared by standard recipe.

Gelatin Nanoparticles	Size in *nm* ± S.Dev	Crosslinking %
Uncrosslinked	231.4 ± 6.1	0
Crosslinked	225.5 ± 7.8	72.5 ± 0.12%

3.4.8. Drug Loading and Release

The entrapment efficiency (E.E) increases with increase in molecular weight. FITC-dextran of 42 kDa showed around 70% E.E, while around 90% entrapment was observed for 167 kDa FITC-dextran. The maximum entrapment was seen for 580 kDa FITC-dextran i.e., ca. 100%, as shown in Figure 3.14. The low entrapment of small molecular weight FITC-dextran is probably due to escape of loosely entrapped FITC-dextran during washing. On the other hand high Mw bigger FITC-dextran molecules are possibly entangled firmly within the nanoparticles matrix, hence resist the leakage during washing step thus showing higher entrapment. Such an increase in entrapment due to increase in molecular weight of FITC-dextran was observed by other investigators as well [152].
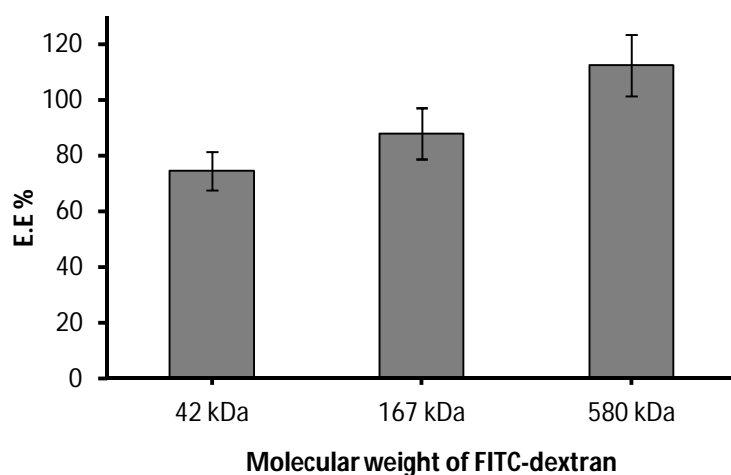

Figure 3.14. Effect of molecular weight of FITC-dextran on entrapment efficiency of gelatin nanoparticles.

The release profile of different molecular weight FITC-dextran is given in Figure 3.14. Which shows that smaller molecular weight FITC-dextran exhibited faster release compared to higher molecular weight FITC-dextran. For instance 42 kDa FITC-dextran showed around 10% release in the initial half hour. Followed by a continuous release for 144 hour where almost half of the drug is released. In case of 167 kDa FITC-dextran, just 10% release was observed in 8 hours. However the release reached to a plateau at 20% in 72 h. Similar slow release was also exhibited by 580 kDa FITC-dextran. This slow release of high molecular weight dextran is not due to involvement of the drug in the crosslinking process, since dextran is a polysaccharide lacking primary amino groups and hence does not participate in the chemical crosslinking process [144]. Most likely there exists a molecular weight cutoff point for diffusion from the nanoparticles matrix. Possibly, 42 kDa is below that limit, hence a continuous release is observed. Contrarily, 167 kDa and 580 kDa seem to be big enough that free diffusion of FITC-dextran molecules from the nanoparticles matrix is hindered. This is reflected in almost similar release profile of 167 kDa and 580 kDa FITC-dextran, where a plateau at 20% indicates no further release of FITC-dextran.
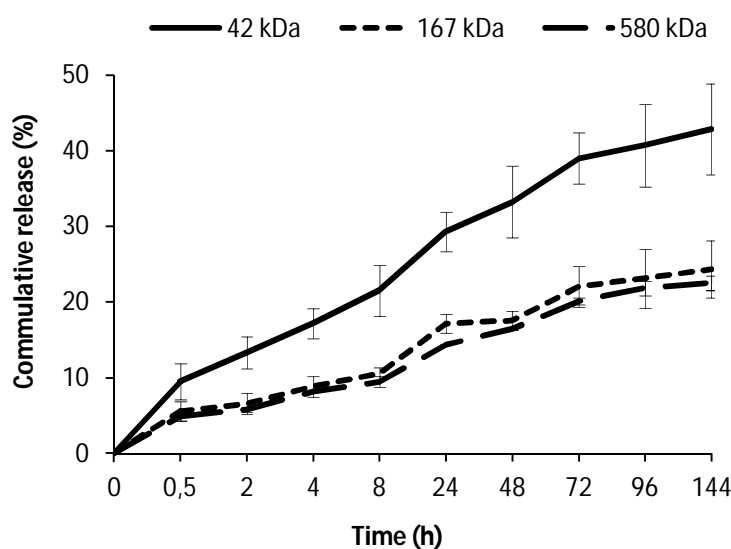
Figure 3.14. Effect of FITC-dextran molecular weight on release from gelatin nanoparticles

The trypsin induced destruction of gelatin network and hence dissolution of particles is evident from the turbidity profile in Figure 3.15. This can be correlated to an abrupt release of about 80% of the loaded FITC-dextran within an hour after tryptic digestion. Gelatin being a protein is composed of amino acids; Ala-Gly-Pro-Arg-Gly-Glu-4Hyp-Gly-Pro [153]. This makes it prone to tryptic digestion. Likewise, trypsin, an endopeptidase which operates by preferentially cleaving the carboxyl side of lysine and arginine residues, i.e. hydrolyzes specific peptide linkages of gelatin. Thus liberating the FITC-dextran encapsulated within the gelatin matrix [154]. It can be concluded that tryptic digestion breaks the crosslinked gelatin network, hence leading to free diffusion of the remaining FITC-dextran from the nanoparticles.
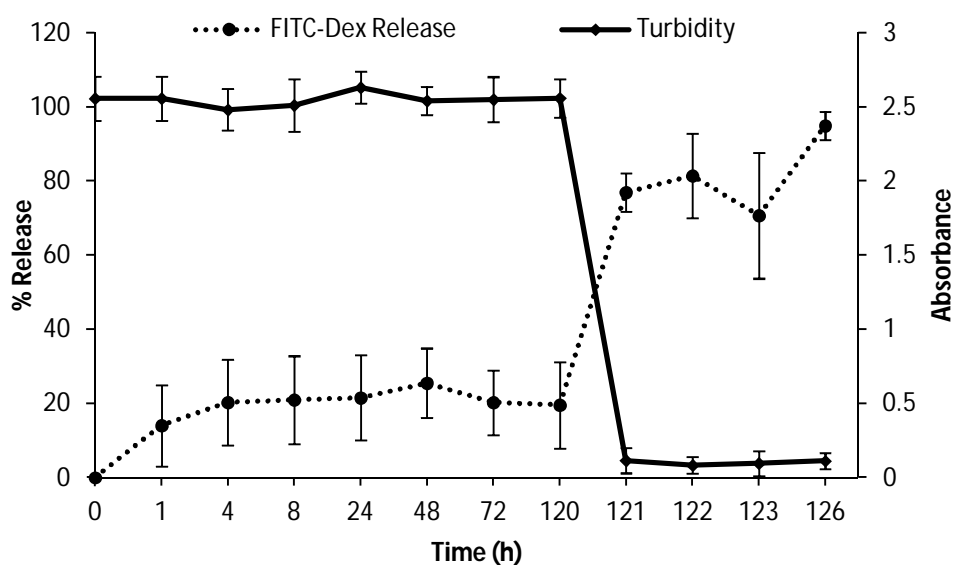
Figure 3.15. In vitro release profile of FITC-dextran and turbidity of gelatin nanoparticles in PBS (pH 7.4), before and after addition of digestive enzyme.

3.4.9. Cytotoxicity Studies

MTT assay was used to assess the cytotoxicity of gelatin nanoparticles. Four different concentrations of gelatin nanoparticles were tested. The results show no substantial cytotoxicity of SKOV-3 and L929 cells incubated with gelatin nanoparticles for 24 hours (Figure 3.16). Thus it can be concluded that the nanoparticles are biocompatible and do not possess any significant toxicity *in vitro*.

Though the charge on surface of gelatin nanoparticles is dependent on the pH of the medium, at neutral or physiological pH the particle are negatively charged (mentioned before). This is a well-known fact that anionic nanoparticles are more compatible with the cell surface than cationic particles [155]. Hence, the biocompatibility of gelatin nanoparticles can be attributed to the negative surface of nanoparticles.
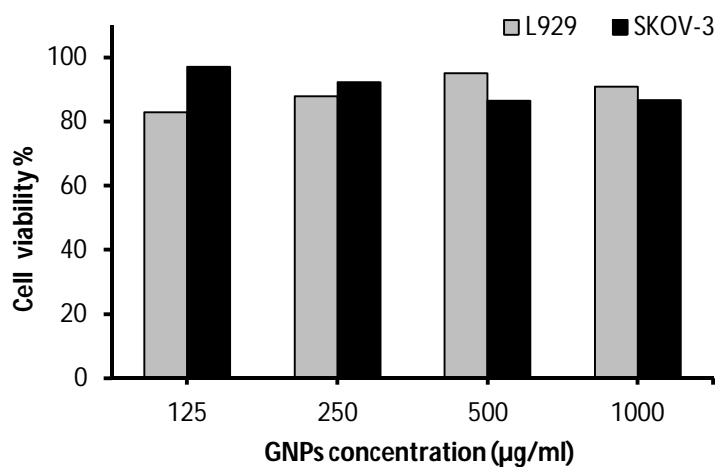
Figure 3.16. Cytotoxicity analyses results by MTT assay after 24 hour incubation with gelatin nanoparticles.

3.5. Conclusion

Gelatin nanoparticles (200-350 nm) could be effectively prepared by nanoprecipitation using poloxamer 407 and poloxamer 188 as stabilizers and ethanol, acetone and acetonitrile as nonsolvent. Particles stability was greatly affected the presence of stabilizers and the respective stabilizer concentration. A minimum of 7% stabilizer concentration was necessary to prevent aggregation during the crosslinking process. The size can be tuned by either varying gelatin concentration in the solvent phase or changing the nonsolvents. However, too high concentration of gelatin led to big visible precipitates. With similar gelatin concentration, two-step desolvation produced smaller particles compared to nanoprecipitation. Additionally, increase in gelatin concentration increased the homogeneity of nanoparticles in case of two-step desolvation. FITC-dextran as a model hydrophilic macromolecule can be effectively loaded into gelatin nanoparticles via nanoprecipitation. The release was dependent on the molecular weight. Faster and continuous release was exhibited by smaller FITC-dextran and vice versa. Total release was possible after digestion with trypsin. No cytotoxicity was observed on L929 and SKOV-3 cell lines. Thus it can be concluded that the system provides a good opportunity for the delivery of macromolecular drugs.

4. Surface Modification of Gelatin Nanoparticles with Polyethylenimine

4.1. Abstract

Gelatin nanoparticles are negatively charged at neutral pH, independent on the type of bulk gelatin used. Since most of the amino groups are crosslinked during the process of nanoparticles preparation. For surface loading of negatively charged substances e.g., oligonucleotides and plasmid DNA, the nanoparticles surface is rendered cationic by introduction of positively charged moieties such as quaternary amines. This is usually done by covalent modification of gelatin before or after nanoparticle formation. This study focuses on cationization of nanoparticles surface without covalent modification. Polyethylenimine (PEI) was physically adsorbed onto the anionic surface of gelatin nanoparticles. The effect on size, PDI, and zeta potential of GNPs after coating with different volume ratio of PEI was studied. The size of crude GNPs increased from 200 nm to around 325 nm with a PDI of around 0.3 after coating with PEI. The size of GNPs after dispersing in PEI solution before centrifuged was around 225 nm which increased to around 350 nm after washing steps. pH of coating solution above 4 was important for successful coating. Uncoated GNPs had a zeta potential of -20 mV while that of PEI coated particles was in the range of shows +45 to +50 mV, regardless of volume of PEI.

4.2. Introduction

Commercially two different types of gelatin (type A & type B) are available depending on the method of collagen hydrolysis. Type A gelatin is obtained by acid hydrolysis of gelatin. Acid processing barely affects the amide groups of glutamine and asparagine, resulting in higher isoelectric point (IEP), i.e., 7-9 [24]. On the other hand, alkaline treatment hydrolyses asparagine and glutamine to aspartate and glutamate, respectively. Thus it possesses a greater proportion of carboxyl groups, rendering it negatively charged and lowering its IEP to 4.5-6.0) [34]. However, contrary to the bulk gelatin, gelatin nanoparticles are negatively charged at neutral pH, independent of the type of gelatin [63].

Therefore, enabling the surface of GNPs to adsorb negatively charged substances like oligonucleotide, plasmids, small interfering (si) RNA, locked nucleic acid (LNA) nucleotide etc., would profit from introducing positively charged moieties such as quaternary amines. This is usually done by covalent modification, which can be done before or after nanoparticle formation. In most of the cases reactive linkers like succinimidyl 3-(2-pyridyldithio) propionate (SPDP), succinimidyl 4-(p-maleimidophenyl) butyrate (SMPB), 1-Ethyl-3-(3-dimethylaminopropyl) carbodiimide hydrochloride (EDC), and dicyclohexyl carbodiimide (DCC) are used [156]. Zwiorek et al [133] and Ziellis et al [132] modified the free carboxylic groups of gelatin nanoparticles with a quaternary amine (cholamine) using EDC as linker. The particles are then incubated with DNA or plasmid DNA solution in order to bind the negatively charged DNA electrostatically [157].

The aim of the present work was to formulate and optimize primary amine modified gelatin nanoparticles. Polyethylenimine was electrostatically deposited on the negatively charged surface of gelatin nanoparticles. The nanoparticles were characterized for size, zeta potential, morphology, and cytotoxicity.

4.3. Experimental

4.3.1. Materials

Gelatin B bloom75 from bovine skin, pluronic F-68 (poloxamer 188), glutaraldehyde (GTA) and polyethylenimine (PEI) were obtained from Sigma-Aldrich, Munich Germany. Acetone was obtained from Merck Millipore, Darmstadt, Germany. Millipore water was used throughout the experiments.

4.3.2. GNPs by Nanoprecipitation

20 mg gelatin was dissolved in 1 ml of millipore water at 50 °C. It was then added drop wise to 15 ml of acetone containing Pluronic® F-68, and subsequently crosslinked with 0.5 ml glutaraldehyde solution (2% w/v). The nanoparticles suspension was stirred overnight for crosslinking.

4.3.3. Coating of GNPs with PEI

Coating of Crude GNPs

Gelatin nanoparticles after overnight crosslinking were diluted with 15 ml water and added to 60 ml PEI solution (2%). After 4 hours of stirring the particles were washed three times by centrifugation (10000×g, 15min) and redispersed in water.

Coating of Centrifuged GNPs

Gelatin nanoparticles after overnight crosslinking were centrifuged at 10000×g for 15min. The pellet was re-dispersed in 30 ml water and added to 60 ml PEI solution (2%). After 4 hours of stirring the particles were washed three times using centrifugation (10000×g, 15min) and redispersed in water.

4.3.5. Size and Zeta Potential of Nanoparticles

The size (z-average mean) and zeta potential of the nanoparticles were analyzed by Zetasizer nano-ZS (Malvern Instruments Ltd., Worcestershire, UK). The nanoparticles suspension was approximately 100 times diluted with de-ionized water at 25°C before measurement. Each sample was analyzed in triplicate.

To see the effect of PEI solution volume, 1 ml of GNPs suspension was added to different volumes (0.25 ml, 1 ml, 2 ml and 4 ml) of PEI solution. Additionally the size and zetapotential was also measured at different centrifugation steps.

The pH of PEI solution was varied between 2-11 to see the effect on size and zetapotential.

4.3.6. Morphological Analysis

TEM (Transmission Electron Microscopy) samples were prepared at ambient condition; a drop of nanoparticles suspension was placed on a TEM grid, stained with 0.1% uranyl acetate and visualized after drying using a JOEL model JEM-2010 instrument (JEOL GmbH, München, Germany).

4.3.7. MTT Assay

Particles were tested for *in vitro* toxicity using MTT assay . This is an assay used to quantify metabolically active cells colorimetrically. Mitochondrial succinate dehydrogenase reduces MTT to a dark purple colored formazan product, which after dissolution in DMSO is quantified spectrophotometrically as a measure for cell viability.

One of the most intensively used cell line for cytotoxicity studies i.e., L929 murine fibroblast, was used. Besides this, SKOV-3 human ovarian carcinoma cell line were used as representative for human cancer.

Nanoparticles suspension was serially diluted with culture medium. 100 µg/ml of cell culture medium containing nanoparticles (i.e., 750 µg/ml, 187.5 µg/ml and 93.75 µg/ml) was added into each well of a 96 well plate containing a density of 1×10^4 cells per well. After incubation at 37ºC for 24 hours 100 µL of cell culture medium containing MTT was added to each well and incubated for further four hours. Then the cell culture medium was removed. Formazan product was dissolved in 100µl DMSO per well and measured with a spectrophotometer at 495nm. Cells without any treatment were used as negative control and TritonX100 was used as positive control. The cell viability was calculated using the following equation.

$$Cell\,Viability\,(\%) \ = \ \frac{(Sample\,\text{-}\,Positive\,control)}{(Negative\,control\,\text{-}\,Positive\,control)} \times 100$$

4.4. Results and Discussion

Gelatin is a polyelectrolyte containing both positive and negative charged groups. The net charge depends on the solution pH. During nanoprecipitation sequential intermolecular charge neutralization in gelatin molecules leads to nanoparticles formation. Crosslinking is an inevitable step in preparation of gelatin nanoparticles. Crosslinkers like glutaraldehyde, formaldehyde links primary amino groups giving a stable solid structure to the particles. It must be realized that the crosslinker does not crosslink all the primary amino groups (evident from the 72% crosslinking degree, discussed in chapter 3). Thus gelatin nanoparticles contain both positively and negatively charged groups, depending on the pH one type of groups predominate the others thus influence the overall surface charge of the particles. At lower pH values carboxylic groups are not deprotonated, thus GNPs are positively charged, and vice

versa at higher pH values. Hence, the effect of pH on the zeta potential is evident from Figure 4.1.
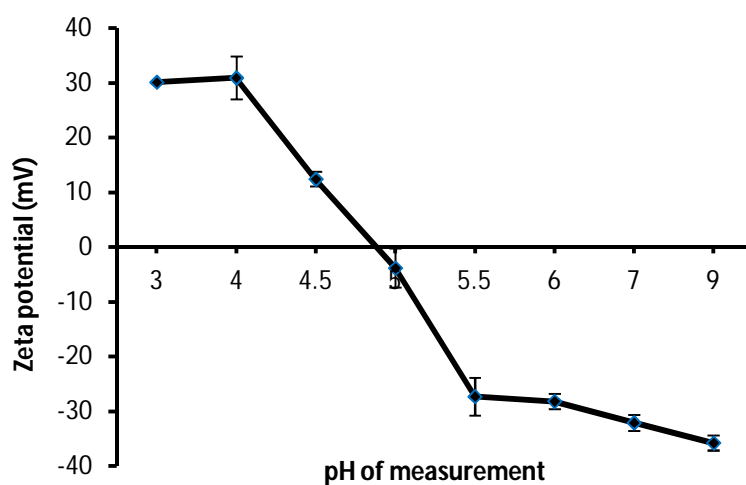
Figure 4.1. Zeta potential of gelatin nanoparticles measured at different pH values.

Hence our strategy was to deposit PEI (a branched poly-anion) on the negatively charged surface of gelatin nanoparticles in neutral condition. Gelatin nanoparticles were prepared by nanoprecipitation technique. The proposed electrostatic binding of PEI to the nanoparticles surface is schematically shown in Figure 4.2.
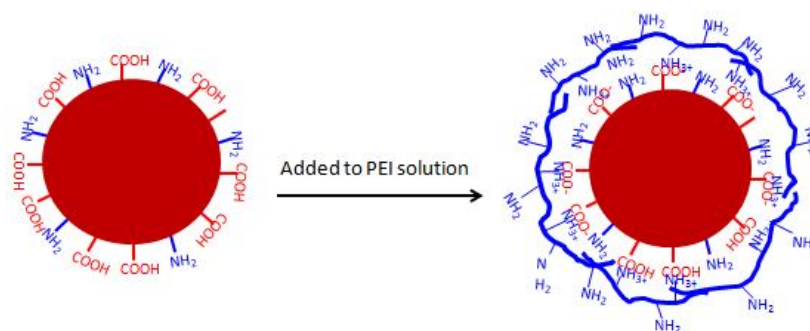
Figure 4.2. Schematic illustration of PEI deposition onto the surface of gelatin nanoparticles

4.4.1. Physicochemical Characterization

Effect of GNPs to PEI Solution Volume Ratio

GNPs were coated with PEI preparing different volume ratios of PEI (2% solution). As shown in Figure 4.3(a), the size of GNPs is around 250 nm after centrifugation, which increased to around 400 nm when coated with PEI. On the other hand, in case of crude GNPs (without centrifugation) the effect of PEI coating on size was comparatively less pronounced, i.e., the size increased from 200 nm to 325 nm after PEI coating (GNPs/PEI volume ratio 1/4 and 1/2). This might be because of the Poloxamer which was used for preparation of GNPs providing steric hindrance during coating and easy redispersion after centrifugation. As a result, the crude particles have lower PDI values compared to centrifuged particles, after PEI coating.

Figure 4.3(b) shows the zeta potential values. The uncoated GNPs had a zeta potential of -20 mV while that of PEI coated particles was in the range of +45 to +50 mV. the PEI volume does not have any effect on zeta potential. This means that the surface of gelatin nanoparticles is fully coated with PEI, independent of the PEI volume.


(a)   (b)
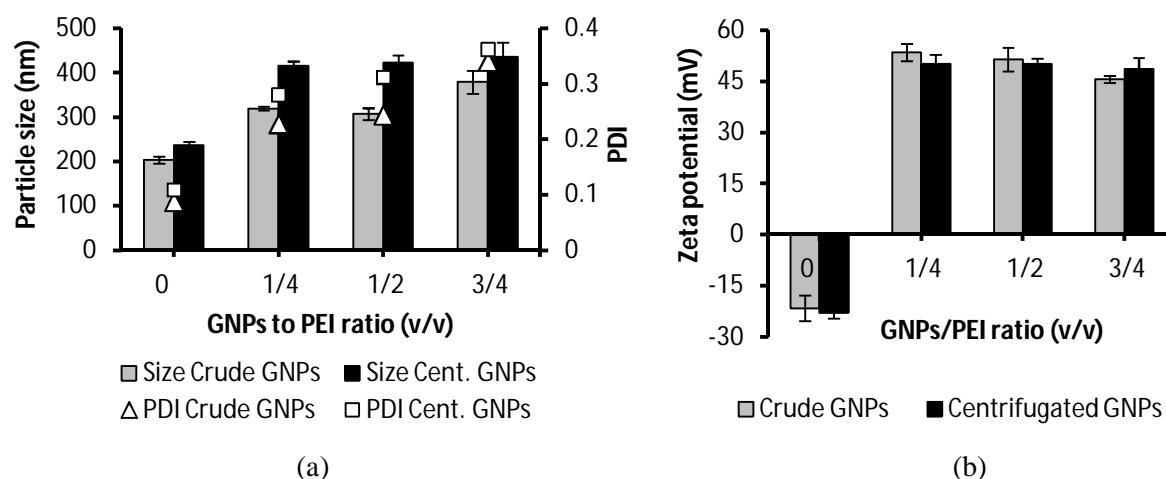
Figure 4.3. Effect of Gelatin/PEI volume ratio on the size, (a) and zeta potential (b) of nanoparticles.

Effect of Centrifugation Step

It was important to see the effect of each centrifugation step on the particles. The size and zeta potential was measured at every centrifugation step.

A slight increase in size and PDI was seen for uncoated particles after first centrifugation. However, the size remained consistent in the range of around 250 during centrifugation-redispersion cycles. On the other hand, the size of PEI coated particles was substantially increased after each consecutive centrifugation step. For example the size of PEI coated GNPs was around 224 nm before centrifugation, however an increase of around 50 nm was observed after first centrifugation. Similarly, second and fourth centrifugation step increased the size by 80 nm and 150 nm, respectively, as shown in Figure 4.4(a). Thus it can be said that the size did not increase primarily due to coating. Rather the centrifugation redispersion step was mainly responsible for the size increase.

The reason for increase in size after PEI coating was not clear, however, size increase after each consecutive step of centrifugation suggests that the increase might be due to interparticular aggregation during centrifugation-redispersion cycle. However, size calculated from SEM and TEM images (section 4.4.2) showed literally bigger particles with uniform sizes, this excludes the possibility of size increase due to interparticular bridging during centrifugation. Perhaps, it might be due to the diffusion of PEI within the nanoparticle matrix which may alter the overall swelling of particles. Additionally, the PEI shell around particles may also be responsible for increasing the hydrodynamic radii of particles
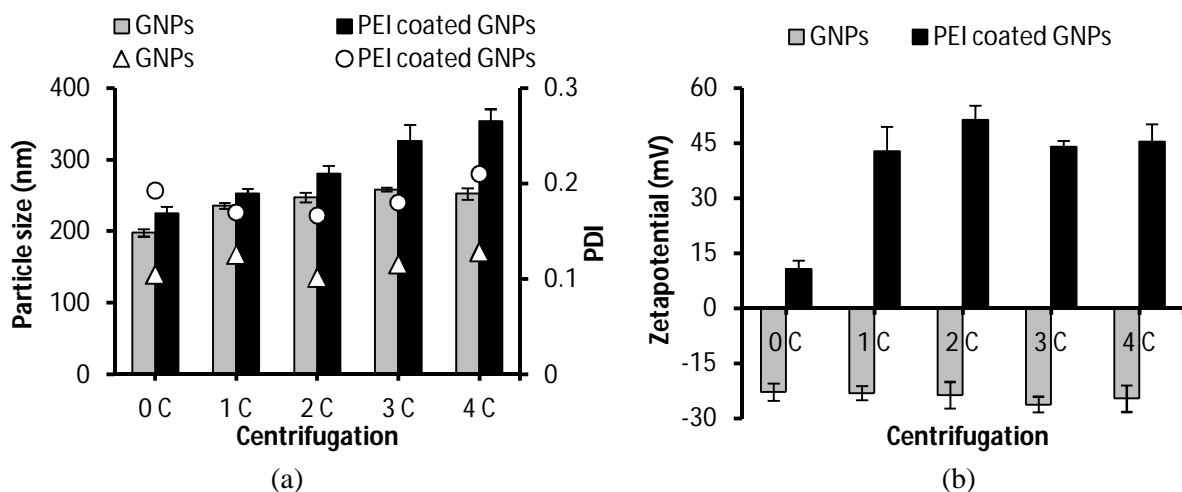
Figure 4.4. Effect of centrifugation on the (a) size and (b) zetapotential of GNPs and PEI coated GNPs.

The zeta potential of uncoated GNPs remained around -20 mV to -25 mV, while PEI coated GNPs showed zeta potential +10 mV before centrifugation and around +45 mV to +50 mV after washing, as shown in Figure 4.4(b).

Effect of PEI Solution pH

It is well known that pH has an influence on the electrostatic interaction of weak polyelectrolytes such as PEI [158]. Therefore, the pH of the PEI solution was systematically varied from 2 to 11 to study the influence on coating onto GNPs. The effect on size and zeta potential was investigated. GNPs coated at pH below 4 could not be re-dispersed after centrifugation. Hence, a substantial increase can be seen in the size and PDI. However, at pH 4 the particles showed comparatively less increase in size. Nevertheless, PDI value is still considerably high (i.e., around 0.4), as shown in Figure 4.5(a). The increase in PDI is probably due to inefficient coating of the nanoparticles, as a result big agglomerates are formed during the centrifugation steps.

It should be noted that, though PEI is a polycation, but the surface charge of GNPs depends on the pH (Figure 4.1). At lower pH GNPs are positively charged and may prevent adsorption

60

of PEI to the surface, which is evident from the zeta potential values, shown in Figure 4.5(b). Normally, GNPs after efficient PEI coating are positively charged (Figure 4.3 and 4.4), but here we see that the particles coated at pH <4 are negatively charged even after coating step. Hence, it can be assumed that, at pH <4 the GNPs could not be coated with PEI.

The possible coating of GNPs at pH 4 is exhibited as a slightly positive zeta potential (7.6 mV). Perhaps, though at pH 4 the GNPs surface is predominantly cationic, however some of the carboxylic groups might be de-protonated. Hence, several PEI molecules might be adsorbed to the surface, thus changing the overall zeta potential of the particles.
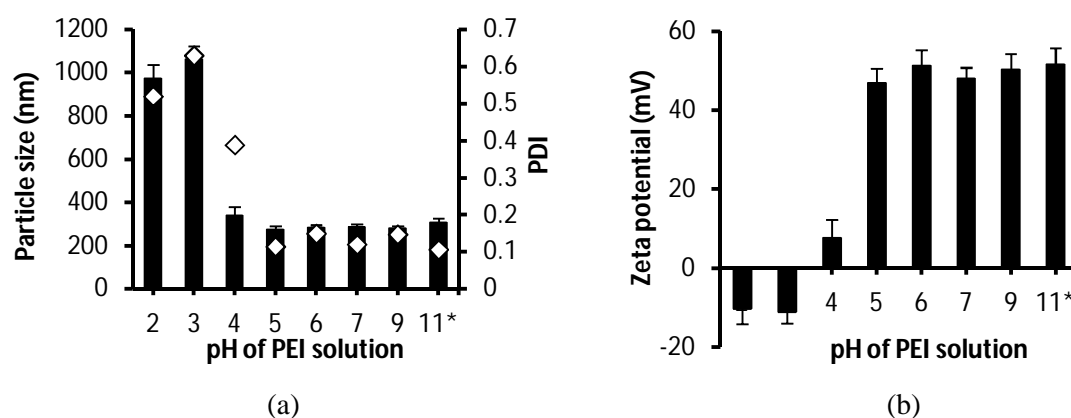

Figure 4.5. Effect of pH of PEI solution on the (a) size and (b) zetapotential of PEI coated GNPs.

4.4.2. Morphological Characterization

SEM and TEM images reveal spherical shape of particles, however the size of PEI coated particles are fairly bigger than that of uncoated GNPs (Figure 4.6).
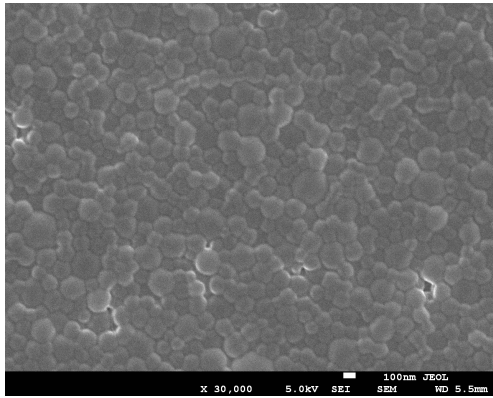
(a)
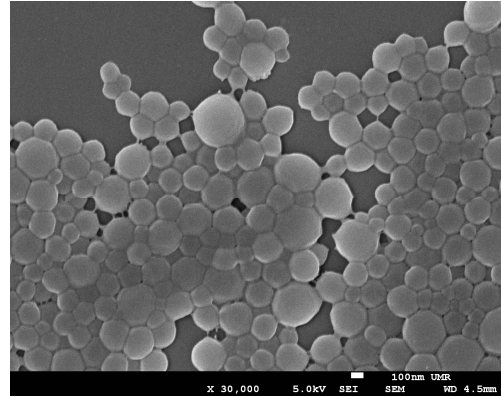
(b)
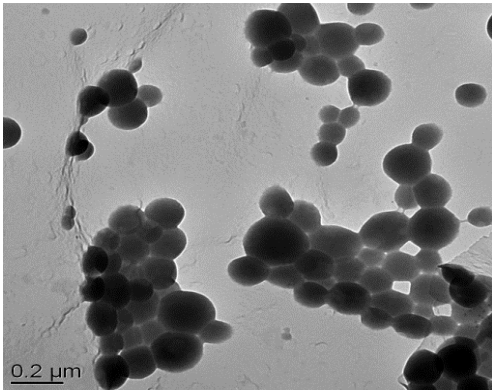
(c)
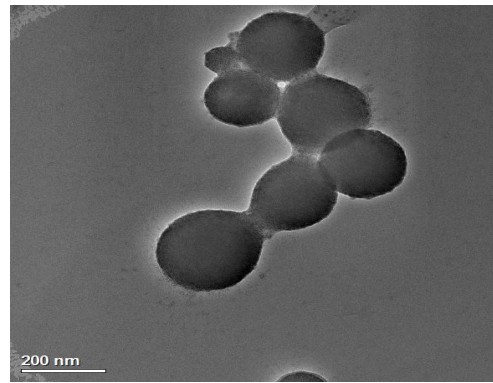
(d)

Figure 4.6. (a) SEM micrographs of uncoated GNPs and (b) SEM micrographs PEI coated GNPs, (c) TEM micrographs of uncoated GNPs and (d) TEM micrographs PEI coated GNPs.

The size of particles calculated using imageJ® from SEM images show an increase of around

70 nm in the size of PEI coated particles compared to that of uncoated GNPs (Table 4.1).

Table. 4.1 Size of nanoparticles from SEM images

Samples	*Size in (nm) ±STDEV
GNPs	182.6 ± 49.2
PEI coated GNPs	256.2 ± 65.8

*50 particles analyzed using ImageJ®

The increase in size cannot be assumed solely due to PEI shell, since a possible shell found on

some of the particles is less than 15 nm (Figure 4.7), which is an observable trend for PEI

shell around nanoparticles [159]. However, we additionally presume PEI might diffuse within

nanoparticles matrix, hence may alters the mechanical properties and swelling properties of

nanoparticles. Consequently, the size of PEI coated GNPs appear larger than that of uncoated ones.

<div align="center">(a)   (b)</div>
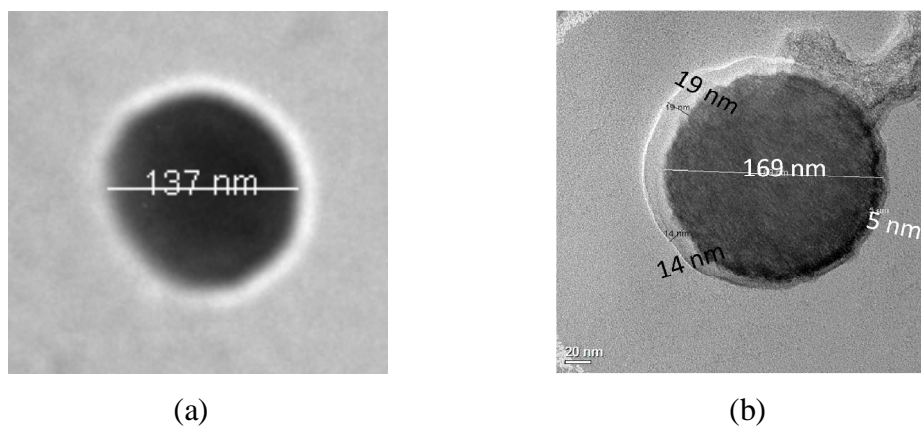
Figure 4.7. TEM micrographs of (a) uncoated GNPs and (b) PEI coated GNPs.

4.4.3. Cytotoxicity Evaluation

MTT assay shows that cytotoxicity of PEI coated GNPs decreased with the decreasing concentration of particles. PEI coated particles were highly toxic in the concentration up to 275 µg/ml, while at lower concentration around 188 µg/ml around 50% of the cells were viable. The cell viability was above 80% when 94 µg/ml particles concentration was used, as shown in Figure 4.8.

As explained in chapter 3, crosslinked gelatin nanoparticles are non toxic up to 1 mg/ml concentration. However, when coated with PEI, the particles turn out to be toxic. Obviously this is due to the extreme cytotoxic behavior of PEI. PEI being adsorbed on the surface may disrupt the cell membrane leading to immediate cell death. Additionally, after internalization of the particles PEI may disrupt the mitochondrial membrane leading to delayed cell death.
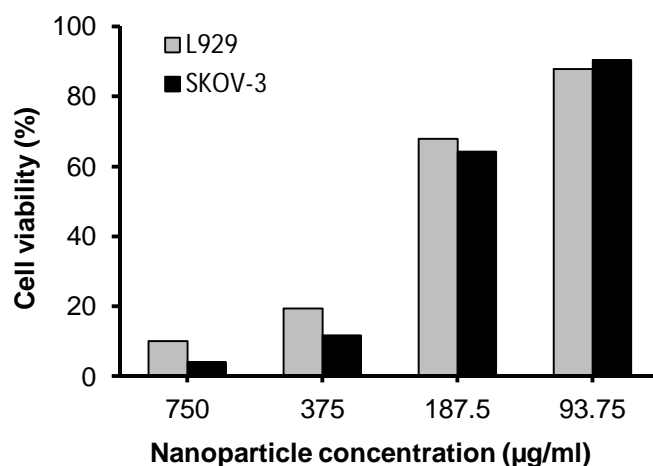
Figure 4.8. Cytotoxicity analysis results by MTT assay after 24 hours incubation with PEI-coated gelatin nanoparticles.

4.5. Conclusion

This study presents that the surface of gelatin nanoparticles can be modified by PEI without the use of covalent modification. PEI coating makes the surface of gelatin nanoparticles positively charged. The size and PDI is increased after coating. The volume of PEI solution cannot be correlated with the size increase, though PDI is higher with lower PEI volume. pH of coating solution must be above 4 for efficient coating. However, PEI coating renders the particle cytotoxic.

5. Stabilization of Gelatin Nanoparticles without Crosslinking

Parts of this chapter are submitted for publication:

5.1. Abstract

Gelatin nanoparticles have intensively been reported to have the potential of being a promising nanocarrier for many therapeutic agents. However, the necessity of crosslinking for stabilization is a serious constraint for the application of gelatin nanoparticles for proteinaceous drugs. This chapter presents an alternative approach to crosslinking. The structural integrity of gelatin nanoparticles was kept intact by coating them with synthetic polymers forming hybrid nanospheres. For preparation, a hybrid technique of nanoprecipitation-emulsion solvent evaporation was employed. The inefficient entrapment and substantial burst release proved PLGA not a suitable polymer for this purpose. While Eudragit® E 100 showed promising result. However, its concentration was found to be critical for morphology and effective entrapment of GNPs. Nanospheres produced with lower Eudragit® E 100 concentration showed spherical depressions of around 90 nm on the surface (termed as porosity here). The porosity decreased with increase in Eudragit® E 100 concentration, which in turn improved gelatin entrapment. Additionally, a raise in Eudragit® E 100 concentration decreased the initial burst release of gelatin from the particles. The final size of nanospheres was mainly determined by homogenization speed. This study is the first step to extend the use of gelatin nanoparticles for the delivery of arbitrary biologicals.

5.2. Introduction

Hydrophilicity is an important characteristic for biocompatibility of gelatin, but it also imparts drawbacks in its use for drug delivery. Gelatin-based devices rapidly swell upon contact with biological fluids, thus lose their structural integrity and release their contents abruptly [160, 161]. Therefore, for improved mechanical properties and extended release, crosslinking is an inevitable step for gelatin based delivery systems. Gelatin nanoparticles are usually stabilized by crosslinking with glutaraldehyde [162], glyoxal [94], carbodiimide [148], Genipin [163], transglutaminase [164], and reduced sugars [165]. A crosslinker links gelatin chains to each other [166]. Particles maintain their structural integrity in aqueous environment, since the gelatin chains are tied together by strong covalent bonds.[167] However, due to the generalized reaction of crosslinker with reactive groups (mainly -NH$_2$), loading of proteinaceous drugs in gelatin nanoparticles before crosslinking with no involvement in crosslinking, seems to be impossible. This impedes efficient loading and application of gelatin nanoparticles for delivery of all kinds of macromolecular drugs.[27]

Therefore, it is worthwhile introducing an alternative approach for gelatin nanoparticles stabilization without crosslinking, in order to protect their structural integrity. This could be an important aspect for application and release of drugs from the gelatin matrix. We proposed an alternative stabilization approach without using crosslinker. Gelatin nanoparticles were entraped in polymeric nanospheres using the concept of nanoparticles in nanospheres (NiNOs). PLGA and Eudragit E100 were employed as polymers for preparation of nanospheres. The effect of different parameters and the physicochemical properties of nanosphere preparation were investigated to get optimum formulation. Gelatin nanoparticles in PLGA nanospheres and Eudragit® E 100 nanospheres, are addressed as GP-NiNOs and GE100-NiNOS, respectively. A dual technique of nanoprecipitation-emulsion solvent

evaporation was employed. Gelatin nanoparticles were produced by nanoprecipitation, which were subsequently entrapped in Eudragit® E 100 (E.100) nanospheres by emulsion solvent evaporation technique. Dynamic light scattering (DLS) studies were performed to ascertain critical factors affecting the size of nanoparticles. Scanning electron microscopy (SEM) measurements were done for size and morphological analysis. Gelatin release from the particles was used as a parameter to determine the effective entrapment of gelatin NPs in nanospheres and hence the integrity of the E.100 shell.

5.3. Experimental

5.3.1. Materials

Gelatin B bloom75 from bovine skin, was obtained from Sigma-Aldrich, Munich, Germany. Dimethyl sulfoxide (DMSO) and dimethyl formamide (DMF) were supplied by Carl Roth GmbH, Karlsruhe, Germany. Acetone and ethyl acetate were obtained from VWR-International, Darmstadt, Germany. PBS ready mix was used to prepare phosphate buffered solution. Mowiol® (PVA) was provided by Kuraray Europe GmbH, Hattersheim, Germany. QuantiPro® BCA kit was from Sigma-Aldrich, Munich, Germany. Eudragit® E100 was provided by Evonik Industries, Darmstadt, Germany. Millipore water with a resistivity of 18.2 MΩ·cm was used throughout the experiments.

5.3.2. Preparation of Gelatin Nanoparticles

40 mg gelatin was dissolved in 1.0 ml DMSO (2% w/v). 250µl of gelatin solution was added drop wise to 1.5 ml acetone-DMF mixture (1:1) while stirring.

With an intention to get smaller monodisperse particles, different gelatin concentration (4-6%), water as solvent phase, and acetone as nonsolvent phase were investigated. The

objective was to produce gelatin nanoparticles small enough to be entrapped in E.100 nanospheres in a subsequent step. Based on the results, 4% Gelatin in DMSO as solvent phase and acetone-DMF (1:1) mixture as nonsolvent phase was chosen for the typical procedure.

5.3.3. Entrapment of Gelatin Nanoparticles in Polymeric Nanospheres

GNPs in PLGA nanospheres (GP-NiNOS)

GNPs were produced using standard procedure. 250µl of stabilizer solution was added to gelatin nanosuspension, and was subsequently added to PLGA solution (2% w/v in ethyl acetate). The organic phase containing GNPs was slowly dropped into 10 ml PVA (2%) solution. The crude emulsion was homogenized using Ultra-Turrax at 15,000 rpm and subsequently diluted with 20 ml water. After an overnight stirring to evaporate ethyl acetate GP-NiNOS were obtained using centrifugation at 10000×g for 15 minutes and freeze dried. Similarly blank PLGA nanospheres for comparison were prepared without gelatin.

In order to vary the droplet size and in turn the nanosphere size, different homogenization speeds (i.e. 5000, 10000, 15000 rpm) were used. PLGA concentration was kept constant at 2%. Furthermore, in different set of experiments PLGA concentration was varied (1.75%-2.5%), while keeping the homogenization speed constant at 15,000 rpm.

GNPs in E.100 nanospheres (GE100-NiNOS)

Gelatin nanosuspension was added to E.100 solution (2% w/v in ethyl acetate). It was dropped slowly into 10 ml PVA (2%) solution. After 30 minutes of vigorous stirring the crude emulsion was homogenized using Ultra-Turrax at 15,000 rpm. Subsequently, about 20 ml water was added. The system was stirred overnight to evaporate ethyl acetate. GE100-NiNOS were isolated by centrifugation at 10,000×g for 15 minutes and resuspended in distilled water before freeze drying.

Blank E.100 nanospheres for comparison were prepared with the same procedure, without addition of gelatin in DMSO.

The size of droplet and hence the final size of nanoparticles is dependent upon the emulsification step. Therefore, keeping E.100 concentration constant (2%), the effect of homogenization speed (i.e. 5000, 8000, 15000 rpm) was studied.

Furthermore, the effect of E.100 concentration in ethyl acetate was also investigated by varying the concentration between 2 to 6% w/v.

5.3.4. Measurement of Particle Size and Zeta Potential

The size (z-average mean) and zeta potential of the nanoparticles were analyzed by dynamic light scattering and laser Doppler anemometry, respectively, using a Zetasizer nano-ZS (Malvern Instruments Ltd., Worcestershire, UK). The nanoparticles suspension was approximately 100 times diluted with distilled water at 25°C before measurement. Each sample was analyzed in triplicate.

5.3.5. Morphological Characterization

Scanning Probe Microscopy (SPM)

The freshly prepared nanosuspension was centrifuged and washed three times with water and later resuspended. A drop of nanosphere suspension was placed on a freshly cleaved mica sheet (Plano GmbH, Wetzlar, Germany) and subsequently dried by overnight evaporation. SPM imaging was performed using a Bioscope® (DI Digital Instruments, Bruker corporation, Billerica, USA) in tapping mode, using a cantilever with a spring constant of 40 N/m (Anfatec Instruments AG, Oelsnitz, Germany) and a scan rate of 0.5 Hz under ambient conditions. Raw data was processed by flattening algorithm to remove background slopes, and analyzed by

Nanoscope SPM software.

Scanning Electron Microscopy (SEM)

For sample preparation, a drop of the washed nanosuspension was dropped onto a silicon wafer mounted on a metal hub using carbon adhesive tape. Samples were dried by overnight evaporation under ambient conditions. Samples were coated with gold, in an argon atmosphere using Q150RES sputter coater (Quorum Technologies Ltd. Laughton, UK). SEM images were obtained on an EVO HD microscope (Carl Zeiss Microimaging, GmbH, Jena, Germany).

Surface Analysis of GE100-NiNOS

In the initial experiments it was observed that the GE100-NiNOS show spherical depressions on the surface. Here termed as "porosity" of the particles. These holes were analyzed in terms of porous particle fraction (i.e. % of all particles), as well as particles to pores surface ratio (PPSR), as follows.

About 60-70 nanoparticles were manually observed for porous particle fraction. It was calculated using the following equation:

$$\text{Porous Particles (\%)} = \frac{\text{Number of Porous Particles}}{\text{Number of Observed Particles}} \times 100$$

For PPSR, the SEM images of different batches (i.e. 2-6% E.100 concentration produced with 8000 rpm homogenization speed) were analyzed. The surface area of particles (i.e. $4\pi r^2$) and the pores area was calculated using imageJ® software. The PPSR was calculated using the following equation:

$$\text{Particles to pores surface ratio (PPSR)} = \frac{\text{Sum of Particles Surface Area}}{\text{Sum of Area of Pores}}$$

71

5.3.6. Measurement of Gelatin Entrapment and Release

In order to estimate how efficiently gelatin nanoparticles have been entrapped within the nanospheres, percent gelatin entrapment was used as a quantitative parameter. It was determined by a bicinchoninic acid protein (BCA) assay using QuantiPro® BCA kit (Sigma-Aldrich, Munich, Germany). Briefly, 10 mg of freeze dried nanospheres were dispersed in 1 ml HCl (0.1 N). After an hour of dissolution a clear solution was obtained, which was neutralized by 1 ml NaOH (0.1 N). The volume was made up to 10 ml and centrifuged at 24,000×g for 15 minutes. 0.1 ml samples were filled into a 96 well plate, followed by addition of BCA reagent. After 2 hours of incubation at 37°C, absorption was measured at 562 nm by Infinite®M200 plate reader (Tecan group Ltd., Männedorf, Switzerland). Calibration curve was prepared with different gelatin concentrations in water. Nanospheres not containing gelatin were used as blank. The percent gelatin entrapment was calculated using the following equation:

$$\text{Gelatin Entrapment (\%)} = \frac{\text{Gelatin in Nanospheres (g) / Nanospheres (g)}}{\text{Gelatin used (g) / Polymer used (g)}} \times 100$$

Since gelatin is a hydrophilic macromolecule, it readily diffuses to the aqueous phase if not stabilized [168]. Therefore, the stabilization effectiveness of gelatin nanoparticles within nanospheres was estimated in terms of gelatin release from nanospheres to aqueous medium. Briefly, 10 mg of Nanospheres were dispersed in 10 ml of phosphate buffer solution (pH 7.4). Aliquots of 1 ml were taken out in different Eppendorf tubes and incubated at 37°C. At different time intervals the tubes were centrifuged at 24,000×g for 15 minutes. Supernatant was collected for gelatin quantification by BCA assay, and sediment was discarded.

In case of GE100-NiNOS a portion of nanospheres in release medium were dissolved after 24 hours by adding 1ml HCl (0.1 N), in order to release the entire entrapped gelatin.

5.4. Results and Discussion

The objective of this research is to introduce a new approach for stabilization of gelatin nanoparticles as a first step to circumvent the use of crosslinking agents. We developed a technique for maintaining the structural integrity of gelatin nanoparticles by entrapping them in polymer nanospheres.

The ampholytic nature of gelatin nanoparticles makes them theoretically susceptible for surface adsorption of cationic and anionic polymers. For instance Shutava et al. coated crosslinked gelatin nanoparticles with different polyelectrolytes using LbL technique [169]. However, coating of uncrosslinked gelatin nanoparticles is a question that has not yet been addressed. Practically it is a big challenge, since uncrosslinked gelatin nanoparticles on one hand dissolve in hydrophilic environment and on the other hand tend to aggregate in organic medium (preliminary experiments).

In this scenario, the concept of gelatin nanoparticles in nanospheres (NiNOS) is put forward, employing a dual technique of nanoprecipitation-double emulsion (schematically given in Figure 5.1). The technique used is associated with the following five steps: (a) preparing of gelatin nanoparticles by nanoprecipitation, (b) dispersing gelatin nanoparticles in organic phase, (c) emulsifying organic phase in aqueous PVA solution, (d) reducing the globule size by high speed homogenization, and (e) evaporating the organic solvent.
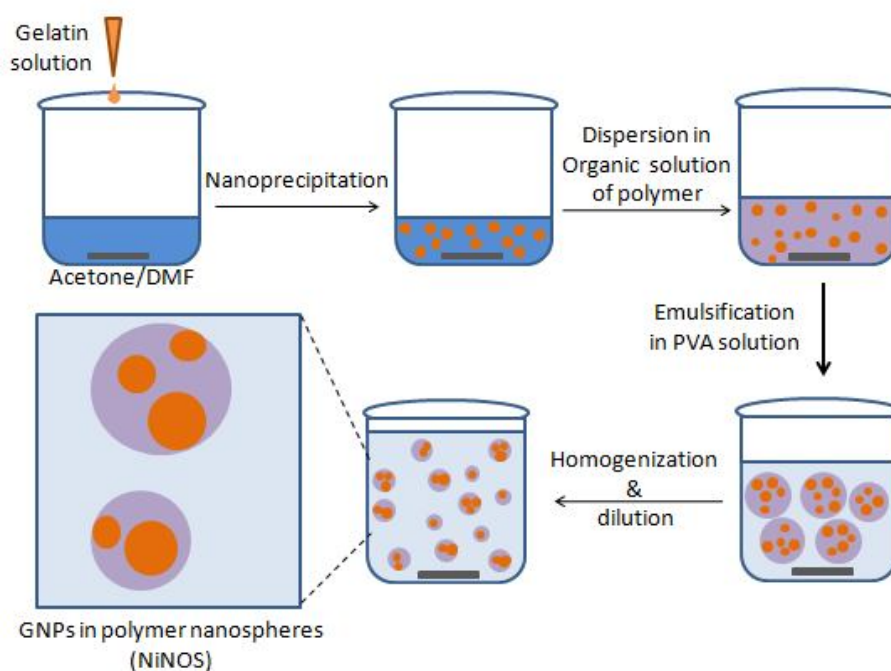
Figure 5.1. Schematic representation of hybrid nanoprecipitation-emulsion solvent evaporation technique for preparation NiNOS.

5.4.1. Gelatin nanoparticles by nanoprecipitation

Gelatin nanoparticles by nanoprecipitation are formed instantly due to rapid diffusion of solvent phase to the nonsolvent phase. The interfacial turbulence created due to solvent diffusion, forms nanodroplets at the interface. Consequently, aggregation of gelatin within the droplets leads to nanoparticle formation [170].

Nanoprecipitation is based on a complex phenomenon associated with the mutual relationship of the polymer–nonsolvent–solvent system. It is governed by the diffusion of solvent into nonsolvent. Therefore, the affinity of the solvent for the nonsolvent is of more importance than the individual solvent characteristics. In this respect, the solvent-nonsolvent interaction parameter, *X*, is of relevance [149]. Therefore, it was calculated using the following equation [150], and was correlated with the nanoparticles size.

74

$$X = \frac{V_{NS}}{RT} (\delta_S - \delta_{NS})^2$$

where V_{NS} is the molar volume of the nonsolvent, R is the gas constant, T is the absolute temperature, and δ_S and δ_{NS} are the Hildebrand solubility parameters of solvent and nonsolvent, respectively. Solubility parameter proposed by J. H. Hilderbrand in 1936 is the square root of the cohesive energy density as a numerical value indicating the solvency behavior of specific solvent.

The size of gelatin nanoparticles correlated with solvent-nonsolvent interaction parameter, is shown in Table 1. DMSO as solvent produced smaller nanoparticles, i.e., around 90 nm. It can be seen that the lower the X_{S-NS} values, the smaller the NP mean size. For instance keeping gelatin concentration constant (i.e., 4% w/v), the size of GNPs increased to 149 nm when three parts of the DMSO were replaced with water in the solvent phase. Furthermore, when acetone alone was used as nonsolvent, the size further increased to around 160 nm. It can be seen that particle size increases with increase in X_{SNS} values. This confirms that the solvent-nonsolvent interaction plays a vital role in the solvent diffusion phenomenon during nanoparticles formation. Lower X_{S-NS} values represent high affinity of the solvent for the nonsolvent, thus leading to formation of smaller nanoparticles, due to faster diffusion [149]. However, the interaction parameter cannot be considered as the sole factor for solvent/nonsolvent affinity. For example when water alone was used as solvent against acetone/DMF mixture the size remained almost unchanged while interaction parameter increased from 13 to 21, as shown in table 5.1.

Table 5.1. Effect of solvent/nonsolvent on the size and polydispersity of gelatin nanoparticles (mean ± standard deviation)

[a]Batch	Solvent Phase	Nonsolvent	Interaction parameter, χ[b]	Size ± S.D.	PDI ± S.D.
1	DMSO	DMF+Acetone	0.63	94.2 ± 6.1	0.16 ± 0.01
2	DMSO +Water (7 : 1)	DMF+Acetone	1.62	102.1 ± 7.3	0.15 ± 0.01
3	DMSO +Water (3 : 1)	DMF+Acetone	2.99	107.5 ± 3.2	0.15 ± 0.02
4	DMSO +Water (5 : 3)	DMF+Acetone	4.83	119.7 ± 1.1	0.15 ± 0.02
5	DMSO +Water (1 : 1)	DMF+Acetone	6.92	131.2 ± 2.3	0.14 ± 0.02
6	DMSO +Water (1 : 3)	DMF+Acetone	12.98	149.4 ± 3.9	0.11 ± 0.03
7	Water	DMF+Acetone	20.61	148.9 ± 6.8	0.07 ± 0.01
8	Water	Acetone	24.10	160.4 ± 2.7	0.12 ± 0.01

[a] All batches were prepared with 250 µl of solvent phase containing 10 mg of gelatin and 1.5 mL of nonsolvent phase.
[b] Calculated for T=25 °C (298 K).

Regarding other effects on the mean size of gelatin nanoparticles, it was found that it increases with increasing concentration of gelatin in the solvent phase; (Figure 5.2). For instance, 2% gelatin produced particles in the size of around 55 nm. The mean size increased to around 90 nm with a gelatin concentration 4%, while about 150 nm particles were produced when the concentration was further increased to 6%. Similarly, a constant increase in polydispersity index (PDI) values was observed with increase in gelatin concentration. For example it was 0.1 with 2% gelatin and increased to 0.16 and 0.18 when gelatin concentration was increased to 4% and 6%, respectively. Nevertheless, the PDI values in all the cases were in the range of 0.1-0.2 which reflects narrow distribution of produced nanoparticles. The improvement in size of nanoparticles with rise in concentration is thought to be due to increased viscosity of the gelatin solution. Since, higher viscosity of the solvent phase due to higher polymer concentration retards appropriate diffusion of the solvent towards the nonsolvent [23]. These results are in accordance with our expectations regarding similar data for other materials described in literature [151].
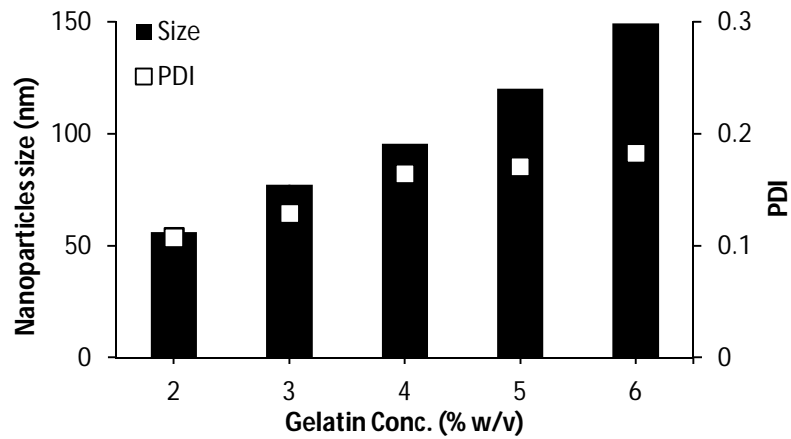
Figure 5.2. Effect of gelatin concentration on the size of nanoparticle produced by nanoprecipitation

5.4.2. Gelatin Nanoparticles in PLGA Nanosphere (GP-NiNOS)

Gelatin nanoparticles are hydrophilic and tend to aggregate in organic solvents. Therefore in order to achieve homogeneous dispersion of gelatin nanoparticles in ethyl acetate, different stabilizers were tested. i.e., gelatin nanoparticles were coated with stabilizers before dispersing them in ethyl acetate containing PLGA (Figure 5.3).
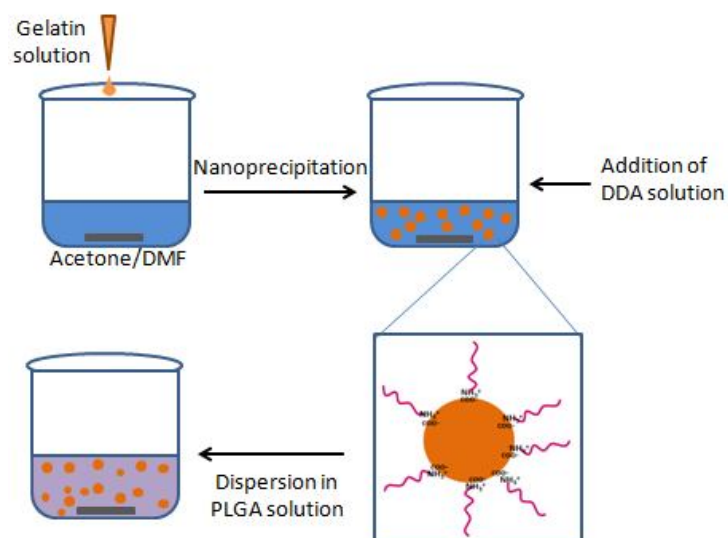

Figure 5.3. Schematic representation of gelatin nanoparticles coating with DDA before dispersion in PLGA solutions.

Among the studied stabilizers dodecylamine (DDA) and polyethylene glycol 1000 (PEG1000) were found to be effective. The final size of nanospheres is not affected by different stabilizers at this stage i.e. the size remains in the range of 200-250 nm (Figure 5.4).
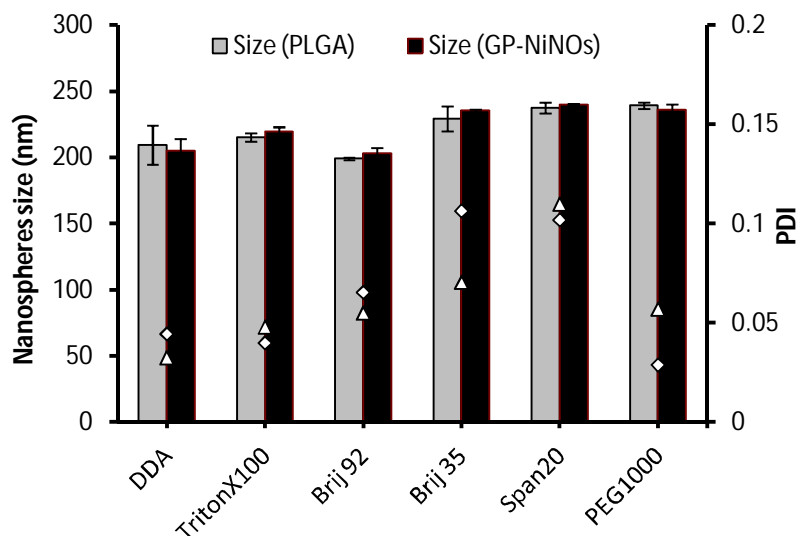

Figure 5.4. Effect of stabilizers for GNPs on the final size of gelatin nanoparticles

Physicochemical Characterization

In our protocol, an emulsion-solvent evaporation step is employed for the entrapment of gelatin nanoparticles in PLGA nanospheres. Thus, homogenization speed is considered to be critical for the final size of GP-NiNOS. Hence, nanospheres were produced with different homogenization speeds. Results are given in Figure 5.5(a). Lower speed of homogenization produced bigger nanoparticles and vice versa. For instance, the size of nanospheres was around 2 µm with a broad size distribution (PDI value around 0.3). Increasing homogenization speed to 10000 rpm decreased the size and the PDI to around 350 nm and 0.2, respectively. The smallest particle size (ca. 200 nm) with a narrow distribution (PDI < 0.1) was observed at 15000 rpm.

Additionally, no considerable difference was observed in the size of blank PLGA nanospheres

as well as GP-NiNOS in all the studied cases, except in the case of 5000 rpm homogenization speed. However, this cannot be considered as a considerable difference with such a huge standard deviation as shown in Figure 5.5(a).

Emulsification of PLGA ethyl acetate solution (containing dispersed GNPs) in PVA solution is actually responsible for gelatin nanoparticles entrapment within the nonpolar phase. For this reason the final size of nanospheres is governed by homogenization speed.

For the effect of polymer concentration in organic phase (PLGA in ethyl acetate solution), different PLGA amounts was investigated. No correlation was observed between the particle size and PLGA concentration, given in Figure 5.5(b). Furthermore, the size of blank PLGA nanospheres as well as GP-NiNOS was around 200 nm with all the studied PLGA concentrations.

(a)   (b)
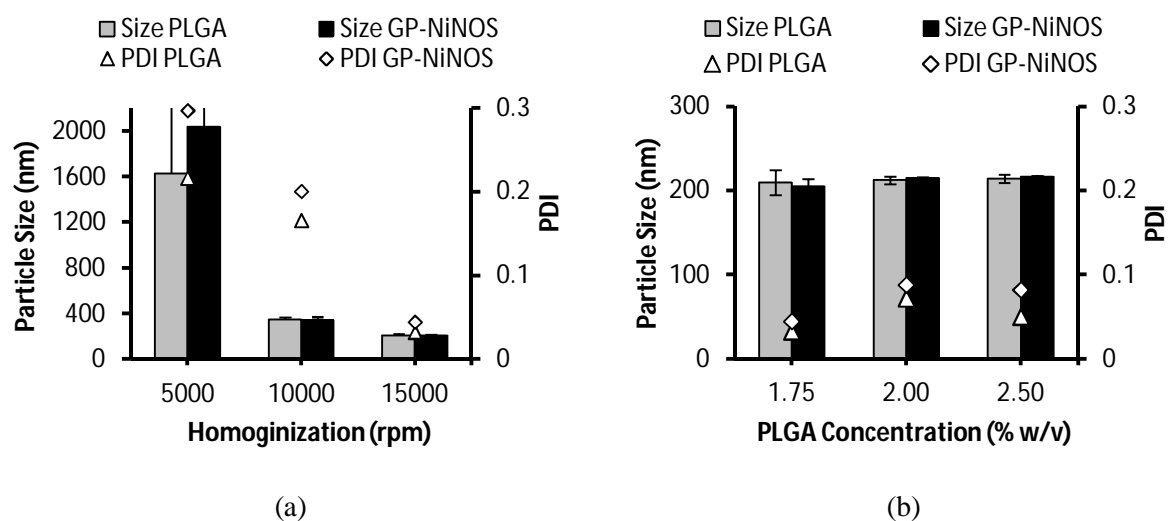
Figure 5.5. Effect of homogenization speed (a) and PLGA concentration (b) on the size and polydispersity of nanospheres.

Morphological Analysis

SPM images showed no apparent difference in the blank PLGA nanospheres and GP-NiNOS. The images showed smooth surface and spherical shape, shown in Figure 5.6.

(a)   (b)
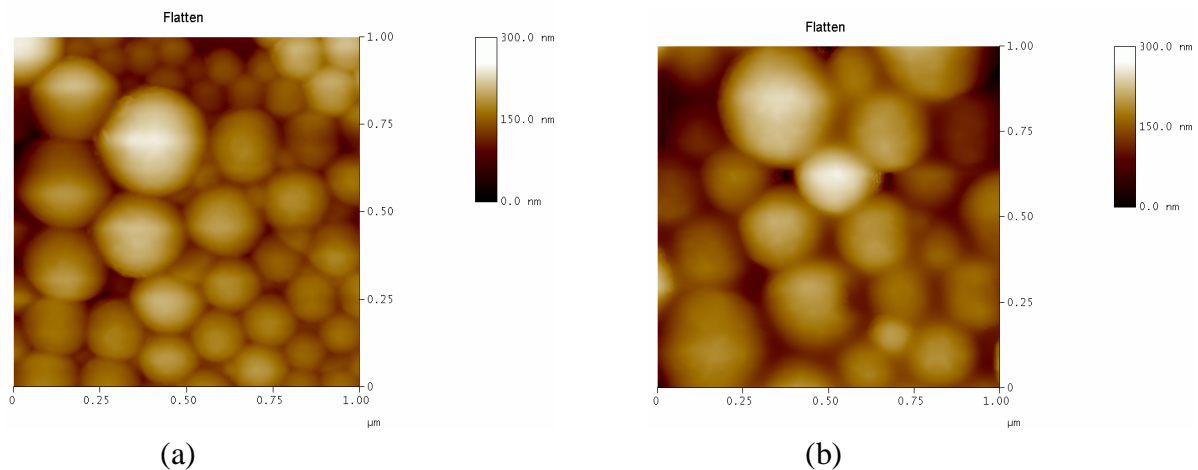
Figure 5.6. SPM micrographs of nanospheres (a) blank PLGA nanospheres, (b) GP-NiNOS. Preparation conditions: 2% PLGA concentration, 15,000 rpm homogenization.

5.4.3. Gelatin Entrapment and Release

The amount of gelatin entrapped was used as a parameter to assess the effective entrapment of gelatin nanoparticles in PLGA nanospheres. As mentioned earlier, different stabilizers were investigated to stabilize gelatin nanoparticles for homogeneous dispersion in PLGA solution. Their effect on gelatin entrapment is given in Figure 5.7. Gelatin entrapment of around 35% was observed with DDA and span20. Maximum entrapment of around 45% was witnessed with PEG1000. While Brij35 exhibited the lowest entrapment i.e. 30%.
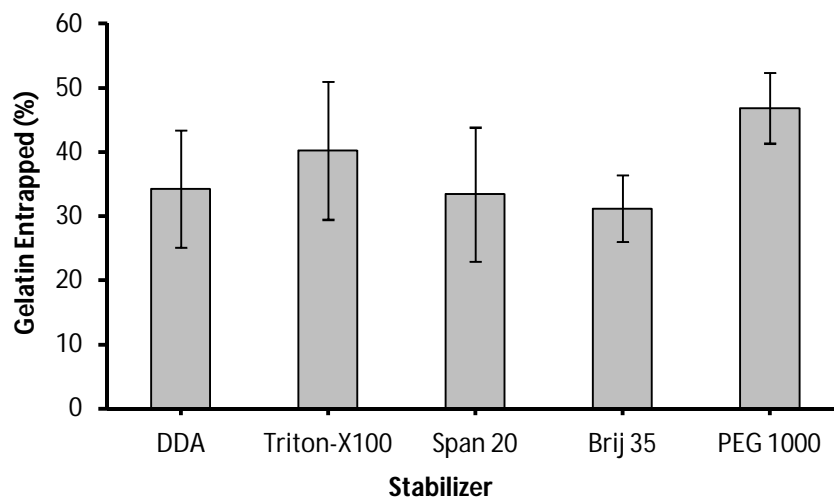

Figure 5.7. Effect of stabilizer used on gelatin entrapment in GP-NiNOS.

Gelatin entrapment slightly decreased with increase in PLGA concentration. For instance, it decreased from around 35% to less than 30 % when PLGA concentration was increased from to 1.75% to 2.5%, shown in Figure 5.8(a). However, homogenization speed inversely affected % gelatin entrapment. For instance, at 5000 rpm and 10000 rpm homogenization speed, approx. 65% gelatin was entrapped. While at 15000 rpm around 35% entrapment was observed, as shown in Figure 5.8(b).

<center>(a)</center><center>(b)</center>
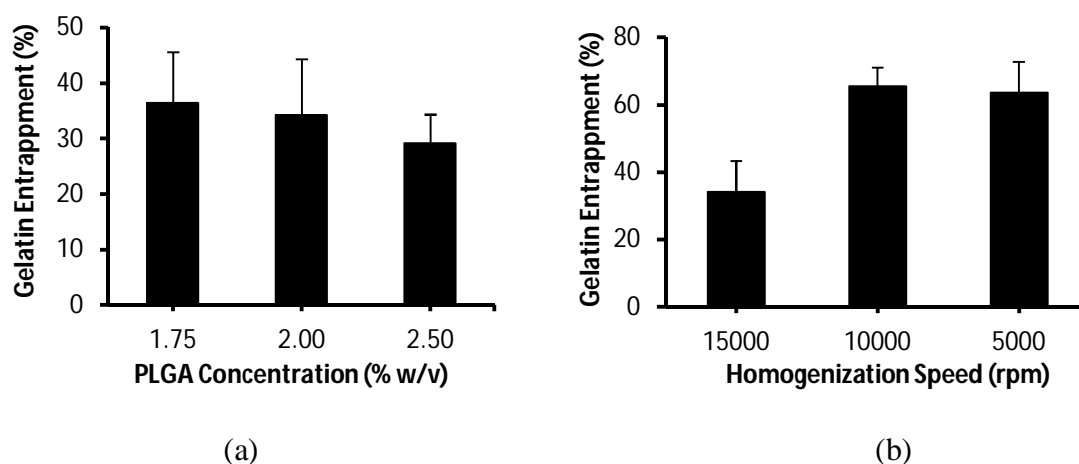
Figure 5.8. Effect of (a) PLGA concentrations and (b) homogenization speed on gelatin entrapment within GP-NiNOS.

The release of gelatin from GP-NiNOS studied in PBS (pH 7.4) showed that around 60% of the entrapped gelatin was released in the first half hour (Figure 5.9) reaching a plateau remaining unchanged for ~48 hours. However, the released amount reached another plateau of 70% after 72 hours.
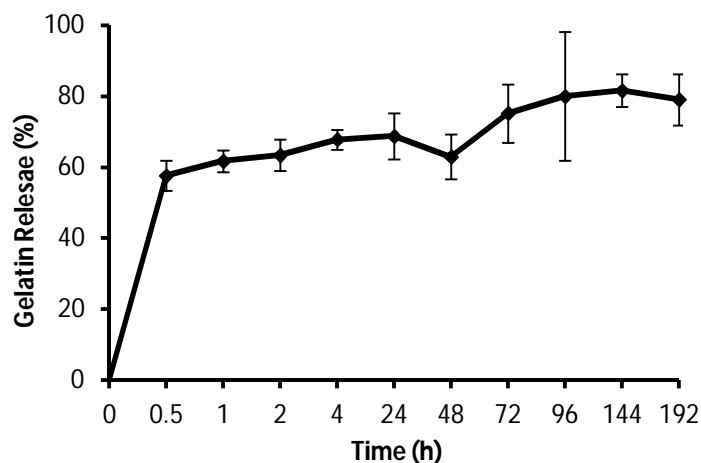
Figure 5.9. Release pattern of gelatin from GP-NiNOS in PBS (pH 7.4) at 37°C

As mentioned above, at 15,000 rpm the nanospheres had gelatin entrapment of less than 40%. Furthermore, the release was as fast as 60% in just half hour. Both these factor contribute to the inefficient entrapment of gelatin nanoparticles in PLGA nanospheres. Therefore, another film forming polymer was tested. In this regard Eudragit®E100 (E.100) served the purpose. Substituting PLGA with E.100 concentration not only improved the entrapment but also eliminated the need for stabilizer before gelatin nanoparticles dispersion in organic phase.

5.4.4. Gelatin Nanoparticles in E.100 Nanospheres (GE100-NiNOS)

Physicochemical Characterization

As mentioned earlier, upon evaporation of ethyl acetate the emulsion droplets were converted into E.100 nanospheres. Thus emulsification of E.100 ethyl acetate solution (containing dispersed GNPs) in PVA solution is actually responsible for gelatin nanoparticles entrapment within the E.100 nanospheres. For this reason the final size of nanoparticles is governed by the homogenization speed, i.e., nanosphere size decreases with increase in homogenization speed and vice versa. As shown in Figure 5.10(a), lower homogenization speed produced nanospheres in the range of 800-1000 nm with a very broad size distribution (PDI value 0.3-0.4). Increasing homogenization speed to 8,000 rpm decreased the size and the PDI to around

400-500 nm and 0.2, respectively. The smallest particle size with a narrow distribution (PDI 0.1) was observed at 15,000 rpm.

Additionally, the size of blank E.100 nanospheres is lower than that of GE100-NiNOS in all the studied cases, except at 15000 rpm. For instance at homogenization speed of 5000 rpm the size of GE100-NiNOS is around 127 nm greater than blank E.100 nanospheres while at 8000 rpm and 1000 rpm this difference in size is of around 55 nm whereas at an homogenization speed of 15000 rpm the difference is not noticeable.

For the effect of polymer concentration in organic phase (E.100 ethyl acetate solution), different E.100 amounts were investigated. It can be seen from the relationship between particle size and E.100 concentration, given in Figure 5.10(b), that 2% E.100 in ethyl acetate produced nanospheres in the size range of 160-180 nm. While an increase in polymer concentration barely affected the size. For instance, hardly 20-30 nm increase in size was observed for a threefold increase in E.100 concentration. Thus it can be said that the effect of polymer concentration on the final droplet size and in turn particle size was not substantial.


(a)   (b)
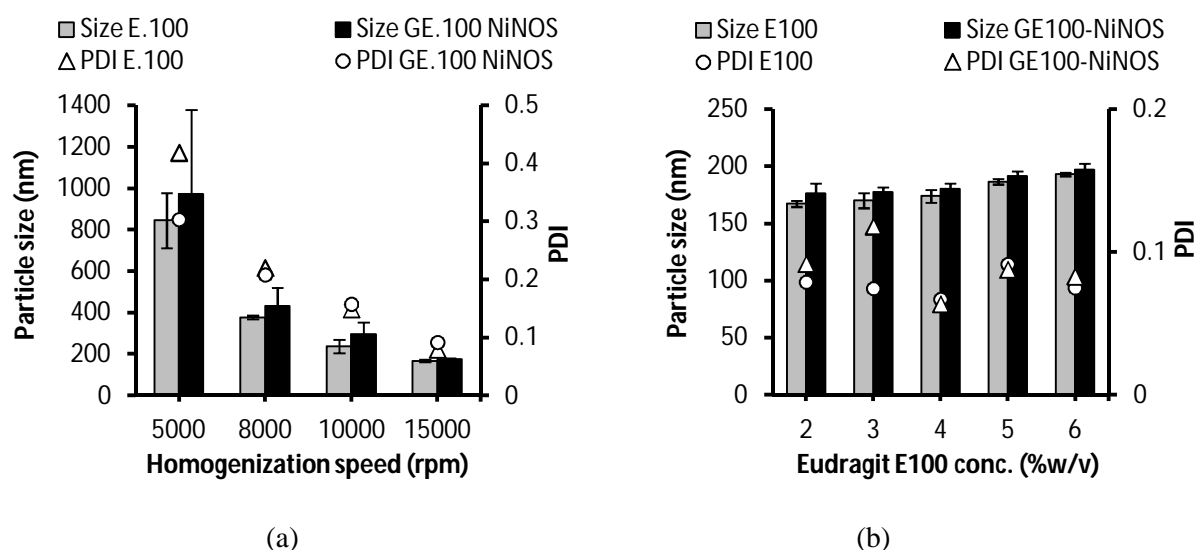
Figure 5.10. Effect of homogenization speed (a) and Eudragit® E 100 concentration (b) on the size and polydispersity of nanospheres.

Analyzing the particles size by SEM revealed smaller sizes than those measured by the Zetasizer (as shown in Table 5.2). This is most likely due to the drying effects of the sample, whereas SPM analysis show slight discrepant results for particles sizes. This is probably due to imprecise boundary of the overlapping particles in SPM image analysis and convolution effects of tip and object geometry [171]. Blank nanospheres reveal a smooth surface (Figure 5.11a). In contrast, the morphological analysis of the GE100-NiNOS shows spherical depressions on the surface (Figure 5.11b).

Table 5.2. Size characterization of nanospheres by DLS, SEM, and SPM

Nanospheres	Size in nm ± S.D		
	Zeta sizer	SEM[*]	SPM[*]
Blank nanospheres	202.4 ± 4.5	194.7 ± 51.6	227.1 ± 36.2
GE100-NiNOS	215.3 ± 8.6	200.1 ± 47.3	212.6 ± 40.6

*data based on analysis of 20 nanospheres.
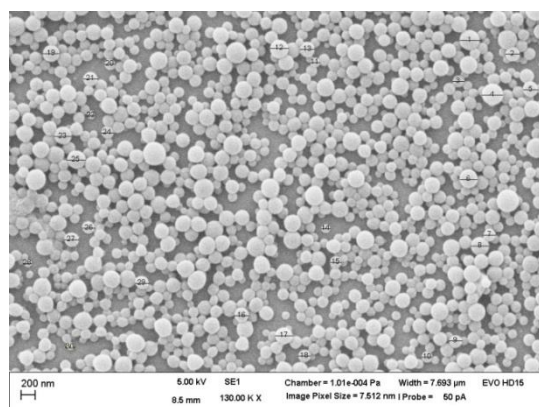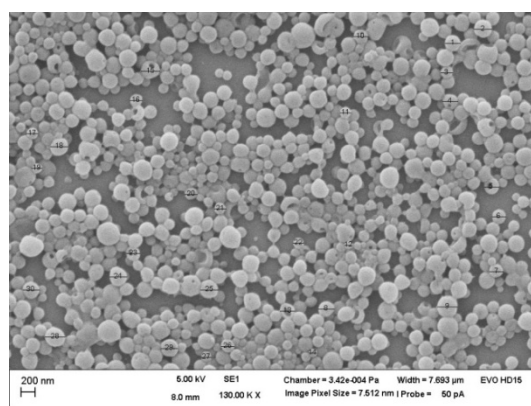
(a)   (b)

Figure 5.11. SEM micrographs of nanospheres (a) blank E.100 nanospheres, (b) GE100-NiNOS. Preparation conditions: 4% E.100 concentration, 15,000rpm homogenization.

Concerning the zeta potential, the values were consistent between +40 and +50 mV for all the studied cases. There is no big difference in the zeta potential values of blank E.100 nanospheres and GE100-NiNOS (Figure 5.12) suggesting that the surface properties of the disperse systems might equal.
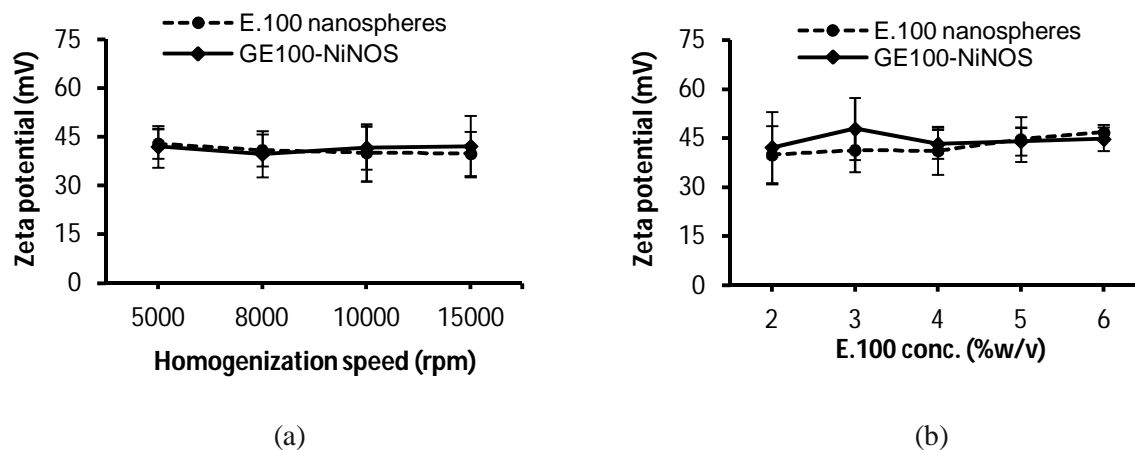
Figure 5.12. Effect of Eudragit® E 100 concentration (a) and homogenization speed (b) on the zeta potential of nanospheres.

Morphological Analysis

As mentioned earlier, SPM and SEM micrographs reveal spherical depressions on the surface of GE100-NiNOS. Two semi-quantitative parameters, i.e., porous particle fraction (% of all particles) and particle surface to pore surface ratio (PPSA), were proposed, to be good parameters to describe the porosity. Nanoparticles were manually analyzed for porous particles fraction. The number of porous particles to the total number of particles was used to determine porous particle fraction.

For PPSA, the surface area of particles and pores were calculated by pixel analysis using imageJ® software. The total surface area of the particles as calculated from their radius was divided by the total area of the pores as derived from the images.

We found that the porosity decreased with increasing E.100 concentration. SEM images from different batches with different E.100 concentration were taken (Figure 5.13) and the surface area of the nanospheres and the pores was determined using imageJ® software.
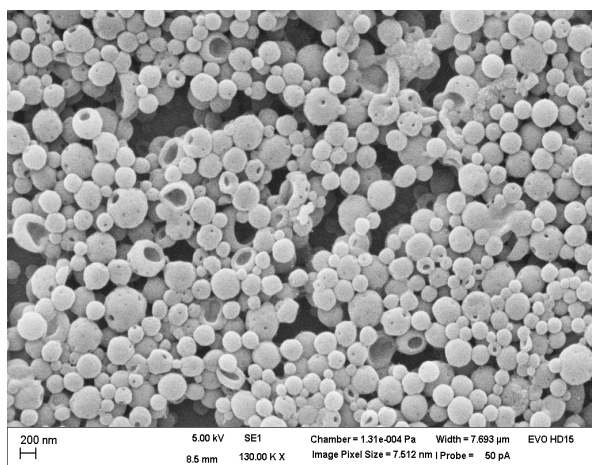
(a)
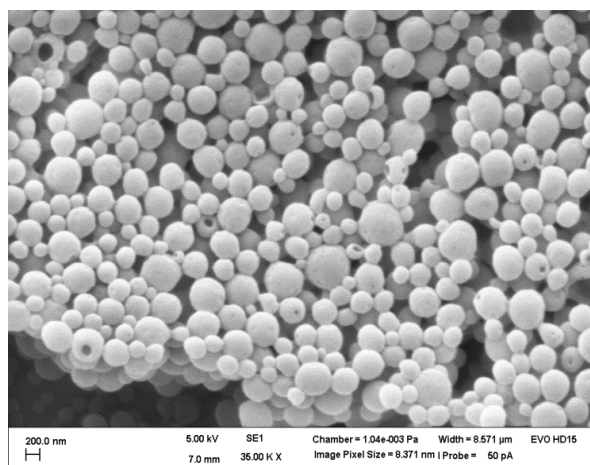
(b)
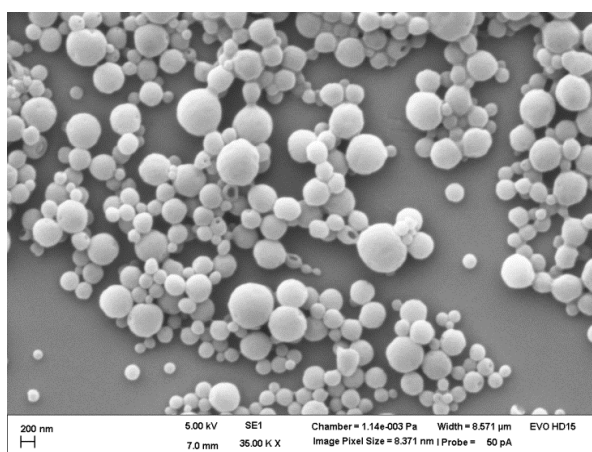
(c)
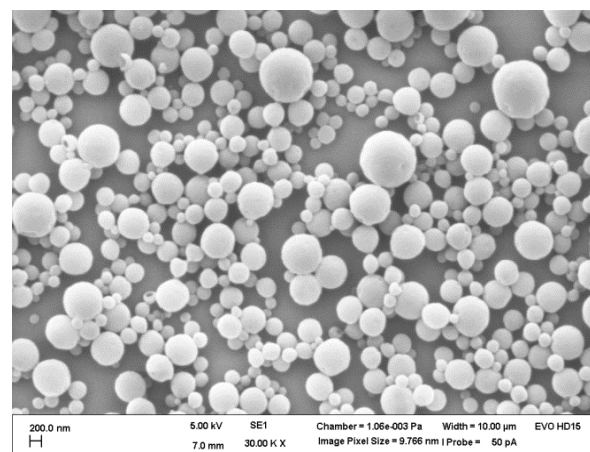
(d)

Figure 5.13. SEM images of GE100-NiNOS produced by hybrid nanoprecipitation-emulsion solvent evaporation technique, at different E.100 concentrations: (a) 2%, (b) 3.6%, (c) 4.2%, and (d) 6%, (constant homogenization speed 8,000 rpm).

The results of this analysis are given in Figure 5.14. An inverse relationship between porous particles fraction and E.100 concentration was observed; increase in E.100 concentration steadily decreased the porous fraction of the nanospheres produced. For instance, about 68% of the nanospheres were porous when 2% E.100 concentration was used. A decline of about 20% was observed when E.100 concentration was increased to 3% (i.e. 51% porous particles). Further increase in E.100 concentration slightly lowered the number of porous particles.

However, a substantial decline was witnessed between 4.5% and 4.8% E.100 concentration, where 27% of the nanospheres were found to be porous. Further rise in E.100 concentration to 5.7 % and 6 %, decreased the porous fraction to 10% and 5 % respectively.

Contrarily, a reciprocal relationship was observed between PPSR value and E.100 concentration; an increase in PPSR value was seen with increase in E.100 concentration. However the effect is somewhat invisible until E.100 concentration 4.5%. This is probably due to the closure of smaller pores (depicted in vanishing of porous fraction, Fig. 6), while the net PPSR remained more or less constant since only porous particles were considered for the calculation. For example, PPSR value of about 50 was seen with 2% E.100, and it remained in the range of 60-100 with E.100 concentration as high as 4.2%. However, further increase in E.100 concentration (4.5%) resulted in a sharp rise in PPSR value to 276, which further increased to around 378 with 5.4 % E.100 concentration. Higher values of PPSR i.e. 530 and 504 were seen at 5.7% and 6% E.100 concentration, respectively. The slight fluctuation in the PPSR value at higher concentration might be because of an analytical error, due to ill-defined boundaries of the pores on the surface, and less number of porous particles available for analysis.

Ultimately the decrease in the number of porous particles and rise in the PPSR values contribute to the fact that porosity of the nanospheres is inversely proportional to E.100 concentration. Thus it can be said that GE100-NiNOS prepared with low E.100 concentration cannot entrap gelatin nanoparticles efficiently. This can be depicted as a decline in gelatin entrapment with decreased E.100 concentration (Figure 5.14). However, with the porosity and the amount of porous particles the burst release could be possibly adjusted and controlled.
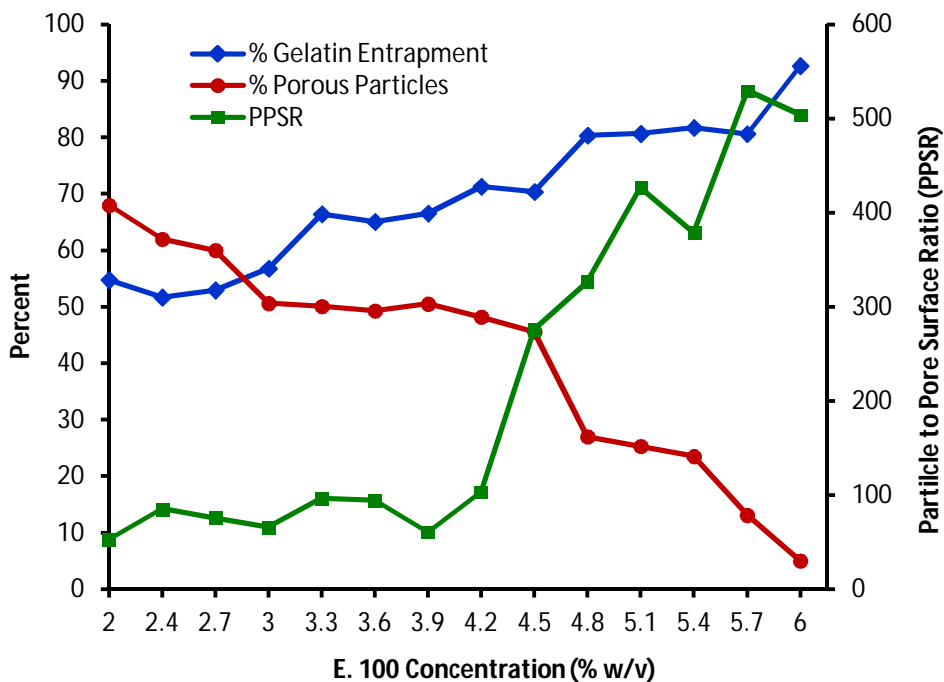
Figure 5.14. Correlation of porosity in terms of % porous particles and PPSA value, in dependence from E.100 concentration.

<center>(a)   (b)</center>
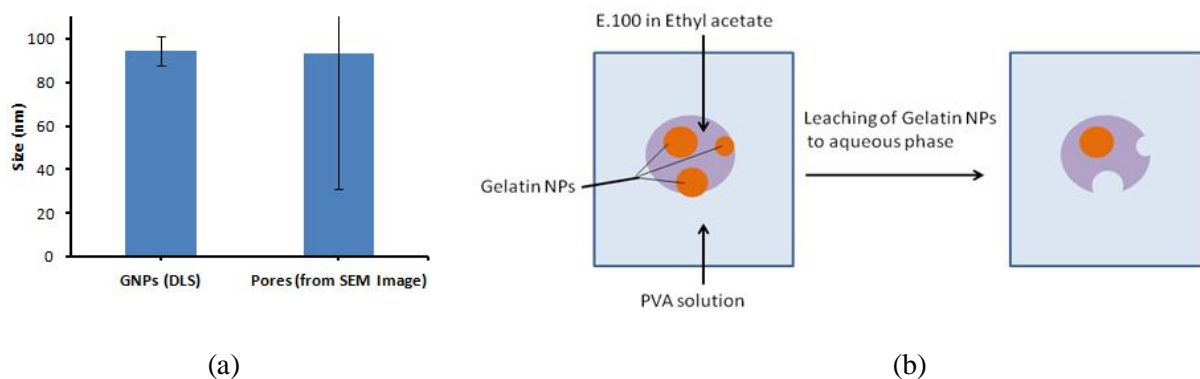
Figure 5.15. (a) Average size of pores on the surface of GE100-NiNOS prepared at 2% E.100 concentration (SEM) and gelatin nanoparticle size by DLS. (b) Schematic representation of possible gelatin leaching from the surface of nanospheres to the aqueous phase.

From the similarity in size of the pores and gelatin nanoparticles (Figure 5.15a), it can be conceived that the pores were apparently formed by leaking of gelatin nanoparticles from the surface to aqueous medium due to incompletely coated GNP, schematically shown in Figure 5.15b. Before emulsification gelatin nanoparticles were primarily dispersed in organic phase

containing E.100. Possibly, at low concentrations of E.100, the amount was insufficient to entrap all gelatin nanoparticles efficiently. Thus gelatin nanoparticles at the surface not fully covered were prone to leak to the external aqueous phase, hence leaving a pore of its size on the surface.

5.4.5. Gelatin Entrapment and Release

Gelatin entrapment diminished with decrease in E.100 concentration. For instance, it decreased from around 100% to 55 % when E.100 concentration was decreased from 6 to 2%. Nevertheless, when homogenization speed was reduced to 8,000 rpm gelatin entrapment was slightly increased to around 65%, compared to 55% at 15,000 rpm, as shown in Figure 5.16.
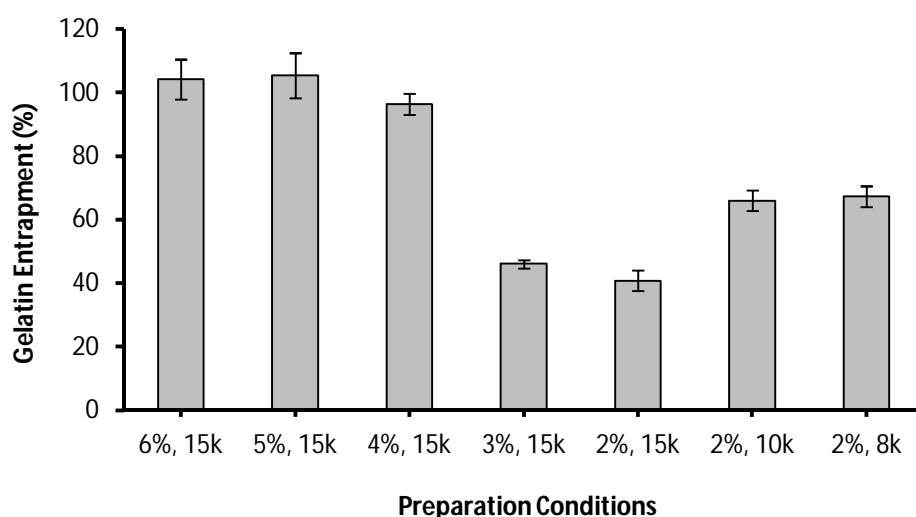
Figure 5.16. Effect of Eudragit® E 100 concentrations and homogenization speed on gelatin entrapment within GE100-NiNOS. k: ×1000 rpm, representing homogenization speed.

The release of gelatin from GE100-NiNOS was studied in PBS (pH 7.4). As shown in Figure 5.17(a), comparatively higher burst release was observed for nanospheres prepared at low concentration of E.100. For instance, nanospheres prepared with 2% and 3% E.100 concentration showed 27.1% and 18.6% initial release, respectively. On the other hand, around 10% of entrapped gelatin was released from nanospheres produced with 4-6% E.100.

89

The comparatively higher initial burst release at lower E.100 concentration could be due to the loosely embedded gelatin nanoparticles in the surface layer. It may also be attributed to the morphology of the nanospheres. Since nanospheres produced with low concentration were more porous (as explained previously), they exposes greater surface area to the release medium.

To see the effect of nanosphere size on release, different sized nanospheres were obtained by lowering the homogenization speed (keeping E.100 concentration constant, i.e., 2%). It was found that the initial burst release was reduced when the size of nanosphere was increased, as shown in Figure 5.17(b). For instance, almost fourfold decrease (i.e. decreased from 27% to 6.7%) in initial burst release was observed when the size of nanospheres was increased from 176 ± 5 nm to 433 ± 88 nm. Similarly, 295 ± 59 nm nanospheres exhibited around 15% release in the first half hour. The reason for this may be the lower surface area of larger nanospheres than that of smaller ones which was expected based on literature [172, 173].

Nevertheless, in all the studied cases the release profile remained unchanged over 24 hours. However, upon acidifying the medium (pH < 5) the entire entrapped gelatin was released. This could obviously be attributed to the dissolution of E.100 at pH values below 5.5 [174].
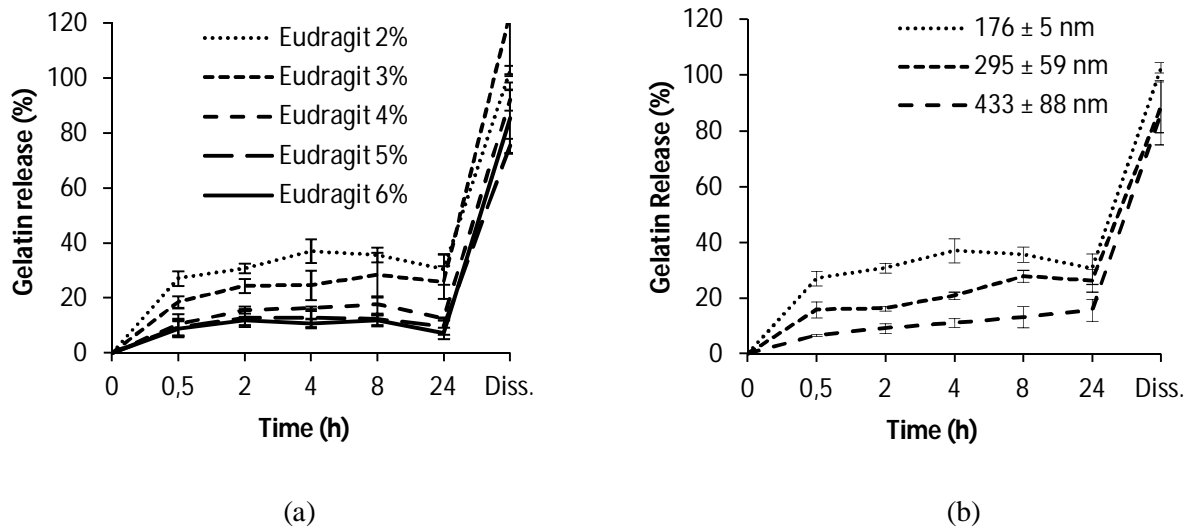
Figure 5.17. Effect of E.100 concentration (a) and nanosphere size (b), on gelatin release from GE100-NiNOS in PBS (pH 7.4) at 37°C, and after dissolution of nanospheres.

5.5. Conclusion

This work demonstrates a novel approach for stabilization of gelatin nanoparticles without the use of crosslinking agents. A unique technique of nanoprecipitation-double emulsion is presented. Gelatin nanoparticles are produced by nanoprecipitation, and are subsequently entrapped in polymeric nanospheres by emulsion-solvent evaporation technique. The final size of nanospheres is mainly affected by homogenization speed. Smaller particles were produced at higher speeds and vice versa. The immense burst release reveals the inefficiency of PLGA for entrapment of gelatin nanoparticles. In case of GE100-NiNOS, the entrapment of gelatin is dependent on concentration. The porosity on nanosphere surface and in turn the initial burst release of gelatin from nanospheres decreases with increase in E.100 concentration. At pH below 5 all the entrapped gelatin is released due to dissolution of E.100. It can be concluded that the system provides a good opportunity for stabilization of gelatin nanoparticles. The study is seemingly a promising step towards stabilization of gelatin nanoparticles without crosslinking.

91

6. Summary and Outlook

Macromolecules are conventionally administered in aqueous solution using needles and syringes. In order to develop delivery systems for other routes, attempts are made to encapsulate macromolecules in polymers, e.g. microparticles, hydrogels, beads, nanoparticles, etc. Nanoparticles have been proved to be one of the most promising delivery system due to its size. However, these systems are mostly based on hydrophobic polymers, which may induce unfolding, and hence inactivation of some macromolecular drugs. Gelatin being a hydrophilic biopolymer may exhibit better compatibility with macromolecular drugs.

During preparation of nanoparticles from gelatin special attention needs to be taken for the interparticular aggregation. For this reason, most of the preparation are either tedious, require specific proportion of certain molecular weight fraction or need a narrow range of appropriate pH. The requirement of extreme acidic or basic pH for successful nanoparticle preparation may affect some sensitive macromolecules. Therefore the first objective was to offer an optimized technique without altering the intrinsic properties of gelatin. In this context, a straight forward technique of nanoprecipitation was optimized. The effects of various parameters involved in the particle preparation process were investigated. The presence of poloxamer was a critical factor for the stability of the nanoparticles. The size of nanoparticles was tuned by changing gelatin concentration in the solvent phase and by changing the nonsolvent composition. The potential of the system for delivery of hydrophilic macromolecules was demonstrated using FITC-dextran as model drug. The release from glutaraldehyde crosslinked gelatin nanoparticles was dependent on the molecular weight of FITC-dextran. Surface modification of the particles was done by physically adsorbing PEI on the surface. Uncrosslinked particles cannot be coated with PEI, while crosslinked gelatin

nanoparticles could effectively bind PEI on its surface rendering the zeta potential positively charged.

It should be noted that release of FITC-dextran cannot be correlated with peptide based macromolecular drugs, since protein based macromolecules contain primary amino groups. Which due to involvement in the crosslinking process, presumably will not only affect the release pattern but also the biological activity of the drugs. Hence, efforts need to be taken to explore other possibilities for stabilization of gelatin nanoparticles without crosslinking. To date, no study has been performed to address this issue of gelatin nanoparticles. Therefore, we presented a novel technique for maintaining the structural integrity of gelatin nanoparticles in polymeric nanospheres, using nanoparticles in nanospheres (NiNOS) concept. PLGA and Eudragit E100 were employed as polymers for preparation of nanospheres. The effect of different parameters and the physicochemical properties of nanosphere preparation were investigated to get optimum formulation. It was found that PLGA could not stabilize gelatin nanoparticles, since gelatin was immediately released from the nanospheres. On the other hand Eudragit E100 was effective in stabilizing gelatin nanoparticles. However, E100 concentration was critical for morphology of the nanospheres, and in turn the stability of gelatin nanoparticles within the nanospheres matrix. Our study is the first step of its kind towards stabilization of gelatin nanoparticles without crosslinking. However, due the limitations in application of Eudragit E100 besides oral route, other biodegradable materials need to be investigated.

In this context, we are planning to investigate the possibility of using spray drying technique. The decisive factor will be to keep the integrity of gelatin nanoparticles in biodegradable polyester microspheres. We are also looking forward to association with our collaborators from University of Leipzig, on the assumption to covalently crosslink nanoparticle surface

without harming the internal core. This will give us the opportunity to load protein based macromolecules within the core of nanoparticles not interfering with the crosslinker being only present on the surface. Furthermore, we are working in close collaboration with our institute members to deliver specific plasmid, intended for application against fibrosis.

7. Bibliography

1. Goldberg, M. and I. Gomez-Orellana, *Challenges for the oral delivery of macromolecules.* Nature Reviews Drug Discovery, 2003. 2(4): p. 289-295.

2. Carter, P.J., *Introduction to current and future protein therapeutics: a protein engineering perspective.* Experimental cell research, 2011. 317(9): p. 1261-1269.

3. *EvaluatePharma, "World Preview 2018 Embracing the Patent Cliff".* 2012.

4. Brown, L.R., *Commercial challenges of protein drug delivery.* Expert opinion on drug delivery, 2005. 2(1): p. 29-42.

5. Selbo, P.K., et al., *Photochemical internalisation: a novel drug delivery system.* Tumor biology, 2002. 23(2): p. 103-112.

6. Bostad, M., et al., *Photochemical internalization (PCI) of immunotoxins targeting CD133 is specific and highly potent at femtomolar levels in cells with cancer stem cell properties.* Journal of Controlled Release, 2013. 168(3): p. 317-326.

7. Asokan, A. and M.J. Cho, *Exploitation of intracellular pH gradients in the cellular delivery of macromolecules.* Journal of pharmaceutical sciences, 2002. 91(4): p. 903-913.

8. Tang, M., et al., *A reversible hydrogel membrane for controlling the delivery of macromolecules.* Biotechnology and bioengineering, 2003. 82(1): p. 47-53.

9. Krebs, M.D., O. Jeon, and E. Alsberg, *Localized and sustained delivery of silencing RNA from macroscopic biopolymer hydrogels.* Journal of the American Chemical Society, 2009. 131(26): p. 9204-9206.

10. Lynam, D., et al., *Augmenting protein release from layer-by-layer functionalized agarose hydrogels.* Carbohydrate Polymers, 2014. 103(0): p. 377-384.

11. Larrañeta, E. and J.R. Isasi, *Non-covalent hydrogels of cyclodextrins and poloxamines for the controlled release of proteins.* Carbohydrate Polymers, 2014. 102(0): p. 674-681.

12. Coulman, S.A., et al., *Minimally invasive cutaneous delivery of macromolecules and plasmid DNA via microneedles.* Current drug delivery, 2006. 3(1): p. 65-75.

13. Kim, Y.-C., J.-H. Park, and M.R. Prausnitz, *Microneedles for drug and vaccine delivery.* Advanced Drug Delivery Reviews, 2012. 64(14): p. 1547-1568.

14. Berkland, C., et al., *Macromolecule release from monodisperse PLG microspheres: control of release rates and investigation of release mechanism.* Journal of pharmaceutical sciences, 2007. 96(5): p. 1176-1191.

15. Carrillo-Conde, B.R., et al., *Chemistry-dependent adsorption of serum proteins onto polyanhydride microparticles differentially influences dendritic cell uptake and activation.* Acta Biomaterialia, 2012. 8(10): p. 3618-3628.

16. Cruz, M.E.M., et al., *Formulation of NPDDS for Macromolecules.* Drug Delivery

Nanoparticles Formulation and Characterization: p. 35.

17.   Bhattacharyya, S., H. Wang, and P. Ducheyne, *Polymer-coated mesoporous silica nanoparticles for the controlled release of macromolecules.* Acta Biomaterialia, 2012. 8(9): p. 3429-3435.

18.   Desai, M.P., et al., *The mechanism of uptake of biodegradable microparticles in Caco-2 cells is size dependent.* Pharmaceutical research, 1997. 14(11): p. 1568-1573.

19.   Treuel, L., X. Jiang, and G.U. Nienhaus, *New views on cellular uptake and trafficking of manufactured nanoparticles.* Journal of The Royal Society Interface, 2013. 10(82).

20.   Chen, M.C., et al., *Recent Advances in Chitosan-based Nanoparticles for Oral Delivery of Macromolecules.* Advanced Drug Delivery Reviews, 2012. 65(6): p. 865–879.

21.   des Rieux, A., et al., *Nanoparticles as potential oral delivery systems of proteins and vaccines: a mechanistic approach.* Journal of Controlled Release, 2006. 116(1): p. 1-27.

22.   Pinto Reis, C., et al., *Nanoencapsulation II. Biomedical applications and current status of peptide and protein nanoparticulate delivery systems.* Nanomedicine: Nanotechnology, Biology and Medicine, 2006. 2(2): p. 53-65.

23.   Bilati, U., E. Allémann, and E. Doelker, *Nanoprecipitation Versus Emulsion-based Techniques for the Encapsulation of Proteins Into Biodegradable Nanoparticles and Process-related Stability Issues.* AAPS PharmSciTech 2005. 6 (4): p. E593-E604.

24.   Mundargi, R.C., et al., *Nano/micro technologies for delivering macromolecular therapeutics using poly(D,L-lactide-co-glycolide) and its derivatives.* Journal of Controlled Release, 2008. 125(3): p. 193-209.

25.   Xu, Y. and Y. Du, *Effect of molecular structure of chitosan on protein delivery properties of chitosan nanoparticles.* International journal of pharmaceutics, 2003. 250(1): p. 215-226.

26.   Vila, A., et al., *Low molecular weight chitosan nanoparticles as new carriers for nasal vaccine delivery in mice.* European journal of pharmaceutics and biopharmaceutics, 2004. 57(1): p. 123-131.

27.   Janes, K., P. Calvo, and M. Alonso, *Polysaccharide colloidal particles as delivery systems for macromolecules.* Advanced drug delivery reviews, 2001. 47(1): p. 83-97.

28.   Dong, L., et al., *Self-assembled FeCo/gelatin nanospheres with rapid magnetic response and high biomolecule-loading capacity.* Small, 2009. 5(10): p. 1153-1157.

29.   Chauhan, I., M. Yasir, and P. Nagar, *Insights into Polymers: Film Formers in Mouth Dissolving Films.* Drug Invention Today, 2012. 3(12).

30.   Gómez-Guillén, M.C., et al., *Functional and bioactive properties of collagen and gelatin from alternative sources: A review.* Food Hydrocolloids, 2011. 25(8): p. 1813-1827.

31.   Karim, A.A. and R. Bhat, *Fish gelatin: properties, challenges, and prospects as an alternative to mammalian gelatins.* Food Hydrocolloids, 2009. 23(3): p. 563-576.

32.   Choi, S.S. and J. Regenstein, *Physicochemical and sensory characteristics of fish gelatin.* Journal of Food Science, 2000. 65(2): p. 194-199.

33.   Patel, Z.S., et al., *Biodegradable gelatin microparticles as delivery systems for the controlled release of bone morphogenetic protein-2.* Acta biomaterialia, 2008. 4(5): p. 1126-1138.

34.   Ninan, G., J. Jose, and Z. Abubacker, *Preparation and characterization of gelatin extracted from the skins of rohu (Labeo Rohita) and common carp (Cyprinus Carpio).* Journal of food processing and preservation, 2010. 35(2): p. 143-162.

35.   Siqueira, G., J. Bras, and A. Dufresne, *New process of chemical grafting of cellulose nanoparticles with a long chain isocyanate.* Langmuir, 2009. 26(1): p. 402-411.

36.   Janes, K.A., et al., *Chitosan nanoparticles as delivery systems for doxorubicin.* Journal of Controlled Release, 2001. 73(2): p. 255-267.

37.   Das, R.K., N. Kasoju, and U. Bora, *Encapsulation of curcumin in alginate-chitosan-pluronic composite nanoparticles for delivery to cancer cells.* Nanomedicine: Nanotechnology, Biology and Medicine, 2010. 6(1): p. 153-160.

38.   Murado, M., et al., *Optimization of extraction and purification process of hyaluronic acid from fish eyeball.* Food and Bioproducts Processing, 2012. 90(3): p. 491-498.

39.   Leathers, T., *Biotechnological production and applications of pullulan.* Applied microbiology and biotechnology, 2003. 62(5): p. 468-473.

40.   Tseng, C.-L., et al., *Development of gelatin nanoparticles with biotinylated EGF conjugation for lung cancer targeting.* Biomaterials, 2007. 28(27): p. 3996-4005.

41.   Kumari, A., S. Yadav, and S. Yadav, *Biodegradable polymeric nanoparticles based drug delivery systems.* Colloids and Surfaces B: Biointerfaces, 2010. 75(1): p. 1-18.

42.   Patil, G.V., *Biopolymer albumin for diagnosis and in drug delivery.* Drug development research, 2003. 58(3): p. 219-247.

43.   ; Available from: http://www.mpbio.com/product.php?pid=05214216.

44.   Shukla, R. and M. Cheryan, *Zein: the industrial protein from corn.* Industrial Crops and Products, 2001. 13(3): p. 171-192.

45.   Park, S., D. Bae, and K. Rhee, *Soy protein biopolymers cross-linked with glutaraldehyde.* Journal of the American Oil Chemists' Society, 2000. 77(8): p. 879-884.

46.   Tanaka, F., *Thermoreversible gelation driven by coil-to-helix transition of polymers.* Macromolecules, 2003. 36(14): p. 5392-5405.

47.   Gao, M., et al., *A gelatin-based sol–gel procedure to synthesize the LiFePO4/C nanocomposite for lithium ion batteries.* Solid State Ionics, 2014. 258(0): p. 8-12.

48.   Parker, N.G. and M.J.W. Povey, *Ultrasonic study of the gelation of gelatin: Phase diagram, hysteresis and kinetics.* Food Hydrocolloids, 2012. 26(1): p. 99-107.

49.   Cheng, Y.-H., et al., *Sustained Delivery of Latanoprost by Thermosensitive Chitosan-Gelatin-*

based Hydrogel for Controlling Ocular Hypertension. Acta Biomaterialia. In press(DOI: 10.1016/j.actbio.2014.05.031).

50. Nur Hanani, Z.A., Y.H. Roos, and J.P. Kerry, *Use and application of gelatin as potential biodegradable packaging materials for food products.* International Journal of Biological Macromolecules. In press(DOI: 10.1016/j.ijbiomac.2014.04.027).

51. Olad, A. and F. Farshi Azhar, *The synergetic effect of bioactive ceramic and nanoclay on the properties of chitosan–gelatin/nanohydroxyapatite–montmorillonite scaffold for bone tissue engineering.* Ceramics International, 2014. 40(7, Part A): p. 10061-10072.

52. Chhabra, H., et al., *Gelatin–PMVE/MA composite scaffold promotes expansion of embryonic stem cells.* Materials Science and Engineering: C, 2014. 37(0): p. 184-194.

53. Hoffmann, H. and M. Reger, *Emulsions with unique properties from proteins as emulsifiers.* Advances in Colloid and Interface Science, 2014. 205(0): p. 94-104.

54. Sovilj, V., J. Milanović, and L. Petrović, *Viscosimetric and tensiometric investigations of interactions between gelatin and surface active molecules of various structures.* Food Hydrocolloids, 2013. 32(1): p. 20-27.

55. Pal, K., A.T. Paulson, and D. Rousseau, *14 - Biopolymers in Controlled-Release Delivery Systems*, in *Handbook of Biopolymers and Biodegradable Plastics*, S. Ebnesajjad, Editor. 2013, William Andrew Publishing: Boston. p. 329-363.

56. Buchweitz, M., et al., *Application of ferric anthocyanin chelates as natural blue food colorants in polysaccharide and gelatin based gels.* Food Research International, 2013. 51(1): p. 274-282.

57. Jamil, R.K., et al., *Evaluation of the thermal stability of a novel strain of live-attenuated mumps vaccine (RS-12 strain) lyophilized in different stabilizers.* Journal of Virological Methods, 2014. 199(0): p. 35-38.

58. Boks, R.H., et al., *Low molecular starch versus gelatin plasma expander during CPB: does it make a difference?* Perfusion, 2007. 22(5): p. 333-337.

59. Santoro, M., A.M. Tatara, and A.G. Mikos, *Gelatin carriers for drug and cell delivery in tissue engineering.* Journal of Controlled Release. In press(DOI: 10.1016/j.jconrel.2014.04.014).

60. Cui, L., et al., *Preparation and characterization of IPN hydrogels composed of chitosan and gelatin cross-linked by genipin.* Carbohydrate Polymers, 2014. 99(0): p. 31-38.

61. Li, J.-H., et al., *Preparation and characterization of active gelatin-based films incorporated with natural antioxidants.* Food Hydrocolloids, 2014. 37(0): p. 166-173.

62. Prata, A.S. and C.R.F. Grosso, *Production of microparticles with gelatin and chitosan.* Carbohydrate Polymers. In press(DOI: 10.1016/j.carbpol.2014.03.056).

63. Azarmi, S., et al., *Optimization of a two-step desolvation method for preparing gelatin nanoparticles and cell uptake studies in 143B osteosarcoma cancer cells* Journal of Pharmacy

and Pharmaceutical Sciences, 2006 9(1): p. 124-132.

64. Rajan, M. and V. Raj, *Formation and characterization of chitosan-polylacticacid-polyethylene glycol-gelatin nanoparticles: A novel biosystem for controlled drug delivery.* Carbohydrate Polymers, 2013. 98(1): p. 951-958.

65. Azimi, B., et al., *Producing Gelatin Nanoparticles as Delivery System for Bovine Serum Albumin.* Iranian biomedical journal, 2014. 18(1): p. 34.

66. Oppenheim, et al., *Injectable compositions, nanoparticles useful therein, and process of manufacturing same* United States Patent 1978. 4107288.

67. Victoria, P.S.o. and Speiser, *Injectable compositions* United Kingdom Patent 1975. GB1516348.

68. Panyam, J. and V. Labhasetwar, *Biodegradable nanoparticles for drug and gene delivery to cells and tissue.* Advanced Drug Delivery Reviews, 2003. 55: p. 329–347.

69. Prow, T.W., et al., *Nanoparticles and microparticles for skin drug delivery.* Advanced Drug Delivery Reviews. 63(6): p. 470-491.

70. Balthasar, S., et al., *Preparation and characterisation of antibody modified gelatin nanoparticles as drug carrier system for uptake in lymphocytes.* Biomaterials, 2005. 26(15): p. 2723-2732.

71. Azarmi, S., W.H. Roa, and R. Löbenberg, *Targeted delivery of nanoparticles for the treatment of lung diseases.* Advanced Drug Delivery Reviews, 2008. 60(8): p. 863-875.

72. Gupta, B., et al., *Preparation and characterization of in-situ crosslinked pectin–gelatin hydrogels.* Carbohydrate Polymers, 2014. 106(0): p. 312-318.

73. Coester, C., P. Nayyar, and J. Samuel, *In vitro uptake of gelatin nanoparticles by murine dendritic cells and their intracellular localisation.* European Journal of Pharmaceutics and Biopharmaceutics, 2006. 62(3): p. 306-314.

74. Bajpai, A.K. and J. Choubey, *In vitro release dynamics of an anticancer drug from swellable gelatin nanoparticles.* Journal of Applied Polymer Science, 2006. 101(4): p. 2320-2332.

75. Cascone, M., et al., *Gelatin nanoparticles produced by a simple w/o emulsion as delivery system for methotrexate.* Journal of Materials Science: Materials in Medicine, 2002. 13: p. 523-526.

76. Gupta, A.K., et al., *Effect of cellular uptake of gelatin nanoparticles on adhesion, morphology and cytoskeleton organisation of human fibroblasts.* Journal of Controlled Release, 2004. 95(2): p. 197-207.

77. Ethirajan, A., et al., *Synthesis and optimization of gelatin nanoparticles using the miniemulsion process.* Biomacromolecules, 2008. 9(9): p. 2383-2389.

78. Leo, E., et al., *Doxorubicin-loaded gelatin nanoparticles stabilized by glutaraldehyde: Involvement of the drug in the cross-linking process.* International Journal of Pharmaceutics,

1997. 155(1): p. 75-82.

79.   Leo, E., et al., *General and cardiac toxicity of doxorubicin-loaded gelatin nanoparticles.* Il Farmaco, 1997. 52(6-7): p. 385-388.

80.   Leo, E., R. Cameroni, and F. Forni, *Dynamic dialysis for the drug release evaluation from doxorubicin-gelatin nanoparticle conjugates.* International Journal of Pharmaceutics, 1999. 180(1): p. 23-30.

81.   Mohanty, B. and H.B. Bohidar, *Systematic of Alcohol-Induced Simple Coacervation in Aqueous Gelatin Solutions* Biomacromolecules, 2003. 4(4): p. 1080 -1086.

82.   Vandervoort, J. and A. Ludwig, *Preparation and evaluation of drug-loaded gelatin nanoparticles for topical ophthalmic use.* European Journal of Pharmaceutics and Biopharmaceutics, 2004. 57(2): p. 251-261.

83.   Kaul, G. and M. Amiji, *Long-circulating poly (ethylene glycol)-modified gelatin nanoparticles for intracellular delivery.* Pharmaceutical research, 2002. 19(7): p. 1061-1067.

84.   Kommareddy, S. and M. Amiji, *Preparation and evaluation of thiol-modified gelatin nanoparticles for intracellular DNA delivery in response to glutathione.* Bioconjugate Chem, 2005. 16(6): p. 1423-1432.

85.   Coester, C., et al., *Preparation of avidin-labelled gelatin nanoparticles as carriers for biotinylated peptide nucleic acid (PNA).* International Journal of Pharmaceutics, 2000. 196(2): p. 147-149.

86.   Lee, E.J., S.A. Khan, and K.-H. Lim, *Gelatin Nanoparticle Preparation by Nanoprecipitation.* Journal of biomaterials science. Polymer edition, 2010. 22(4-6): p. 753-771.

87.   Bajpai, A. and J. Choubey, *Release study of sulphamethoxazole controlled by swelling of gelatin nanoparticles and drug-biopolymer interaction.* Journal of macromolecular science. Pure and applied chemistry, 2005. 42(3): p. 253-275.

88.   Janes, K.A., P. Calvo, and M.J. Alonso, *Polysaccharide colloidal particles as delivery systems for macromolecules.* Advanced Drug Delivery Reviews, 2001. 47: p. 83-97.

89.   Landfester, K., *The generation of nanoparticles in miniemulsions.* Advanced Materials, 2001. 13(10): p. 765-768.

90.   Gupta, A., Reena, and H.B. Bohidar, *Free-energy landscape of alcohol driven coacervation transition in aqueous gelatin solutions.* The Journal of Chemical Physics, 2006. 125(054904).

91.   Mohanty, B., et al., *Small-angle neutron and dynamic light scattering study of gelatin coacervates.* Indian Academy of Sciences, 2005. 63(2): p. 271-276.

92.   Mohanty, B., et al., *Length Scale Hierarchy in Sol, Gel, and Coacervate Phases of Gelatin.* Journal of Polymer Science: Part B: Polymer Physics, 2006. 44: p. 1653-1667.

93.   Kaul, G. and M. Amiji, *Biodistribution and targeting potential of poly (ethylene glycol)-modified gelatin nanoparticles in subcutaneous murine tumor model.* Journal of drug

targeting, 2004. 12(9-10): p. 585-591.

94.	Kaul, G. and M. Amiji, *Tumor-targeted gene delivery using poly (ethylene glycol)-modified gelatin nanoparticles: in vitro and in vivo studies.* Pharmaceutical research, 2005. 22(6): p. 951-961.

95.	Kaul, G. and M. Amiji, *Cellular interactions and in vitro DNA transfection studies with poly (ethylene glycol) modified gelatin nanoparticles.* Journal of pharmaceutical sciences, 2005. 94(1): p. 184-198.

96.	Kommareddy, S. and M. Amiji, *Poly(ethylene glycol)-modified thiolated gelatin nanoparticles for glutathione-responsive intracellular DNA delivery.* Nanomedicine: Nanotechnology, Biology and Medicine, 2007. 3(1): p. 32-42.

97.	Kommareddy, S. and M. Amiji, *Biodistribution and pharmacokinetic analysis of long circulating thiolated gelatin nanoparticles following systemic administration in breast cancer bearing mice.* Journal of pharmaceutical sciences, 2007. 96(2): p. 397-407.

98.	Ofokansi, K., et al., *Matrix-loaded biodegradable gelatin nanoparticles as new approach to improve drug loading and delivery.* European Journal of Pharmaceutics and Biopharmaceutics, 2010. 76(1): p. 1-9.

99.	Zwiorek, K., *Gelatin Nanoparticles as Delivery System for Nucleotide-Based Drugs*, in *Department of Pharmacy, Pharmaceutical Technology and Biopharmaceutics.* Ph.D dissertation, 2006, Ludwig-Maximilians-Universität München.

100.	Farrugia, C.A. and M.J. Groves, *Gelatin Behaviour in Dilute Aqueous Solution: Designing a Nanoparticulate Formulation.* Journal of Pharmacy and Pharmacology, 1999. 51(6): p. 643-649.

101.	Fuchs, S., *Gelatin Nanoparticles as a Modern Platform for Drug Delivery-Formulation Development and Immunotherapeutic Strategies*, in *Department of Pharmacy, Pharmaceutical Technology and Biopharmaceutics.* Ph.D dissertation, 20010, Ludwig-Maximilians-Universität München.

102.	Zillies, J.C., *Gelatin Nanoparticles for Targeted Oligonucleotide Delivery to Kupffer Cells–Analytics, Formulation Development, Practical Application*, in *Department of Pharmacy, Pharmaceutical Technology and Biopharmaceutics.* Ph.D dissertation, 2007, Ludwig-Maximilians-Universität München.

103.	Narayanan, D., et al., *Poly-(ethylene glycol) modified gelatin nanoparticles for sustained delivery of the anti-inflammatory drug Ibuprofen-Sodium: An in vitro and in vivo analysis.* Nanomedicine: Nanotechnology, Biology and Medicine, 2013. 9(6): p. 818-828.

104.	Karthikeyan, S., et al., *Anticancer activity of resveratrol-loaded gelatin nanoparticles on NCI-H460 non-small cell lung cancer cells.* Biomedicine & Preventive Nutrition, 2013. 3(1): p. 64-73.

105. Rodriguez, S.G., et al., *Physicochemical parameters associated with nanoparticle formation in the salting-out, emulsification-diffusion, and nanoprecipitation methods.* Pharmaceutical Research, 2004. 21(8).

106. Fessi, H., et al., *Nanocapsule formation by interfacial polymer deposition following solvent displacement.* International Journal of Pharmaceutics, 1989. 55(1): p. R1-R4.

107. Guerrero, D.Q., et al., *Preparation techniques and mechanisms of formation of biodegradable nanoparticles from preformed polymers.* drug development and industrial pharmacy, 1998. 24(12): p. 1113-1128.

108. Khan, F., et al., *Versatile biocompatible polymer hydrogels: scaffolds for cell growth.* Angewandte Chemie, 2009. 121(5): p. 996-1000.

109. Lee, S.J., et al., *Biocompatible gelatin nanoparticles for tumor-targeted delivery of polymerized siRNA in tumor-bearing mice.* Journal of Controlled Release, 2013. 172(1): p. 358-366.

110. Reis, C.P., et al., *Nanoencapsulation I. Methods for preparation of drug-loaded polymeric nanoparticles.* Nanomedicine: Nanotech. Bio Med . 2006. 2 p. 8- 21.

111. Reis, C.P., et al., *Nanoencapsulation II. Biomedical applications and current status of peptide and protein nanoparticulate delivery systems.* Nanomedicine: Nanotechnology, Biology, and Medicine, 2006. 2: p. 53- 65.

112. Han, S., et al., *Construction of amphiphilic copolymer nanoparticles based on gelatin as drug carriers for doxorubicin delivery.* Colloids and Surfaces B: Biointerfaces, 2013. 102(0): p. 833-841.

113. Lai, P., et al., *Overview of the preparation of organic polymeric nanoparticles for drug delivery based on gelatine, chitosan, poly(d,l-lactide-co-glycolic acid) and polyalkylcyanoacrylate.* Colloids and Surfaces B: Biointerfaces, 2014. 118(0): p. 154-163.

114. El-Shabouri, M., *Positively charged nanoparticles for improving the oral bioavailability of cyclosporin-A.* International Journal of Pharmaceutics, 2002. 249(1): p. 101-108.

115. Singh, V. and A.K. Chaudhary, *Development and characterization of rosiglitazone loaded gelatin nanoparticles using two step desolvation method.* International Journal of Pharmaceutical Sciences Review and Research, 2010. 5(1): p. 100-13.

116. Kaur, A., S. Jain, and A.K. Tiwary, *Mannan-coated gelatin nanoparticles for sustained and targeted delivery of didanosine: in vitro and in vivo evaluation.* Acta Pharmaceutica, 2008. 58(1): p. 61-74.

117. Lu, Z., et al., *Paclitaxel-loaded gelatin nanoparticles for intravesical bladder cancer therapy.* Clinical Cancer Research, 2004. 10(22): p. 7677.

118. Saxena, A., et al., *Effect of molecular weight heterogeneity on drug encapsulation efficiency of gelatin nano-particles.* Colloids and Surfaces B: Biointerfaces, 2005. 45(1): p. 42-48.

119. Bajpai, A.K. and J. Choubey, *Design of gelatin nanoparticles as swelling controlled delivery system for chloroquine phosphate.* Journal of Material Science Material in Medicine, 2006. 17(4): p. 345-358.

120. Nahar, M., et al., *In vitro evaluation of surface functionalized gelatin nanoparticles for macrophage targeting in the therapy of visceral leishmaniasis.* Journal of drug targeting, 2010. 18(2): p. 93-105.

121. Nahar, M., et al., *Development, characterization, and toxicity evaluation of amphotericin B-loaded gelatin nanoparticles.* Nanomedicine: Nanotechnology, Biology and Medicine, 2008. 4(3): p. 252-261.

122. Rose, J.B., et al., *Gelatin-Based Materials in Ocular Tissue Engineering.* Materials, 2014. 7(4): p. 3106-3135.

123. Li, J.K., N. Wang, and X.S. Wu, *Gelatin nanoencapsulation of protein/peptide drugs using an emulsifier-free emulsion method.* Journal of microencapsulation, 1998. 15(2): p. 163-172.

124. Yilmaz, H. and S.H. Sanlier, *Preparation of magnetic gelatin nanoparticles and investigating the possible use as chemotherapeutic agent.* Artificial Cells, Nanomedicine, and Biotechnology, 2013. 41(2): p. 69-77.

125. Huang, J.-Y., et al., *Cholaminchloride hydrochloride-cationized gelatin/calcium-phosphate nanoparticles as gene carriers for transgenic chicken production.* Process Biochemistry, 2012. 47(12): p. 1919-1925.

126. Kommareddy, S., D.B. Shenoy., and M. Amiji, *Gelatin Nanoparticles and Their Biofunctionalization.* Nanotechnologies for the Life Sciences, 2007.

127. Kim, K.J. and Y. Byun, *Preparation and characterizations of self-assembled PEGylated gelatin nanoparticles.* Biotechnology and Bioprocess Engineering, 1999. 4(3): p. 210-214.

128. Tseng, C.-L., et al., *The use of biotinylated-EGF-modified gelatin nanoparticle carrier to enhance cisplatin accumulation in cancerous lungs via inhalation.* Biomaterials, 2009. 30(20): p. 3476-3485.

129. Tseng, C.-L., et al., *Targeting efficiency and biodistribution of biotinylated-EGF-conjugated gelatin nanoparticles administered via aerosol delivery in nude mice with lung cancer.* Biomaterials, 2008. 29(20): p. 3014-3022.

130. Dinauer, N., et al., *Selective targeting of antibody-conjugated nanoparticles to leukemic cells and primary T-lymphocytes.* Biomaterials, 2005. 26(29): p. 5898-5906.

131. Zwiorek, K., et al., *Delivery by cationic gelatin nanoparticles strongly increases the immunostimulatory effects of CpG oligonucleotides.* Pharmaceutical research, 2008. 25(3): p. 551-562.

132. Zillies, J.C. and C. Coester, *Evaluating gelatin based nanoparticles as a carrier system for double stranded oligonucleotides.* J Pharm Pharm Sci, 2005. 7(4): p. 17–21.

133.   Zillies, J.C., et al., *Formulation development of freeze-dried oligonucleotide-loaded gelatin nanoparticles.* European Journal of Pharmaceutics and Biopharmaceutics, 2008. 70(2): p. 514-521.

134.   Oppenheim, R.C., J.J. Marty, and P. Speiser, *Injectable compositions, nanoparticles useful therein, and process of manufacturing same.* 1978, Google Patents.

135.   Harsha, S., *Pharmaceutical suspension containing both immediate/sustained-release amoxicillin-loaded gelatin nanoparticles: preparation and in vitro characterization.* Drug design, development and therapy, 2013. 7: p. 1027.

136.   Coester, C., et al., *Gelatin nanoparticles by two step desolvation a new preparation method, surface modifications and cell uptake.* Journal of microencapsulation, 2000. 17(2): p. 187-193.

137.   Xu, J., F. Gattacceca, and M. Amiji, *Biodistribution and pharmacokinetics of EGFR-targeted thiolated gelatin nanoparticles following systemic administration in pancreatic tumor-bearing mice.* Molecular pharmaceutics, 2013. 10(5): p. 2031-2044.

138.   Jing, X. and A. Mansoor, *Therapeutic Gene Delivery and Transfection in Human Pancreatic Cancer Cells using Epidermal Growth Factor Receptor-targeted Gelatin Nanoparticles.* Journal of Visualized Experiments, 2012(59).

139.   Gan, Z., et al., *Temperature-triggered enzyme immobilization and release based on cross-linked gelatin nanoparticles.* PloS one, 2012. 7(10): p. e47154.

140.   Galindo-Rodríguez, S.A., et al., *Comparative scale-up of three methods for producing ibuprofen-loaded nanoparticles.* European Journal of Pharmaceutical Sciences, 2005. 25(4): p. 357-367.

141.   Murakami, H., et al., *Preparation of poly (DL-lactide-co-glycolide) nanoparticles by modified spontaneous emulsification solvent diffusion method.* International Journal of Pharmaceutics, 1999. 187(2): p. 143-152.

142.   Stainmesse, S., et al., *Formation and stabilization of a biodegradable polymeric colloidal suspension of nanoparticles.* Colloid & Polymer Science, 1995. 273(5): p. 505-511.

143.   Govender, T., et al., *PLGA nanoparticles prepared by nanoprecipitation: drug loading and release studies of a water soluble drug.* Journal of Controlled Release, 1999. 57(2): p. 171-185.

144.   Bancroft, J.D. and M. Gamble, *Theory and Practice of Histological Techniques* 6ed. 2008, Amsterdam: Elsevier Health Sciences. 56.

145.   Ofner III, C.M. and W.A. Bubnis, *Chemical and swelling evaluations of amino group crosslinking in gelatin and modified gelatin matrices.* Pharmaceutical Research, 1996. 13(12): p. 1821-1827.

146.   Gupta, A. and H. Bohidar, *Free-energy landscape of alcohol driven coacervation transition in aqueous gelatin solutions.* The Journal of Chemical Physics, 2006. 125: p. 054904.

147. Bigi, A., et al., *Mechanical and thermal properties of gelatin films at different degrees of glutaraldehyde crosslinking.* Biomaterials, 2001. 22(8): p. 763-768.

148. Qazvini, N.T. and S. Zinatloo, *Synthesis and characterization of gelatin nanoparticles using CDI/NHS as a non-toxic cross-linking system.* Journal of Materials Science: Materials in Medicine, 2011. 22(1): p. 63-69.

149. Galindo-Rodriguez, S., et al., *Physicochemical parameters associated with nanoparticle formation in the salting-out, emulsification-diffusion, and nanoprecipitation methods.* Pharmaceutical Research, 2004. 21(8): p. 1428-1439.

150. Bilati, U., E. Allémann, and E. Doelker, *Development of a nanoprecipitation method intended for the entrapment of hydrophilic drugs into nanoparticles.* European Journal of Pharmaceutical Sciences, 2005. 24(1): p. 67-75.

151. Hornig, S., et al., *Synthetic polymeric nanoparticles by nanoprecipitation.* Journal of Materials Chemistry, 2009. 19(23): p. 3838-3840.

152. Hines, D.J. and D.L. Kaplan, *Mechanisms of controlled release from silk fibroin films.* Biomacromolecules, 2011. 12(3): p. 804-812.

153. Tungkavet, T., D. Pattavarakorn, and A. Sirivat, *Bio-compatible gelatins (Ala-Gly-Pro-Arg-Gly-Glu-4Hyp-Gly-Pro-) and electromechanical properties: effects of temperature and electric field.* Journal of Polymer Research, 2012. 19(1): p. 1-9.

154. Digenis, G.A., T.B. Gold, and V.P. Shah, *Cross‐linking of gelatin capsules and its relevance to their in vitro‐in vivo performance.* Journal of pharmaceutical sciences, 1994. 83(7): p. 915-921.

155. Asati, A., et al., *Surface-charge-dependent cell localization and cytotoxicity of cerium oxide nanoparticles.* ACS nano, 2010. 4(9): p. 5321-5331.

156. Kommareddy, S. and M. Amiji, *Antiangiogenic gene therapy with systemically administered sFlt-1 plasmid DNA in engineered gelatin-based nanovectors.* Cancer gene therapy, 2007. 14(5): p. 488-498.

157. Kuo, W.-T., et al., *Surface modification of gelatin nanoparticles with polyethylenimine as gene vector.* Journal of Nanomaterials, 2011. 2011: p. 28.

158. Carneiro-da-Cunha, M.G., et al., *Influence of concentration, ionic strength and pH on zeta potential and mean hydrodynamic diameter of edible polysaccharide solutions envisaged for multinanolayered films production.* Carbohydrate Polymers, 2011. 85(3): p. 522-528.

159. Zhu, J., et al., *Amphiphilic core-shell nanoparticles with poly (ethylenimine) shells as potential gene delivery carriers.* Bioconjugate chemistry, 2005. 16(1): p. 139-146.

160. Elzoghby, A.O., *Gelatin-based nanoparticles as drug and gene delivery systems: Reviewing three decades of research.* Journal of Controlled Release, 2013. 172(3): p. 1075-1091.

161. Kushibiki, T., H. Matsuoka, and Y. Tabata, *Synthesis and physical characterization of poly*

(ethylene glycol)-gelatin conjugates. Biomacromolecules, 2004. 5(1): p. 202-208.

162. Lee, E., et al., *Studies on the characteristics of drug-loaded gelatin nanoparticles prepared by nanoprecipitation.* Bioprocess and Biosystems Engineering, 2012. 35(1-2): p. 297-307.

163. Won, Y.-W. and Y.-H. Kim, *Recombinant human gelatin nanoparticles as a protein drug carrier.* Journal of Controlled Release, 2008. 127(2): p. 154-161.

164. Fuchs, S., et al., *Transglutaminase: New insights into gelatin nanoparticle cross-linking.* Journal of microencapsulation, 2010. 27(8): p. 747-754.

165. Hiwale, P., et al., *In vitro release of lysozyme from gelatin microspheres: effect of cross-linking agents and thermoreversible gel as suspending medium.* Biomacromolecules, 2011. 12(9): p. 3186-3193.

166. Kim, Y., et al., *Effect of cross-linking on the performance of micelles as drug delivery carriers: a cell uptake study.* Biomacromolecules, 2012. 13(3): p. 814-825.

167. Loth, T., et al., *Reactive and stimuli-responsive maleic anhydride containing macromers– multi-functional cross-linkers and building blocks for hydrogel fabrication.* Reactive and Functional Polymers, 2013. 73(11): p. 1480-1492.

168. Bigi, A., et al., *Stabilization of gelatin films by crosslinking with genipin.* Biomaterials, 2002. 23(24): p. 4827-4832.

169. Shutava, T.G., et al., *Layer-by-layer-coated gelatin nanoparticles as a vehicle for delivery of natural polyphenols.* ACS nano, 2009. 3(7): p. 1877-1885.

170. Lee, E.J., et al., *Studies on the characteristics of drug-loaded gelatin nanoparticles prepared by nanoprecipitation.* Bioprocess and Biosystems Engineering, 2012. 35(1-2): p. 297-307.

171. Schneider, M., M. Brinkmann, and H. Möhwald, *Adsorption of polyethylenimine on graphite: an atomic force microscopy study.* Macromolecules, 2003. 36(25): p. 9510-9518.

172. Bohr, A., et al., *Release profile and characteristics of electrosprayed particles for oral delivery of a practically insoluble drug.* Journal of The Royal Society Interface, 2012. 9(75): p. 2437-2449.

173. Üner, M. and G. Yener, *Importance of solid lipid nanoparticles (SLN) in various administration routes and future perspectives.* International journal of nanomedicine, 2007. 2(3): p. 289.

174. Anand, V., R. Kandarapu, and S. Garg, *Preparation and evaluation of taste-masked orally disintegrating tablets of prednisolone.* Asian J Pharm Sci, 2007. 2(6): p. 227-38.

8. Scientific Output

Publications

1. **Saeed Ahmad Khan**, Marc Schneider, Improvement of Nanoprecipitation Technique for Preparation of Gelatin Nanoparticles and Potential Macromolecular Drug Loading. Macromolecular Bioscience,2013, 13(4):455-63.
2. **Saeed Ahmad Khan**, Marc Schneider, Nanoprecipitation versus two step desolvation technique for the preparation of gelatin nanoparticles, SPIE conference proceedings volume:8595 (Colloidal Nanocrystals for Biomedical Applications VIII, 2013).
3. **Saeed Ahmad Khan**, Marc Schneider, Stabilization of gelatin nanoparticles without crosslinking, Submitted. Macromolecular Bioscience, submitted.

Patents

1. Delivery of antibiotics by nanospheres prepared by MJR technology (with MJR PharmJet GmbH, in preparation).

Poster Presentation

1. Clemens Tscheka, Eman Haimour, **Saeed Ahmad Khan**, Marc Schneider, Novel filamentous carrier systems for drug delivery to bio-films, 2nd HIPS Symposium on Pharmaceutical sciences devoted to infection research, 28. June 2012, Saarland University, Germany.
2. **Saeed Ahmad Khan**, Marc Schneider, Hydrophilic nanoparticles for hydrophilic macromolecular drugs, CRS local chapter meeting, 21-22 Mar. 2013, Ludwigshafen, Germany.Clemens Tscheka, **Saeed Ahmad Khan**, Mohamed Tawfik, Eman Haimour, Marc Schneider, Novel filamentous Carrier Systems based on biodegradable Hydrogels, CRS local chapter meeting, 21-22 Mar. 2013, Ludwigshafen, Germany.
3. **Saeed Ahmad Khan**, Marc Schneider, Gelatin nanoparticles as a potential nanocarrier for macromolecular drugs**,** DPhG annual conference 2013, drug delivery inspired by nature 9-11 Oct. 2013, Freiburg University, Germany.
4. **Saeed Ahmad Khan**, Marc Schneider, Crosslinked gelatin nanoparticles for the delivery of macromolecules, CRS local chapter meeting, 27-28 Feb. 2014, University of Kiel, Germany.
5. **Saeed Ahmad Khan**, Marc Schneider, Effect of molecular weight on encapsulation and release of macromolecular drugs from gelatin nanoparticles, 10th international conference and workshop on Biological Barriers, 16-21 February 2014, Saarland University, Germany.
6. **Saeed Ahmad Khan**, Marc Schneider, Tuning the size of gelatin nanoparticles, Sino-German Workshop "Functional (nano-) biomaterials, 2,3 April, 2014, Department of Physics, Phillips University, Marburg.

Curriculum Vitae

Personal Information

Name	Saeed Ahmad Khan
Date of Birth	10th May 1981
Place of Birth	Buner (Pakistan)

Academic Record

2011-2014	Doing PhD (Pharmaceutical Technology), Phillips University Marburg, Germany, and Saarland University, Saarbrücken, Germany.
2006-2008	MS (Chemical Engineering), Daegu University, South Korea. **Thesis title:** Biopolymer coating, Nanoprecipitation: A novel method for the preparation of gelatin nanoparticles and its evaluation for drug loading.
1999-2003	Bachelor of Pharmacy, University of Peshawar, Pakistan.

Practical Experience

2003-2004	Trainee at Abbott Laboratories Pakistan ltd.
2004-2005	Consultant at Parke-Davis and co. ltd.
2006-2008	Research assistant at the department of chemical engineering, Daegu University, South Korea.
2008-2010	Lecturer at the Department of Pharmacy, Sarhad University of Science and Information technology, Peshawar, Pakistan.
2010-2014	Lecturer at the Department of Pharmacy, Kohat University of Science and Technology, Kohat, Pakistan.

Acknowledgment

(HIPS) for SEM analysis, Peter Meiers (Uni. Saarland) for his help in routine laboratory practice. My respects and thanks to our cooperative and helpful secretaries; Julia Michaelis (Uni. Marburg), Isabelle Conrad-Kehl (Uni. Saarland), Sarah Müller (HIPS) and Karin Groß (Uni. Saarland) for administrative assistance.

Appreciations and respects are extended to Dr. Nicole Daum, Dr. Brigitta Loretz, Dr. Steffi Hansen, Dr. Eva Collnot for sharing with me their excellent knowledge and experience in a couple of graduate courses.

I was lucky for having Hussain Ali and other Pakistani friends in Saarbrücken before I moved there. It eased my settlement and adjustment to the new environment. Thanks for giving me a nice company.

I am gratefully acknowledging all my teachers specially Prof. Muhammad Saeed for his guidance and advices. I owe special thanks to Dr. Taous Khan and Dr. Hamayun Khan, Prof. Kwang-Hee lim, Dr. Nauman and Dr. Khalid for introducing me to the excellent world of research.

Lastly, I would like to thanks my parents (late) who tried hard to meet all my desires. I wish I could share my happiness with them, who sacrificed their wishes for our prosperity and happiness. I thank my brother and sisters for being around me, for typifying the feeling of my parents. I am grateful to my parents-in-law, my cousin Abdul Hamid and my relatives for taking care of my family in my absence. Without their support my aim wouldn't have been accomplished. And most of all I owe immense gratitude to my loving, supportive wife, whose patience and faithful support made it possible. I feel sorry to my wife and kids for not being able to give them the time they deserve. But I hope the compromises we all have made will bear fruit in future. I am anxiously waiting to be together soon.

I gratefully acknowledge HEC, Pakistan and DAAD whose funding made my PhD possible.

Saeed Ahmad Khan